UiT The Arctic University of Norway

Department of Medical Biology, Faculty of Health Sciences

A study on the interactions between perfluorosulfonic acids and P-glycoprotein in the Caco-2 cell line model

Tetyana Voloshyna

Master's thesis in Biomedicine (MBI-3911), May 2021

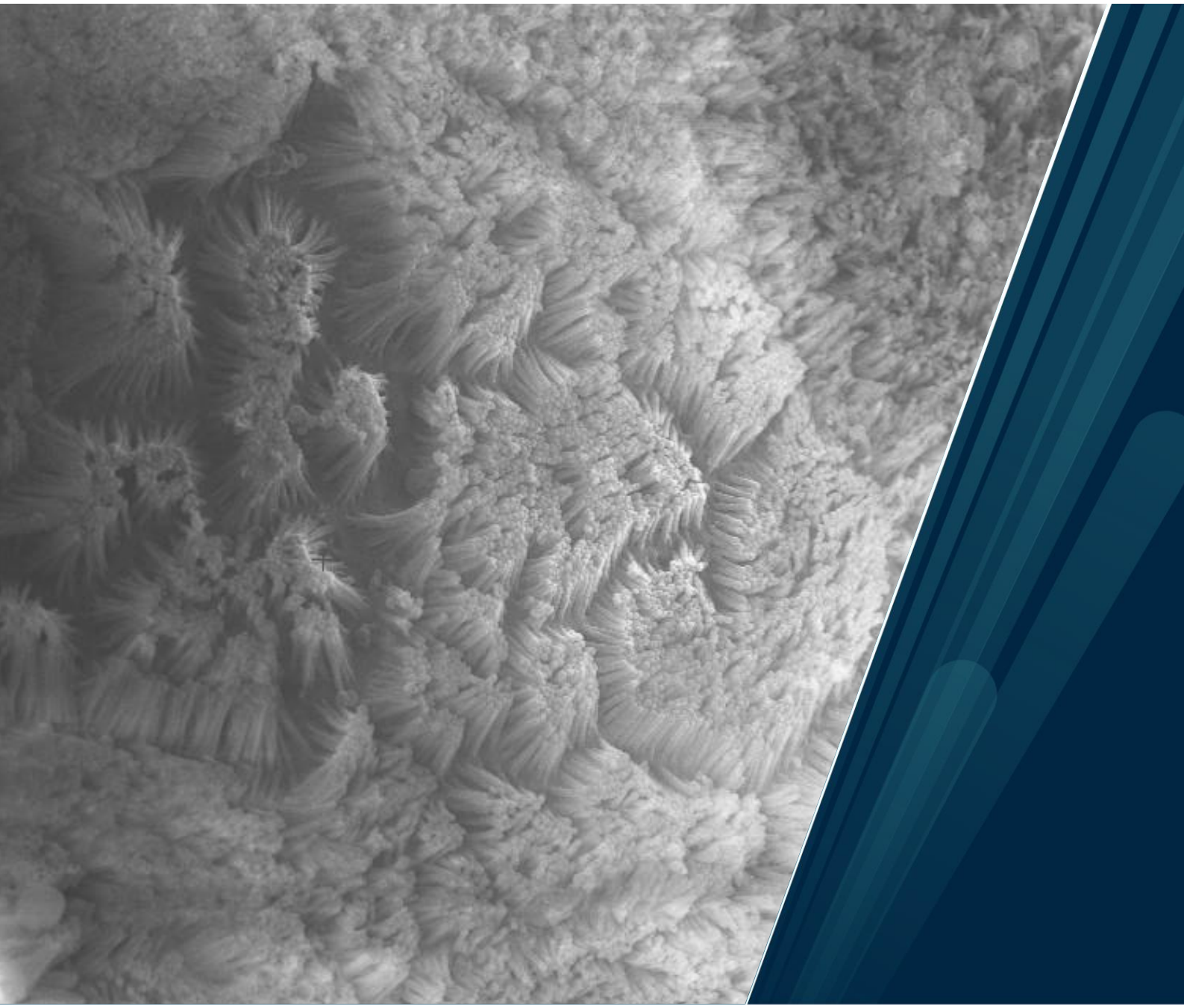

Acknowledgments

This master's thesis was conducted at Experimental and Clinical Pharmacology, at the Department of Medical Biology, at the University of Tromsø between August 2020 and May 2021. It has been an enriching experience, and I cannot express enough how grateful I am for the great deal of support, guidance, and assistance I received during my work.

I would like to thank my main supervisor Erik Sveberg Dietrichs for all the guidance and supervision throughout this study. Thank you for your patient support and for all the opportunities I was given during this work. A special thanks goes to Natalia Smaglyukova for all the support and assistance I received throughout the project. Thank you for always being prepared to help and for all the fun moments together. I would also like to express my gratitude to Sandra Huber for your invaluable expertise, guidance, encouragement, and support throughout the study and your irreplaceable help in the LC-MS analysis of my samples. A huge thanks to Ole Martin Fuskevåg for your invaluable expertise and guidance. I am incredibly grateful for your help in the LC-MS analysis of my samples.

A huge and special thanks to Roy Andre Lysså for the illustrations used in the thesis, for constructing the equipment used in the experimental procedure and for all the support, encouragement, and advice I have received. Timofey Kondratyev, thank you for the contribution in constructing the equipment used in the experimental procedure, and thank you for all the advice and help I have received. Thank you, Merete Skar, for your aid in solution handling and preparation. Lena Aronsen, thank you for sharing your work and insights, your contribution eased my tasks a great deal. A huge thanks to Georg Sager and Aina Westrheim Ravna for expert advice. A special thanks to Randi Olsen, Tom-Ivar Eilertsen and Kenneth Bowitz Larsen for making it possible taking the outstanding electron microscopy and confocal microscopy images for this thesis.

Finally, I would like to thank my mom and my boyfriend Bård for supporting and encouraging me throughout this whole time.

This thesis would not be possible to complete without all of you!

Abstract

Perfluoroalkyl substances (PFAS) have received a great deal of attention due to the ubiquitous occurrence and persistence in the environment, resistance to degradation, and biological accumulation in wildlife and humans. PFAS are being detected around the globe, raising concerns regarding the toxicity and health risks to humans. Studies have shown that environmental toxicants, including PFAS, can interact with transporter proteins involved in the absorption and distribution, as well as detoxification, of drugs, xenobiotics and other toxicants. In this study, the effects of PFAS of different carbon chain lengths, perfluorooctane sulfonic acid (PFOS), perfluorohexane sulfonic acid (PFHxS) and perfluorobutane sulfonic acid (PFBS), on the activity of P-glycoprotein (P-gp) were investigated using the Caco-2 cell line model. Additionally, it was investigated whether PFOS, PFHxS and PFBS cross the Caco-2 cell monolayer. Two known P-gp substrates, quinidine and verapamil, were used to inhibit P-gp in Caco-2 cells, to examine whether PFOS, PFHxS and PFBS might be substrates of P-gp. No interaction between the tested compounds and digoxin were observed, suggesting that these individual PFAS did not modulate the activity of P-gp. Nevertheless, it was observed that PFOS, PFHxS and PFBS crossed the Caco-2 monolayer. Inhibition of P-gp by known inhibitors caused a slight decrease in the rate of PFOS and PFHxS, but not PFBS, in the apical to basolateral direction and in the basolateral to apical direction, suggesting that active uptake and efflux might be involved in the transport of PFOS, PFHxS, but not PFBS, across the Caco-2 monolayer.

Table of Contents

Abbreviations

PFAS	Per- and polyfluoroalkyl substances
PFCAs	Perfluorocarboxylic acids
PFSAs	Perfluorosulfonic acids
PFOS	Perfluorooctane sulfonic acid
PFOA	Perfluorooctane carboxylic acid
PFHxS	Perfluorohexane sulfonic acid
PFBS	Perfluorobutane sulfonic acid
PFNA	Perfluorononane carboxylic acid
PFDA	Perfluorodecane carboxylic acid
PFUdA	Perfluoroundecane carboxylic acid
ABC	ATP-binding cassette
ATP	Adenosine 5’-triphosphate
TMD	Transmembrane domain
NBD	Nucleotide binding domain
POP	Persistant organic pollutant
P-gp	P-glycoprotein
MDR	Multidrug resistance
OATP	Organic anion transporting polypeptide
AB	Apical to basolateral
BA	Basolateral to apical
ER	Efflux ratio
SEM	Scanning electron microscopy
TEM	Transmission electron microscopy
TEER	Transepithelial electrical resistance

1 Introduction

The last decade, per- and polyfluoroalkyl substances (PFAS) have received great amount of attention due to their ubiquitous occurrence, persistence in the environment and resistance to biological degradation. Some of the analogues have been detected in wildlife and humans around the globe and demonstrated toxic properties (1).

1.1 Per- and polyfluoroalkyl substances

PFAS have been in production since the 1940s and utilized during manufacture of a wide range of products. It is a class of more than 4000 synthetic fluorinated chemicals that consist of a hydrophobic carbon chain of varying length with at least one fully fluorinated carbon atom and a hydrophilic functional group (1). PFAS have the general chemical structure: C_nF_{2n+1}-R, and based on the functional group, these can be divided into different groups (2, 3). The groups perfluorocarboxylic acids (PFCAs) and perfluorosulfonic acids (PFSAs) have received most attention, with perfluorooctane carboxylic acid (PFOA) (Figure 1A) and perfluorooctane sulfonic acid (PFOS) (Figure 1B) being the most studied compounds. PFAS can be both linear and branched in their molecular structure (4). Because of the strong covalent bond between carbon and fluorine, PFAS are highly stable – both chemically and thermally (5, 6).

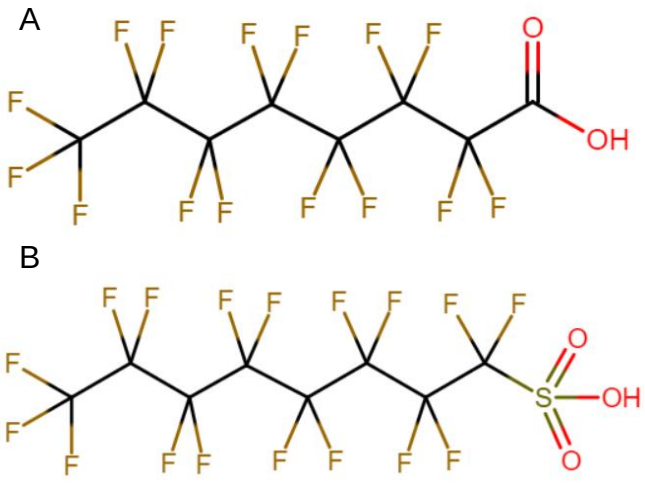

Figure 1: Chemical structure of PFOA (A) and PFOS (B). Constructed in Marvin JS.

1.1.1 Applications and uses

Due to the unique physicochemical properties, PFAS are ideal as surfactants and have been widely used in commercial products such as non-stick cookware, food packaging, stain- and water-proof coating for clothing, furniture and carpets, in cosmetics and hygiene products, as well as in fire-fighting foams and in other industrial applications (1, 5, 7-15).

1.1.2 Concerns regarding environmental distribution

The extensive use of PFAS and their emission have led to a wide distribution in the environment. This wide distribution has been attributed to bioaccumulation and resistance to degradation in ecosystems, as the chemical stability makes many PFAS highly persistent in the environment (16-20).

Although the manufacture of fluoropolymers is one of the main sources of environmental emission in the northern hemisphere, PFAS are mobile in the environment, and can be transported through air and water to remote places, and additionally through animals and humans (21). PFAS are lifestyle-related chemicals, and are more present levels in industrialized rather than in less-developed areas (1). In countries with no fluoropolymer industries, the occurance of PFAS is still common, because of the extensive use of products containing these substances, in addition to industrial use of for instance fire-fighting foams (22). This results in point sources in populated areas. Thus, there are multiple pathways of exposure to PFAS, as depicted in Figure 2.

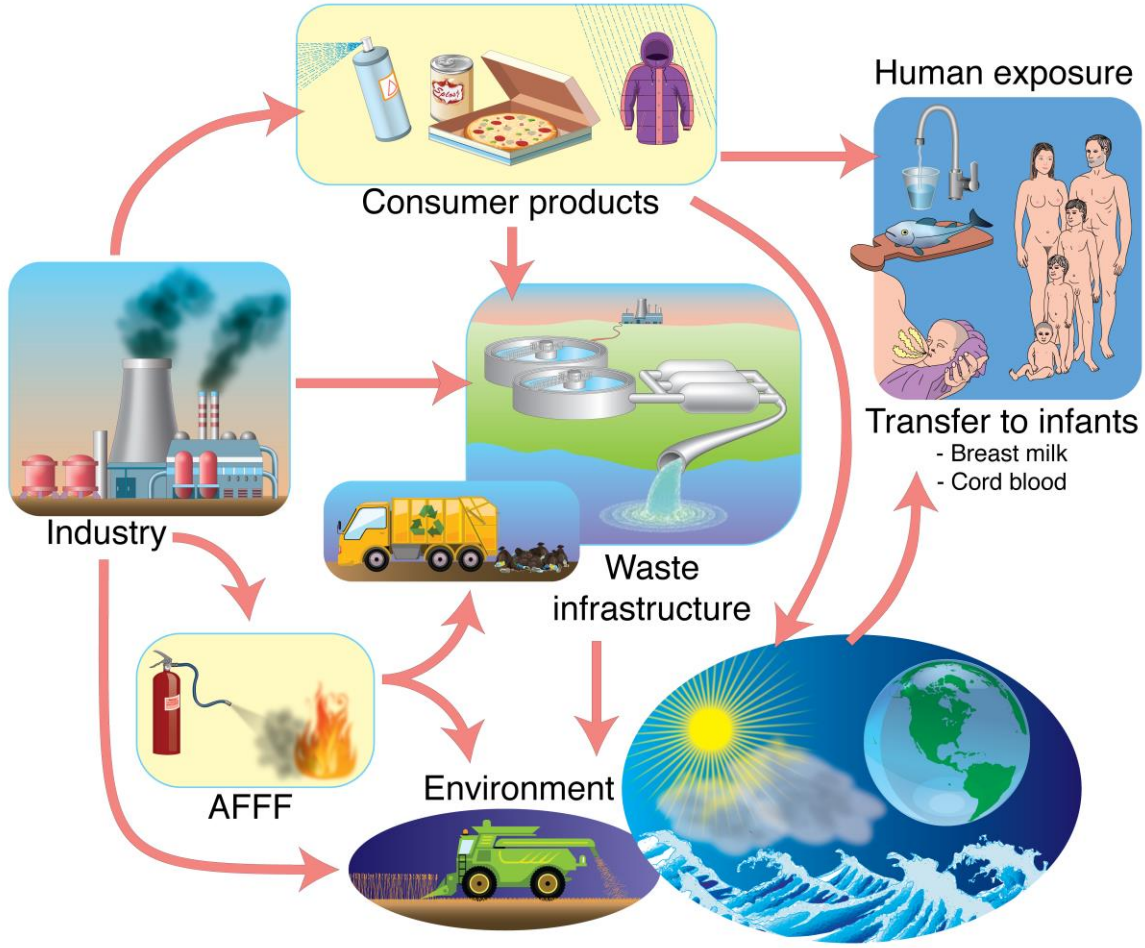

Figure 2: Different pathways of exposure to PFAS. Humans are mostly exposed to PFAS through consumer products, dust, ingestion of contaminated food and water, and through the environment. However, it is all interrelated with the industry or production site, and waste infrastructure. Figure by Roy Lysås.

Since the early 2000s, many studies have been conducted to measure and understand PFAS, especially focusing on single compounds as PFOA and PFOS in the beginning, and later also including long-chain PFAS (23-26). Long-chain PFAS refer to perfluoroalkyl carboxylic acids with 7 or more perfluorinated carbon atoms and perfluoroalkyl sulfonic acids with 6 or more perflouorinated carbons atoms (27).

The most studied compounds, PFOA and PFOS have been detected globally, even in the Arctic (28). In addition to being widely detected in the environment and wildlife, these compounds have been detected in human serum from the general population (16, 19, 21, 29-

35). PFOA and PFOS are however not the only PFASs detected in human serum, other long-chain PFAS like perfluorohexane sulfonic acid (PFHxS), perfluorononane carboxylic acid (PFNA), perfluorodecane carboxylic acid (PFDA), and perfluoroundecane carboxylic acid (PFUdA) are also present, and have even been detected in human breast milk (35-37). Higher serum concentrations of PFAS are common in individuals involved in PFAS manufacturing and individuals living in high proximity to production areas and contaminated areas compared to individuals without occupational exposure (38, 39).

1.1.3 Phaseout

Long-chain PFAS have been recognised as highly persistent, bioacciumulative, and toxic global contaminants of high concern (1, 40). The concerns about persistence in the environment and accumulation in organisms has resulted in PFOS and PFOA being phased out in many developed countries in the beginning of 2000s, and replaced with shorter chain PFAS, which have been shown to be less bioaccumulative (41, 42). PFOA and PFOS were added to Stockholm Convention's list of restricted Persistent Organic Pollutants (POP) in 2009 and 2019 respectively, while PFHxS is proposed for listing under the Convention (30, 43). However, little knowledge is available concerning potential health effects of lower concentrations of the longer chain PFAS, as well as the potential health effects of the shorter chain PFAS in general.

1.1.4 PFAS and health concerns

Bioaccumulation and biomagnification in mammals and other top predators, including humans, as well as the long half-lives, have raised concerns about the toxicity of PFAS and health risks to humans (1). In humans, the half-life of PFOS is several years, but in animals it is considerably shorter (37, 44-47). PFAS have been shown to bind to serum proteins, with albumin being the major carrier protein (34). Nevertheless, the occurrence of PFAS have been confirmed in many tissues of the human organism, such as the brain, liver, lung, bone, and kidney (48, 49). In addition to serum, the liver has been shown to be the major target for bioaccumulation of PFOS (50-52).

Although the health effects of PFAS on the general population are little studied, the exposure to these has been related to a range of health concerns. Adverse outcomes include disruption in the endocrine system where higher serum concentrations of PFNA have been associated

with elevated free thyroxine in adolescent and young adults, and exposure to PFOS and PFOA has been associated with delay in age of menarche, increased total serum cholesterol levels and low-density lipoprotein cholesterol, reduced testosterone levels in men, and reduced birth weight when exposed to PFOA utero (5, 19, 34, 53-61). Moreover, several animal studies, both in vivo and in vitro studies, have suggested that PFAS exposure may lead to adverse health effects in humans, including hepatoxicity, neurotoxicity, reproductive toxicity, immunotoxicity, thyroid disruption, cardiovascular toxicity, pulmonary toxicity and renal toxicity (48, 50, 62-67). However, the toxic effects and mechanisms are not fully understood due to the complexity of the human organism and elimination kinetics of PFAS (48).

The knowledge about the pharmacokinetics and pharmacodynamics of PFAS in general and how individual single substances as well as PFAS-mixtures may affect the absorption of nutrients or drugs and their transport across biological membranes, is however, limited.

1.2 Intestinal absorption and transport of molecules across biological barriers

There are multiple pathways of exposure to PFAS, including ingestion of contaminated food and drinking water (19). The small intestine is the principle site of absorption of ingested compounds, whether they are dietary, therapeutic, or toxic (68). Its surface contains circular folds covered with projections known as villi (Figure 3). These villi are covered in intestinal epithelial cells whose surface membranes form microvilli, also known as the brush border. The presence of these projections significantly increases the surface area of the small intestine and thus maximizes its absorptive capacity (69).

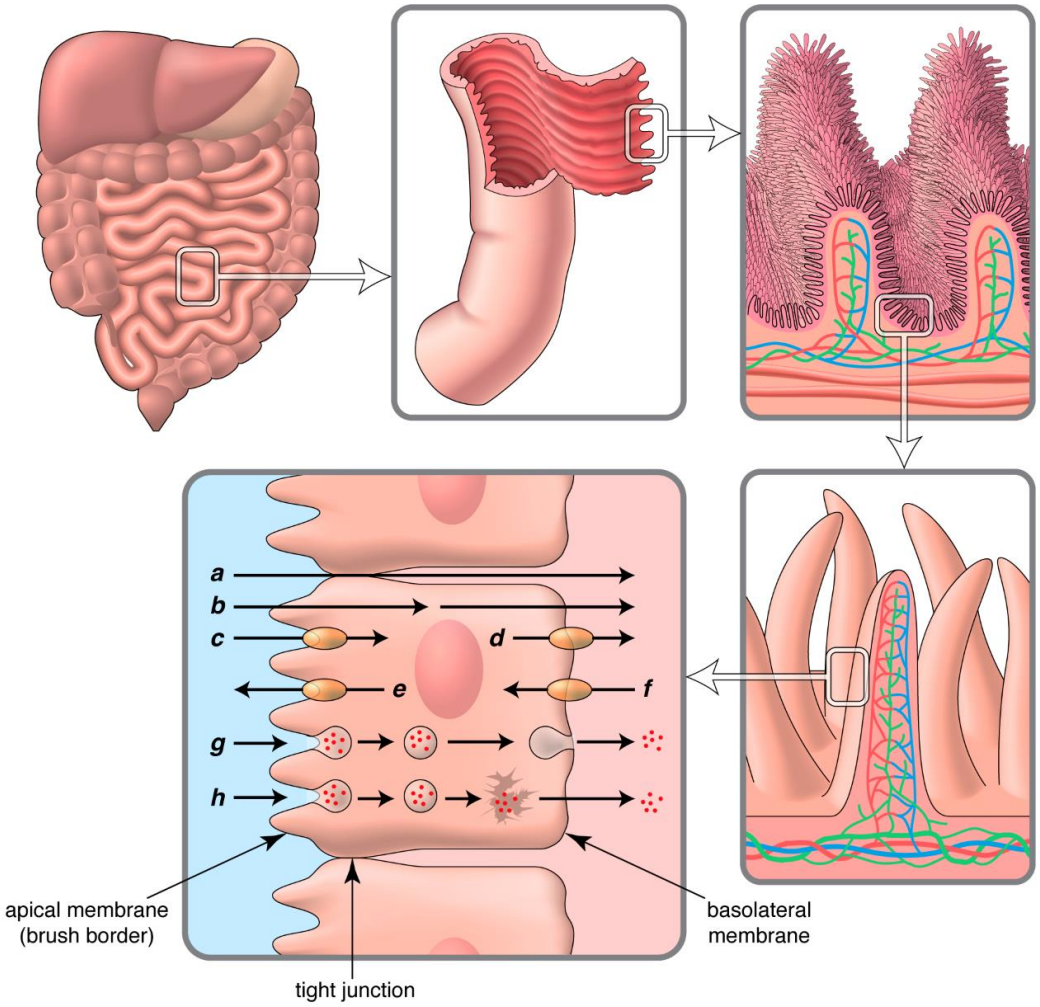

Figure 3: Structure of the small intestine showing the invaginations covered in villi and intestinal enterocytes with microvilli, and transport across intestinal enterocyte, including paracellular passive transport (a), transcellular passive transport (b) facilitated or active transport through membrane transporters (c, d, e, f) as well as endocytosis (g, h). Figure by Roy Lysså.

Intestinal enterocytes, which are the major cell type in the intestinal epithelium, play an important role in the absorption of nutrients and solutes from the intestinal lumen (68, 70, 71). The general routes by which orally ingested compounds may be absorbed, are the paracellular and the transcellular routes (Figure 3). However, for a compound to be absorbed, it must cross biological barriers, including the cell membrane. The cell membrane is a selectively permeable barrier and consists of an amphipathic phospholipid bilayer. Whether a compound is able to cross the cell membrane depends largely on its molecular size, charge, and lipid solubility (72). While water and small nonpolar, molecules can readily diffuse across the membrane due to their lipophilic character, polar molecules, ions, macromolecules, and

solutes require specialized membrane transporters to facilitate their cellular uptake or transport (73). Thus, the selectivity and flexibility of the cell membrane to control the flux of substances in and out of the cell, can be attributed to transporter proteins (72).
There are several ways the absorption of compounds can occur, including passive diffusion, carrier-mediated transport, and vesicular transport (Figure 3) (71). Passive diffusion can be divided into paracellular and transcellular passive diffusion (Figure 3, a and b) (71). Some small hydrophilic ionized compounds may be absorbed by the paracellular route, however, the absorption by this pathway is rather low because the tight junctions restrict free movement between epithelial cells (68). Lipophilic substances and xenobiotics, on the other hand, might undergo passive transcellular absorption or be facilitated by special transporters involved in the absorption of nutrients and micronutrients (71).

Transporters are proteins that are embedded in the membrane and may be divided into following classes based on their function and phylogeny: Channels and pores, electrochemical potential-driven transporters, primary active transporters, group translocators, transport electron carriers, accessory factors involved in transport, as well as incompletely characterized transport systems (74).

These transporter proteins can be active or passive. The passive transport of substrates occurs by facilitated diffusion, where the interaction of the solute with a binding site of the membrane transporter moves the solute across the biological membrane. This process does not require energy and is driven by the concentration gradient of the solute, however, the rate of transport is dependent on the availability of the binding site on the transporter and binding capacity of the solute to the transporter (72). Active transporters, on the other hand, utilize cellular energy to transport solutes across a biological barrier against the concentration gradient, from lower solute concentration to higher solute concentration. Symporters move molecules in the same direction, while antiporters transport substrates in opposite directions of each other. While primary active transport is dependent on a primary source of chemical energy, such as ATP-hydrolysis, to move substrates across a biological membrane, secondary active transporters are driven by the electrochemical gradients of the transported molecules, to transport these against their concentration gradient (74).

The intestinal mucosa contains different transporter proteins like transporters of di- or tripeptides, large neutral amino acids, bile acids, nucleosides and monocarboxylic acids, and some of these might play a role in the absorption of xenobiotics. Consequently, enterocytes also form a selective barrier to xenobiotics (68, 70, 71). Some transporters are influx transporters, which bind the molecule from the intestinal fluid on the apical side and transports it to the basolateral side of the enterocyte. The H+/oligopeptide cotransporter (PEPT1) is an example of an influx transporter and functions as an uptake transporter for peptidomimetic drugs (71). Other transporters transport molecules from the cell cytoplasm and into the intestinal lumen, which reduces the absorption of the compound. Substances that cross the apical membrane might thus be substrates for apical efflux transporters, and be extruded back into the lumen (68). P-glycoprotein (P-gp), which is a member of the ATP-binding cassette transporters (ABC transporters), is known for decreasing the absorption of many drugs as it is responsible for the efflux of drugs or xenobiotics out of the cell (71, 75).

Transporters might thus greatly influence the absorption, distribution, metabolism and excretion of a number of chemical compounds. Moreover, the specific transport systems that are present are important in determining the overall bioavailability and potential toxicity of ingested chemicals (68).

1.3 Efflux mechanisms as barriers to intestinal absorption

Organisms have several ways of handling with xenobiotics and toxic compounds. The general mechanisms of detoxification involve enzymatic modification or cleavage, alteration of accessibility to targets, decreased membrane permeability and active efflux by membrane transporters (76). The latter system includes P-gp (ABCB1), as well as other proteins of the ABC-transporter family. Increased excretion can result in multidrug resistance, which is a limitation to cancer chemotherapy, treatment with antibiotics and HIV medication. P-gp, and transporters in the subfamilies ABCA, ABCB, ABCC and ABCG, are known to be involved in multidrug resistance (77).

ABC transporters proteins belong to the class of primary active transporters. They are transmembrane transporters and are a part of the ABC superfamily, which consists of structurally related members that have a common intracellular motif that exhibit ATPase

activity (78, 79). ABC transporters utilize a primary source of energy, in form of ATP hydrolysis, to actively transport a broad variety of substrates against their concentration gradient (Figure 4).

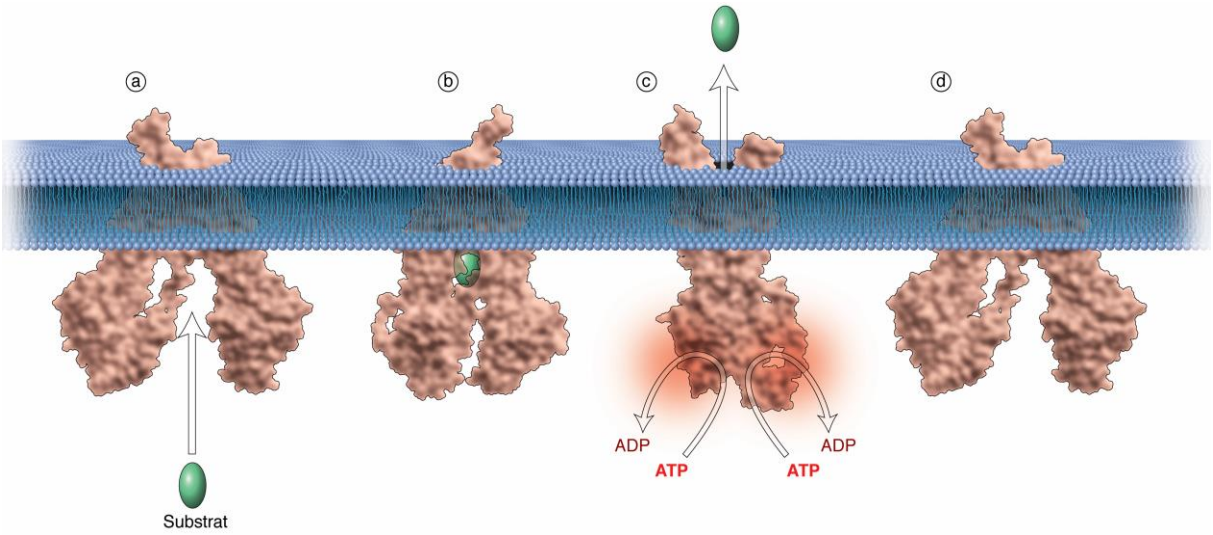

Figure 4: Cycle of transport for ABCC5. a) The transporter recognizes the substrate. b) Substrate binds to the binding site of the transporter and causes conformational change of the transporter. c) Stimulation of ATPases results in ATP hydrolysis, where the hydrolysis of the energy-rich phosphate bond releases energy. Conformational change of the transporter and opening on the extracellular side is caused by energy release and releases the substrate into the extracellular space out from the cell. d) Transporter returns to native state. Figure by Roy Lysså.

More than 40 ABC transporters are encoded in the human genome, and these have been divided into five different subfamilies based on phylogenetic analysis: ABCA, ABCB, ABCC, ABCD and ABCG (80). Members of ABC transporters are involved in a range of different functions, among these are uptake of nutrients, transports of ions and peptides, cell signaling and the extrusion of xenobiotics and toxic compounds (81). Though every transporter has its own substrate specificity, ABC transporters transport a wide range of substrates, such as small inorganic and organic molecules, ions, sterol, sugars, amino acids, vitamins, lipids, xenobiotics and larger molecules (77, 82).

The functional unit of ABC transporters consists of two ATP-binding domains (nucleotide-binding domains, NBDs) and two transmembrane domains (TMDs) (Figure 5).

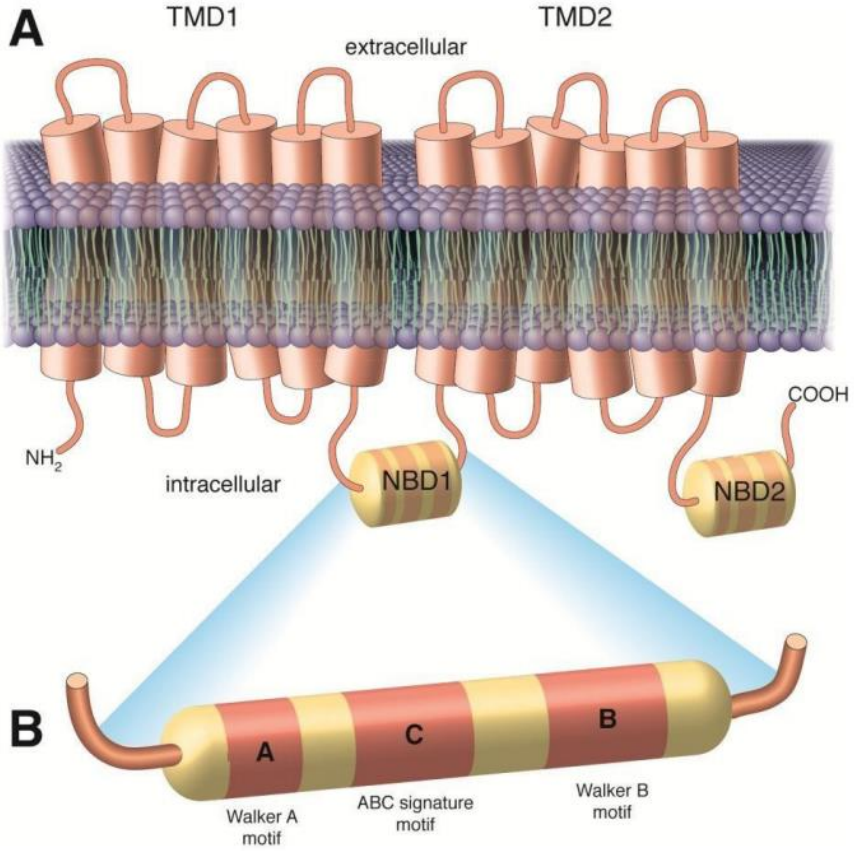

Figure 5: General structure of the ABCC-transporter, showing the extracellular transmembrane domains and intracellular nucleotide binding domains consisting of walker motifs. Figure by Roy Lyså.

1.3.1 P-glycoprotein

P-gp was identified in 1976, and initially described as a 170-kDa surface glycoprotein present in ovary cells of Chinese hamster, resistant to colchicine, a natural drug compound (83). P-gp was the first characterized human ABC transporter and belongs to the subfamily ABCB. It is encoded by the multidrug resistance gene (MDR1), and classified as multidrug resistance-associated protein 1, or ABCB1 (84). Structurally, P-gp is composed of two ATP-binding domains that are located on the intracellular side of the protein. The overall topology is divided into transmembrane domain 1 (TMD1) – nucleotide-binding domain 1 (NBD1) – transmembrane domain 2 (TMD2) – nucleotide-binding domain 2, as shown in Figure 5. The Walker A or phosphate binding loop, and Walker B motifs, are located in the nucleotide-binding domains, while the transmembrane domains contribute to the translocation events of the substrate, including recognition, translocation and release (79).

P-gp has a broad substrate specificity and mediates the active transport of a variety of unrelated lipophilic and amphiphilic substrates, and often chemotherapeutic drugs (77, 79). The overexpression of P-gp in tumor cells can lead to multidrug resistance, which is a major obstacle in cancer therapies (85). Modulators of P-gp, which are known to inhibit active drug efflux and restore drug sensitivity in multidrug resistant cells are, amongst others, verapamil and quinidine (75). P-gp is ubiquitously expressed at lower levels, however, in epithelia in several organs and organ systems such as intestinal enterocytes in the gastrointestinal tract, hepatocytes in the liver, pancreas, proximal renal tubule in the kidney, in addition to endothelial cells of the brain, testes, and adrenal glands, it is expressed at higher levels (75, 86). Thus, P-gp can effect oral bioavailability, renal clearance, and brain penetration of chemicals that are substrates for this transporter (75).

In the gastrointestinal tract, P-gp is located in the apical, or luminal, membrane of the intestinal enterocyte, and induces basolateral to apical efflux of xenobiotics. The physiological role of P-gp as a detoxifying system has been suggested as it is perfectly situated to secrete foreign and potentially toxic compounds and xenobiotics that enter the body through ingestion and thereby limit their absorption (44, 75, 87, 88). Compounds already in the blood might undergo blood-to-intestinal lumen secretion that is facilitated by transporters (68).

Previous studies have suggested that environmental toxicants can interact with transporter proteins, such as P-gp (76, 89-95). Toxicants have been shown to be poorly transported, but the interaction has led to inhibition of the transporter function. Of concern is that this inhibition reduces the efficacy of the transport, sensitizing animals and humans to toxic chemicals that would otherwise be subjects for efflux (91). Experimental studies determining the effects of environmental toxins on human transporter function is therefore of high importance.

1.4 Cell culture and the Caco-2 cell line

Human cell cultures are an extensively used technique, which enables studying cellular and molecular processes *in vitro* (96). The initial culture derived from *in vivo* material is known as primary culture (96). Although primary cultures are preferred when studying normal

physiology, as they are more similar to the original tissue, their lifespan is rather limited. When the growth of the culture progresses beyond the primary culture, it results in a cell line, which can provide a renewable source of material for a study (96). Established cell lines are widely used in research because of several advantages, such as cost-effectiveness, easy use, unlimited supply of material, and pure population of cells which gives reproducible results. Cell lines used should thus display and maintain functional features as close to primary cells as possible (97).

The Caco-2 cell line is derived from human epithelial colorectal adenocarcinoma cells and is the most common and extensively characterized *in vitro* model utilized for investigation and prediction of intestinal drug absorption (88, 98, 99). Although the cell line has cancerous origin as the cells are derived from colon adenocarcinoma, Caco-2 cells have the ability to imitate normal physiology and are similar to enterocytes in the small intestine (100).

Caco-2 cells have the intrinsic ability to undergo spontaneous enterocytic differentiation when grown to confluence under appropriate culture conditions. This involves processes like cell polarization, formation of tight junctions that separate the apical and basolateral surfaces of the plasma membrane, as well as progressive maturation leading to morphological changes like the development of the brush-border (100-102). After 21 days in culture, the Caco-2 monolayer is considered fully differentiated and polarized and portrays functional and morphological similarities to normal intestinal enterocytes, with well-developed tight junctions and brush border (100-102).

The Caco-2 cell model is a complex biological model and encompasses the pathways that are involved in intestinal absorption, i.e. paracellular and transcellular passive diffusion, carrier-mediated transport and vesicular transport. This allows the study of absorption mechanisms of drugs in controlled conditions (102, 103).

Fully differentiated Caco-2 cells express brush border enzymes, such as some cytochrome isoenzymes and phase II enzymes, and several active transport systems located both at the apical and the basolateral compartments, as in the walls of the intestine (86, 102). The active transport systems include a range of uptake (PepT1, HPT1, OATP2B1, OCTN2 and OCT1-3) and efflux (P-gp, MRP2 and BCRP) transporters (75). Other transport systems expressed in the Caco-2 cell line model include MDRP1-6, MCT1 and PepT1 (88).

The apparent permeability coefficients determined by the Caco-2 cell line model has shown good correlation with the in vivo absorption of orally administered drugs in humans, thus, the model has become a gold standard for intestinal permeability research (98). The model is widely accepted by both the pharmaceutical industry and by regulatory authorities, and is also used to assess the transport of drug candidates and lead compounds (75, 98). Moreover, the Caco-2 cell model is also valuable in the identification of substrates or inhibitors of drug transporters and can be used to screen conventional drugs and new chemicals for potential drug-drug interactions (88, 104). Digoxin is a well-known substrate of P-gp and is often used to assess transporter-mediated transport and inhibition of the Caco-2 permeability assay (104, 105).

2 Background for the project

PFAS have received great amount of attention due to their ubiquitous occurrence, persistence in the environment and resistance to biological degradation. PFAS are used in a wide range of consumer products surrounding us in our daily lives, and some of the analogues have been detected in wildlife and humans around the globe. Questions have been raised concerning toxicity to humans, as PFAS have been associated with a range of adverse effects in humans and animal models. PFOS and PFOA are the most studied PFAS, however, less attention has been given to the shorter chain PFAS, such as PFBS. Previously published studies have shown that PFAS can interact with and alter the activity of P-gp in different model organisms, however, few studies are published on the effects of PFAS on human P-gp. Potential interactions or inhibition of P-gp by PFAS could reduce the efficacy of the transport, sensitizing animals and humans to toxic chemicals that would otherwise be subjects for efflux. Experimental studies determining the effects of PFAS on human P-gp function is therefore of high importance.

There is little knowledge available on how and whether PFAS, upon entering the body by ingestion, are transported across the human intestinal enterocytes, and whether these are substrates for active efflux by P-gp. It is thus of importance to establish whether P-gp might be involved in the active efflux of certain PFAS, thereby protecting the body from the potential toxicity of PFAS. The Caco-2 cell line model has been widely used to study drug-drug interactions and identification of substrates or inhibitors of transporters, and in this study, the model will be used to investigate the effects of PFOS, PFHxS and PFBS, on P-gp. In addition, it will be used to examine if these PFSAs might be substrates for P-gp themselves.

3 Aims of the study

- Identify whether PFOS, PFHxS or PFBS are inhibitors/modulators of P-glycoprotein
- Examine whether the carbon chain length of the individual PFAS affect their potential to inhibit or P-gp
- Identify whether PFOS, PFHxS or PFBS cross the monolayer of Caco-2 cells
- Examine whether PFOS, PFHxS and PFBS themselves are substrates of active efflux by P-gp

4 Materials and methods

4.1 Reagents and solutions

4.1.1 Reagents

Table 1. Reagents

Reagent	**Manufacturer**	**Catalogue number**
Dulbecco's Modified Eagle's Medium – high glucose	Sigma-Aldrich	D5796
Trypsin-EDTA solution 0.25 %	Sigma-Aldrich	T4049
MEM Non-essential Amino Acid Solution (100x)	Sigma-Aldrich	M7145
Fetal Bovine Serum	Sigma-Aldrich	F7524
Penicillin-Streptomycin	Sigma-Aldrich	P0781
Dulbecco's Phosphate Buffered Saline	Sigma-Aldrich	D8537
Hank's Balanced Salt Solution	Sigma-Aldrich	H8264
HEPES	Sigma-Aldrich	H4034
HEPES potassium salt	Sigma-Aldrich	H0527
Digoxin	Sigma-Aldrich	D6003
D3-Digoxin	Toronto Research Chemicals	D446577
Mannitol	Sigma-Aldrich	M4125

D-Mannitol-d8	Toronto Research Chemicals INC	M165002
Perfluorooctane sulfonic acid, potassium salt (PFOS), 97 % purity	ABCR	AB120443
Tridecafluorohexane-1-sulfonic acid potassium salt (PFHxS), >89 % purity	Merck/Sigma-Aldrich	50929-10G-F
Potassium nonafluoro-1-butanesulfonate (PFBS), 98 % purity	Merck/Sigma-Aldrich	294209-10G
PFAS ISTD, 99 % purity L-PFBS L-PFHxS L-PFOS	Wellington Laboratories	In-house mixture
PFAS RSTD, Perfluoro-3,7-dimethyloctanoic acid; 97% Perfluoro-3,7-dimethyloctanoic acid; 97% Perfluoro-3,7-dimethyloctanoic acid; 97% Perfluoro-3,7-dimethyloctanoic acid; 97%	ABCR	AB134739

4.1.2 Solutions

Preparations for electron microscopy

- 4X PHEM Buffer:
  36,28 g PIPES buffer, 13 g HEPES buffer, 7,6 g EGTA, 1,98g $MgSO_4$, pH to 7.0 with 10 M KOH
- Malachite green fixative:
  1 % malachite green, 25 % glutaraldehyde, 2x PHEM buffer, 16 % formaldehyde, ddH_2O
- 1x Fixative:
  0.5 % glutaraldehyde, 4 % formaldehyde, 0.05 % malachite green, 0.1 M PHEM buffer
- 4 % Potassium ferricyanide (K3Fe(CN)6)
- 4 % Osmium tetroxide solution ((OsO4 (aq))
- 1 % Tannic acid solution
- 1 % Uranyl acetate
- EPON resin

Preparations for transport studies

- Stock solutions of PFAS test substances were prepared in 96% ethanol and Milli-Q water (1:1) at following concentrations:
  PFOS 52,88 mM
  PFHxS 40,24 mM
  PFBS 40,18 mM
- Digoxin 150 µM stock solution dissolved in 96 % ethanol

PFAS stock solutions were diluted with HBSS to following concentrations, where the percentage of ethanol did not exceed 0.2 %

- PFOS 1 mM
- PFHxS 1 mM
- PFBS 1 mM

Preparation of donor solutions for transport studies with PFAS and digoxin

- HBSS with 20 mM HEPES, 1 µM digoxin, PFOS (0,001 µM, 0,01 µM, 0,1 µM, 1 µM and 10 µM)
- HBSS with 20 mM HEPES, 1 µM digoxin, PFHxS (0,001 µM, 0,01 µM, 0,1 µM, 1 µM and 10 µM)
- HBSS with 20 mM HEPES, 1 µM digoxin, PFBS (0,001 µM, 0,01 µM, 0,1 µM, 1 µM and 10 µM)

Solvents for digoxin extraction procedure for LC-MS

- 50 mmol/L ammonium formate, adjusted to pH 3.1 with formic acid
- 0.2 mol/L ammonium carbonate buffer, adjusted to pH 9.3 with ammonia
- Ethylacetate/heptane/dichloromethane (3:1:1)

Solvents for analytical procedures on LC-MS

- Methanol, MS grade
- Acetonitrile, MS grade

Preparation of donor solutions for PFAS transport across Caco-2 monolayer

- HBSS with 20 mM HEPES, 1 µM of PFOS
- HBSS with 20 mM HEPES, 1 µM of PFHxS
- HBSS with 20 mM HEPES, 1 µM of PFBS

Preparation of donor solutions for PFAS transport across Caco-2 monolayer with inhibitors

- HBSS with 20 mM HEPES, 1 µM PFOS and verapamil (0,01, 0,1, 1, 10 and 100 µM)
- HBSS with 20 mM HEPES, 1 µM PFHxS and verapamil (0,01, 0,1, 1, 10 and 100 µM)
- HBSS with 20 mM HEPES, 1 µM PFBS and verapamil (0,01, 0,1, 1, 10 and 100 µM)
- HBSS with 20 mM HEPES, 1 µM PFOS and quinidine (0,01, 0,1, 1, 10 and 100 µM)
- HBSS with 20 mM HEPES, 1 µM PFHxS and quinidine (0,01, 0,1, 1, 10 and 100 µM)

- HBSS with 20 mM HEPES, 1 μM PFBS and quinidine (0,01, 0,1, 1, 10 and 100 μM)

4.1.3 Other equipment

- Microbiological safety cabinet Class II, Thermo Electron Industries
- Transwell® Polycarbonate Membrane Insert, 3413 Corning Life Sciences
- Tissue culture plate, 6 well, 353046 Falcon
- MilliCell®-ERS, Millipore
- Contess™ - automated cell counter, Invitrogen
- In-Vitrocell CO_2 Incubator, CuVerro Nu-5810, NuAire
- Fume hood
- Centrifuge Kubota 5100, swinging bucket
- Centrifuge Minor, MSE
- RK 20 RKS Refrigerating circulating bath chiller, Lauda Brinkmann
- Specially constructed CO_2 incubator for use inside the fume hood
- Specially constructed nitrogen evaporator
- Waters Xevo TQ-S UPLC tandem mass spectrometry system
- Waters UPLC-tandem mass spectrometry system
- Transmission electron microscope, Hitachi HT7800
- Scanning electron microscope, ZEISS ZIGMA
- Ultra microtome Leica EM UC6
- Gold/palladium-sputter coater, Leica EM ACE600
- Laboratory microwave oven, Pelco BioWave Pro 36500
- Critical point dryer, Leica EM CPD300
- IncuCyte S3, Sartorius

4.2 Experimental procedure

4.2.1 Cell culture

Human intestinal Caco-2 cell line was previously obtained from American Type Culture Collection (ATCC) and stored in liquid nitrogen. The cells were maintained in DMEM supplemented with 10 % fetal bovine serum, 1 % non-essential amino acids and 1 % penicillin-streptomycin and incubated in CuVerro Nu-5810 CO_2 incubator at 37 °C in a humidified atmosphere with 5 % CO2. The cells in this study were used within 10 passages.

All cell work was performed aseptically and under sterile conditions in a laminar flow hood to avoid any infection and contamination of the culture. To exclude infection of the cell culture, microscopic monitoring was performed frequently where the cell density and morphology was examined. The batches of cells used in the study were tested for mycoplasma beforehand and were free of mycoplasma contamination.

Expansion of the cell culture

The cells were frozen and thawed according to established procedures. The ampullas containing Caco-2 cells were removed from the liquid nitrogen tank and thawed at room temperature. Each ampulla was transferred to their corresponding centrifuge tube. 10 mL of preheated medium was added dropwise while carefully stirring the tube to prevent osmotic shock. The tubes were centrifuged at 700 rpm for 5 minutes using a MSE Minor centrifuge. The supernatant was removed by aspiration and the cells were then resuspended in fresh media. This is done to remove DMSO prior to seeding the cells in culture flasks, as DMSO might inhibit the proliferation of some cell lines. DMSO is a cryoprotectant added to cells prior to freezing, which reduces ice crystal formation within the cells that would otherwise puncture the cell membrane. The cells were then transferred to their corresponding culture flasks, stirred to prevent clustering and placed in the incubator for culturing. The cell line was expanded for a couple of weeks after thawing, while monitoring the growth rate to ensure optimal health before proceeding with further experiments.

The media was changed every second or third day to assure that it was not depleted of nutrients, and to remove any byproducts of cellular metabolism that may be toxic to the

culture as they accumulate. The media was removed by aspiration, and carefully replaced with new, preheated media, without disturbing the cell layer.

When a culture fills the available substrate area, it has reached confluency and requires subculture to maintain a healthy growth. Caco-2 cell culture was subcultured when it reached 70-90 % confluency and split in a ratio that would keep the culture in a logarithmic growth phase. The medium was removed by aspiration, and the cells were washed carefully with preheated phosphate buffered saline (PBS) to ensure removal of remaining media, without disturbing the cell layer. Media is supplemented with serum that contains plasma proteins that act as protease inhibitors, thus, surplus of media could neutralize trypsin, which is a proteolytic enzyme that breaks the cell-cell and cell-substrate attachment, producing a single cell suspension. Trypsin was then added to the cell layer, just enough to cover the surface and incubated at 37 °C for 5 minutes or until the cells dissociated from the surface. Fresh, preheated media was added to the culture to neutralize the action of trypsin and resuspended to prevent cell clustering. The suspension was split at a suitable ratio.

4.2.1.1 Proliferation assay

The growth characteristics of the cell line were to be determined to ensure a healthy proliferation pattern of the culture prior to conducting any experiments. Two different batches of caco-2 cells were seeded in a 6 well plate at a density of $1x10^4$ cells/mL and cultured for 7 days.

Contess™ Automated Cell Counter

The cells were counted using Contess Automated Cell Counter, which performs cells count and viability measurements using trypan blue method of dead-cell staining and advanced image analysis. The culture was brought into a suspension and an aliquot was taken for cell count. The cell suspension was mixed with trypan blue in 1:1 ratio and pipetted onto counting chamber slides which were inserted into Contess.

IncuCyte® S3 Live-Cell Analysis System

The proliferation assay was conducted using IncuCyte® Live-Cell Analysis system. This system enables to conduct real-time, non-invasive, quantitative cell assays and gives a

measure of proliferation in a non-invasive manner, by taking images of the cell culture at a user-defined time schedule. The number of images taken per well is defined by the user. For the proliferation assay, the software automatically acquires and analyzes real-time images of the cells and performs a cell count based on phase area confluence. As a result, a growth curve could be generated. Figure 6 figure shows the user-defined plate, with the black dots representing images taken by IncuCyte of each well.

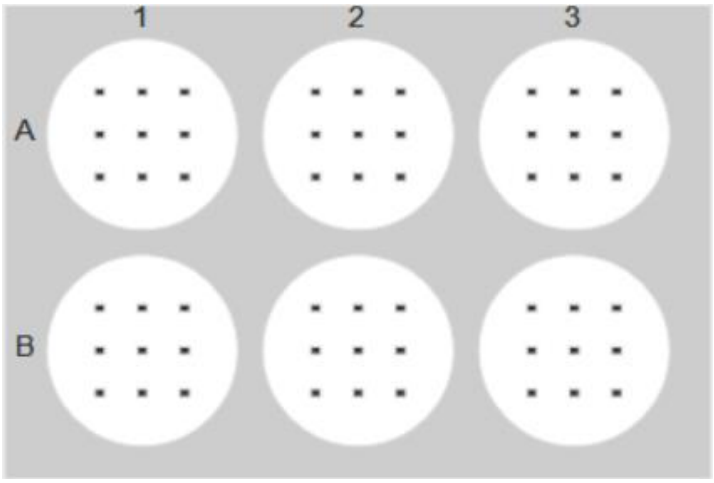

Figure 6: The figure is scan pattern taken from the IncuCyte software during the schedule of a new assay and shows the setup of a 6 wells plate used for the proliferation assay in the IncuCyte. The placement and number of the black dots in each well represent the images taken by IncuCyte.

4.2.2 Caco-2 transport studies – methodological considerations

Caco-2 cells are cultured on inserts with a semi-permeable membrane, thus, establishing an apical and a basolateral side, resembling the normal physiology of the intestinal lumen and the blood side of the small intestine. The two chambers are connected only by the monolayer of cells growing on the membrane.

During Caco-2 transport experiments, the compounds of interest are added to either the apical or the basolateral chamber, while the complementary chamber is left with fresh transport buffer, to stimulate the influx or efflux of the compounds across the monolayer. In a bidirectional transport study, the transport of compounds of interest is studied both in the apical to the basolateral direction, and in the basolateral to the apical direction.

The quantification of compounds in Caco-2 permeability assays has been considerably improved by the implementation of liquid chromatography mass spectrometry (LC-MS) and

LC-tandem mass spectrometry (LC-MS/MS) an by its higher sensitivity compared to the use of radioactive labelling and quantification by scintillation.

4.2.3 Mass spectrometry – methodological considerations

Mass spectrometry (MS) is a powerful analytical tool used in various disciplines and sub-disciplines within chemistry, biochemistry, physics, and pharmacy, and is used to identify, quantify, and characterize, both endogenous and exogenous compounds (106). The specificity, dynamic range, and sensitivity of the instrument to distinguish between closely related metabolites in a complex matrix, and by these means identify and quantify these metabolites, has made MS an important tool in drug discovery and development. However, MS has a broad application range, and is also of great importance in environmental research, where it can be used to analyze pesticides and a broad range of other environmental toxicants both in environmental and human samples.

The most common separation and sample delivery methods include gas chromatography (GC) and liquid chromatography (LC). The choice of the separation and sample delivery methods depend on the physiochemical properties of the targeted analyte. LC or GC separates the sample components and introduces them to an ionization source coupled to the mass spectrometer. A mass spectrometer can only analyze a molecule after converting the molecule to a gas-phase ion. These ions are then separated in the mass spectrometer, and detected and measured according to their mass-to-charge ratio (m/z) For this to happen, an electrical charge is applied to the molecules, and the resultant flux of electrically charged ions can be converted into a proportional electrical current that can be read by a data system, converted to digital information, and be displayed as a signa (e.g. mass spectrum, transition, peak, etc.) The data may be used to provide information about the molecular weight of the analyte, identity and quantity of specific target components in the sample.

4.2.4 Culture of Caco-2 cells on permeable membrane inserts

The cells were seeded into 6.5 mm Costar Transwell 24-well cluster plate with 0.4 μm pore polycarbonate membrane inserts, at a density of $1x10^5$ cells/mL and cultured for 21-28 days.

To improve cell attachment to the membrane, the plates with membrane inserts were incubated with the recommended volume of medium at 37 °C for at least 1 hour prior to

seeding. The medium was first added to the plate well, followed by the inside of the insert. The inserts have three openings for standard pipette tips that allow for easy access to the lower compartment, as seen in Figure 7.

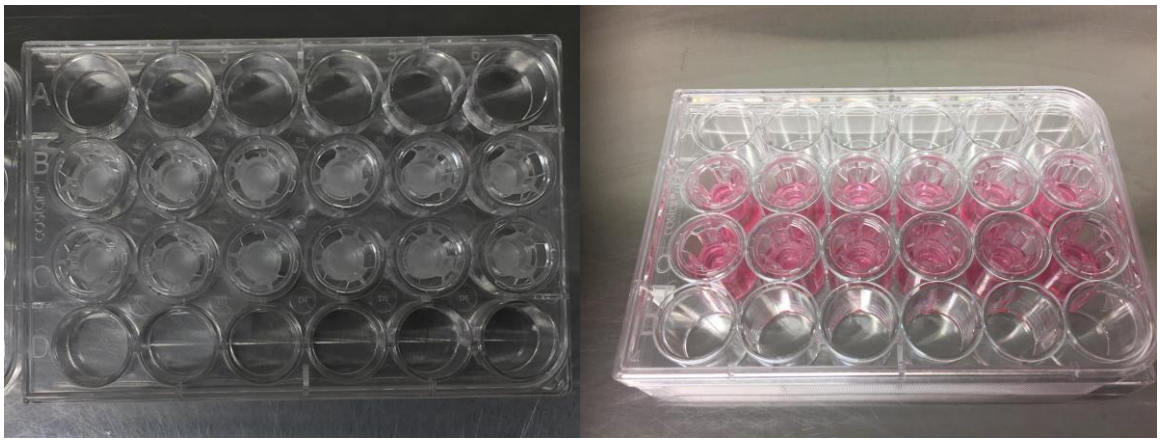

Figure 7: Costar Transwell 24-well cluster plate with 0.4 µm pore polycarbonate membrane insert without and with media, showing the membrane inserts and the openings in the insert for easy access to the lower compartment.

After the initial equilibrium period, the medium inside the insert was replaced with fresh medium containing cell suspension of desired concentration and the plate was returned to the incubator. The media was changed every other or third day. It was removed by aspiration and exchanged with new, with great caution, to not disturb the cell layer or puncture the membrane.

4.2.4.1 Transepithelial electrical resistance (TEER)

The cell layer growing on polycarbonate membrane inserts is not visible in light microscope. Thus, Millipore Millicell®-ERS was used to examine the transepithelial electrical resistance (TEER) across the monolayer, which is a measure of cell monolayer health and cell confluence. The Millicell®-ERS (Electrical Resistance System) uses alternating current to measure the membrane potential and resistance of epithelial cells in culture. The Millicell-ERS is equipped with small chopstick electrodes (Figure 8), and TEER is measured by immersing the longer electrode in the basolateral chamber and the shorter electrode inside the insert. The measurements were done carefully, without touching the cell layer.

Figure 8: The Millicell®-ERS with connected electrodes used for measurements of the transepithelial electrical resistance (TEER).

Before using the Millicell®-ERS, the system was tested, and the electrodes were equilibrated according to the user guide. Before each use, the electrodes were sterilized according to manufacturer's manual in order to avoid contamination of the cell culture.

The resistance was first measured in two inserts without cells, which served as blanks. The average value of the blanks was later subtracted from the sample-well resistance. R_{sample}-R_{blank}=$R_{monolayer}$. To correct for the area covered by the cell monolayer, the product of the area and the resistance was calculated.

4.2.5 Quality control of Caco-2 cell morphology by electron microscopy

Caco-2 cells undergo a spontaneous differentiation into enterocyte-like cells and obtain a distinct morphology with microvilli and tight junctions. Thus, prior to conducting transport experiments, a quality control of the cell monolayer was performed to assess whether the cells were fully differentiated after 21 days in culture. The morphology of Caco-2 cells was examined with help of scanning and transmission electron microscopy (SEM and TEM). TEM was also used to examine whether the cells grow in a monolayer.

Caco-2 cells were seeded into a 24 well Corning Transwell with 0.4 μm pore polycarbonate membrane insert, at densities of $1 \cdot 10^5$ cells/mL, $2 \cdot 10^5$ cells/mL and $3 \cdot 10^5$ cells/mL and cultured for 21 days.

The entire fixation process was performed in Corning Transwell plates with inserts. The detailed fixation protocol is provided in Table 1 in the appendix.

General principles of electron microscopy

There are two basic types of electron microscopes, SEM (scanning electron microscopy) and TEM (transmission electron microscopy) and there are some fundamental differences in how these instruments work and images they produce. While the transmission electron microscope projects electrons through a very thin slice of specimen to produce a two-dimensional image, the scanning electron microscope uses a spot of electrons that scans the surface of a given specimen and generates secondary electrons that are detected by a sensor, to produce a three-dimensional image of the surface of a given specimen.

During preparation of specimen for electron microscopy, every step of the procedure is critical for the outcome, thus, the specimen must be processed according to prescribed methods and with understanding of the process.

The preparation for electron microscopy can be divided into several major steps: primary fixation, washing, secondary fixation, dehydration, critical point drying or resin infiltration. There are, however, some differences regarding sample preparation for TEM and SEM that will be mentioned in more detail later.

Fixation procedure

The cells were fixated to preserve the structure of the living tissue and prevent alterations in the cell structure caused by cellular decomposition after tissue death. The fixative used combined glutaraldehyde with low concentrations of formaldehyde, and osmium tetroxide that is reduced with ferrocyanide. Formaldehyde penetrates the tissue more rapidly than glutaraldehyde, however, it does not form covalent bonds and can thus be reversible. Glutaraldehyde, on the other hand, penetrates the tissue slowly, but in contrast to

formaldehyde, it forms covalent bonds and fixates the tissue irreversibly. Glutaraldehyde cross-links proteins through amine groups.

Osmium tetroxide works as a secondary fixative by reacting primarily with lipids moieties, such as the cell membrane. Osmium tetroxide is also involved in stabilization of many cell components. It is thought that osmium tetroxide oxidizes unsaturated fatty acids and is reduced to black metallic osmium. The reduced heavy metal adds density and contrast to the biological tissue. Because of the high molecular weight (254.2), it is effective in scattering electrons and is therefore an important stain that dyes tissues intensely black after exposure. The penetration rate of osmium tetroxide is slower than for glutaraldehyde, and compact tissues will not be penetrated more than 0.5 cm in an hour, and little additional penetration occurs afterwards.

During fixation, it was important to keep the osmolarity within the physiological range, to prevent osmotic shock of the cells that could result in either swelling or shrinking of tissue. Without a buffering system, the pH would lower drastically during the fixation process, and could lead to formation of artifacts. PHEM buffer, containing the organic buffers PIPES and HEPES was used as buffer during the fixation process.

To remove the remaining unreacted glutaraldehyde within the cells, the cells were washed with double-distilled water. Otherwise, remaining aldehydes would be oxidized by osmium tetroxide.

Samples were prepared both for scanning and transmission electron microscopy. In the end of the fixation process, ethanol dehydration series were performed with 25%, 50%, 75%, 95% and 100% ethanol, thus, replacing the water in the cells with a fluid that can act as a solvent between the hydrophobic embedding media and the aqueous environment of the cell. For scanning electron microscopy, the subsequent step after the dehydration series was the critical point dryer. After the dehydration, the specimen intended for SEM were mounted on a metal stub, using silver-containing glue for increased conductivity. These were coated with a mixture of gold and palladium for enhanced conductivity.

Specimen intended for transmission electron microscopy were infiltrated in resin. Resin infiltration involved gradual replacement of ethanol with resin. Excess resin was removed,

and the samples were put in the oven at 50 °C overnight for polymerization. Then, the specimen for TEM were cut into cross-sections using a ultramicrotome.

The microscopy was performed by the Randi Olsen and Tom-Ivar Eilertsen at the Advanced Microscopy Core Facility at UiT The Arctic University of Norway.

4.2.6 Quality control of the Caco-2 monolayer by confocal microscopy

Additionally, a quality control of the Caco-2 cells was performed by confocal microscopy, to ensure that the cells were growing in a monolayer. The procedure was performed by Kenneth Bowitz Larsen at Advanced Microscopy Core Facility, UiT The Arctic University of Norway.

4.2.7 PFAS background identification in equipment and solutions

Since different per- and polyfluorinated compounds are often used in industry and manufacturing, all the equipment and solutions to be used in transport studies were analyzed for PFAS background. This was done to control the exposure of the cells to PFAS during the transport assays. In this manner, we could be certain that the PFAS detected by means of analysis of MS originate from cellular transport and not from plastic equipment used in the experiment or reagents contaminated during production processes.

The solutions to be tested were transferred to vials using PFAS-free pipette tips and diluted with MS-grade methanol in a 1:1 ratio. The equipment was thoroughly rinsed with MS grade methanol, which then was transferred to vials for further LC-MS-analysis.

4.2.8 Precautions and safety measures when working with PFAS

Precautions were taken when handling PFOS, PFHxS and PFBS solutions in order to avoid contamination of laboratory areas and carry over from high to low exposure experiments. The stock and incubation solutions were prepared by senior scientist and special advisor Sandra Huber at the Environmental Pollutant Laboratory, University Hospital of Northern Norway. Glass vials containing these solutions were stored in a box wrapped in aluminum foil to prevent contamination of surfaces in the laboratory. Weight control was performed before and after handling of the solutions in order to control for possible evaporation during storage. Glass vials were opened only in the fume hood designated for work with environmental toxicants, and with great caution, to avoid spillage and contamination. The fume hood was covered with aluminum foil, which was exchanged after each transport experiment. Personal

protective equipment was used when handling PFOS, PFHxS and PFBS, and gloves were frequently changed. The waste bin was placed inside the fume hood to avoid contamination of the air and laboratory, as PFOS, PFHxS and PFBS are semi-volatile substances, but also due to personal safety reasons since especially PFOS is known to be toxic.

4.2.9 Study of digoxin transport across the Caco-2 cell monolayer

PFOS, PFHxS and PFBS were to be characterized as potential inhibitors of P-gp. Two different batches of Caco-2 cells were used, and five time-independent studies were conducted.

Caco-2 cells were cultured on Transwell permeable membrane inserts and used for transport studies between 21 and 28 days of culture. The functionality of the monolayer was evaluated by the measurement of the transepithelial electrical resistance across the monolayer over a 7 to 28 days period. The membrane integrity was in addition assessed prior to transport study, and the wells showing transepithelial electrical resistance (TEER) values above 250 Ω cm^2 were selected.

Per- and polyfluorinated compounds are known to bind to albumin, which is the most abundant serum protein. Serum proteins present in medium could interact with the experimental compounds and reduce the free fraction of PFAS available in the donor solution. Thus, the inserts and the wells were washed with preheated Hank's balanced salt solution (HBSS) three times prior to the transport experiment to remove residual medium and serum.

All proceeding work was performed in a fume hood, to minimize PFAS contamination of the air, laboratories, and equipment, as these compounds are semi-volatile. As the volume of a solution increases with increased temperature, the glass vials containing the incubation solutions were room tempered to ensure that the correct volume and concentration was added to the cells. Moreover, the glass vials containing the PFOS, PFHxS and PFBS solutions were heavily vortexed before use, as these compounds tend to adsorb to surfaces. This step ensured that the desired concentration of the compounds was maintained in the solution.

To determine the effect of increasing concentration of PFOS, PFHxS and PFBS on the transport of digoxin by P-gp, a bidirectional transport study was conducted. Caco-2 monolayers cultured on Transwell permeable membrane inserts were incubated with 1 μM

digoxin and the desired concentration (0.001, 0.01, 0.1, 1 and 10 μM) of PFOS, PFHxS or PFBS, dissolved in HBSS supplemented with 20 mM HEPES buffer. The control group contained 1 μM digoxin dissolved in HBSS supplemented with 20 mM HEPES buffer. The concentration of 1 μM digoxin was chosen based on previous unpublished studies conducted in the group, which proved the linearity of the transport of 1 μM digoxin across the Caco-2 monolayer over a period of 180 minutes, suggesting that P-gp is saturated by 1 μM over a period of 180 minutes. Each of the compounds, PFOS, PFHxS and PFBS, were incubated on their corresponding plate. The experimental setup is shown in Table 2 below.

Table 2. Experimental setup. Transport study across Caco-2 cell monolayer.

Transport direction	PFAS[1] concentrations (μM) 1 μM digoxin					
A→B	Control	0.001	0.01	0.1	1	10
B→A	Control	0.001	0.01	0.1	1	10
						Blank[2]

1) Separate plate was used for PFOS, PFHxS and PFBS.
2) An insert without cells was used as a blank for TEER measurements

Donor solutions containing digoxin and PFOS/PFHxS/PFBS were added to either the apical compartment (row A→B in Table 2) or basolateral compartment (row B→A in Table 2), while the complementary compartment was left with fresh HBSS. The plates were incubated for 90 minutes at 37 °C and 5 % CO_2. The incubator was placed inside the fume hood and was constructed for this study specifically. It consisted of a Plexiglas cabinet with an attached lid. Three heating plates connected to a water bath were placed in the cabinet to maintain the desired temperature of 37 °C. Moreover, the cabined was connected to constant air flow and flow of CO_2. The level of CO_2 was adjusted automatically by the built-in CO_2 sensor to maintain 5 %. To fulfil the requirements for the physical environment, the lid was tightly closed during incubation. After the incubation, aliquots were taken from the recipient compartments, proceeding with the extraction procedure for digoxin.

4.2.9.1 Digoxin extraction procedure

50 µL of the sample was mixed with 50 µL of digoxin internal standard and 25 µL 0.2 M ammonium carbonate buffer in extraction tubes. The samples were extracted with 1 mL ethylacetate/heptane/dichloromethane (3:1:1) by rough shaking by hand for at least one minute. After centrifugation at 4640 g (Kubota 5100) the organic phase was transferred to a new extraction tube and evaporated to dryness under nitrogen. The residue was then dissolved in 100 uL cold acetonitrile/water (50:50) and mixed thoroughly using a vortex. After centrifugation at 4640 g (Kubota 5100), the solution was transferred to polypropylene vials for LC-MS analysis.

Standard solutions of digoxin of 1024, 512, 256, 128, 64, 32, 16 and 8 nM were prepared simultaneously and extracted by the same method as described above.

4.2.9.2 LC-MS analysis of digoxin

Samples were analysed by LC-MS/MS using a Waters Acquity UPLC I-Class FTN system with an autosampler and a binary solvent delivery system interfaced to Waters Xevo TQ-XS benchtop tandem quadrupole mass spectrometer. The procedures for instrumental analysis have previously been described in detail (107). The mass spectrometer was operated in positive electrospray ion mode (ES+). The system was controlled by MassLynx version 4.2 software. The analysis was performed by associate professor Ole-Martin Fuskevåg.

4.2.10 Transport of PFOS, PFHxS and PFBS across the Caco-2 monolayer

During a pilot study, it was discovered that PFOS crossed the Caco-2 cell monolayer. It was thus of interest to investigate further whether PFOS, PFHxS and PFBS are substrates for P-gp and actively transported across Caco-2 monolayer. Three time-independent studies were performed.

Prior to the study, TEER was assessed and the cells were washed with HBSS as described in chapter 4.2.9. Caco-2 cell monolayers were incubated with either PFOS, PFHxS or PFBS of the desired concentration (0.001, 0.01, 0.1, 1 and 10 µM) dissolved in HBSS supplemented with 20 mM HEPES buffer, as described above for the bidirectional transport study with digoxin across the Caco-2 monolayer. After 90 minutes of incubation, aliquots were taken from the recipient compartment and stored in vials at -20 °C for further analysis.

The samples were diluted prior to LC-MS analysis to avoid contamination of the extremely sensitive instrument. Too high PFAS concentrations could give a carry-over effect on subsequent samples and contaminate the instrument, making it unable to detect lower PFAS concentrations in the future. The samples were diluted with methanol and Milli-Q water, and internal standard (ISTD) and external standard (RSTD) were added. The exact dilution procedure is provided in Table 2 in the appendix.

4.2.11 Transport of PFOS, PHFxS and PFBS across the Caco-2 monolayer with P-glycoprotein inhibitors

To investigate whether P-gp is involved in the active efflux of PFOS, PFHxS, and PFBS, a bidirectional transport study with known P-gp inhibitors, quinidine and verapamil, was conducted. Three time-independent experiments were performed. A pilot study was carried out with 1 μM PFOS, which showed that PFOS crossed the Caco-2 cell monolayer both in the apical to basolateral direction, and in the basolateral to apical direction. Thus, this concentration was chosen for the subsequent transport studies.

Prior to the experiment, TEER was measured and the cells were washed with preheated HBSS. The transport study was carried out as described in chapter 4.2.9. Caco-2 cell monolayers were incubated with 1 μM of either PFOS, PFHxS or PFBS and the desired concentrations of verapamil and quinidine (0.01, 0,1, 1, 10 and 100 μM) dissolved in HBSS supplemented with HEPES. The control group contained 1 μM of either PFOS, PFHxS or PFBS dissolved in HBSS, supplemented with HEPES buffer, without the addition of P-gp inhibitors. Following the 90-minute-long incubation, aliquots were taken from the receiver chamber and stored in vials at -20 °C. Three time-independent studies were conducted.

Prior to the LC-MS analysis, samples were diluted with methanol and Milli-Q water and ISTD and RSTD was added after the same principle as for experiments without the inhibitors. For details see Table 2 in the appendix.

4.2.12 Time trend of PFAS across the Caco-2 cell monolayer

To prove the linearity of the transport of 1 μM PFOS, PFHxS and PFBS across Caco-2 cell monolayer, a time trend was conducted. Prior to the transport study, TEER was measured and the cells were washed three times with prewarmed HBSS. The transport study was performed as described in chapter 4.2.9, except that the cells were incubated with 1 μM PFOS, PFHxS

and PFBS dissolved in HBSS supplemented with 20 mM HEPES, over a period of 150 minutes at 37 °C. Aliquots were taken from the receiver chamber every 30 minutes, and immediately replaced with the same volume of fresh HBSS and placed back into the incubator for further incubation. The samples were stored in vials at -20 °C for further analysis.

The study was run in parallels for each compound. Prior to LC-MS analysis, the samples were diluted with methanol and Milli-Q water and RSTD and ISTD were added. The dilution scheme is provided in Table 3 in the appendix.

4.2.13 LC-MS analysis of PFAS

PFAS were analyzed by ultrahigh pressure liquid chromatography tandem mass spectrometry (UHPLC-MS/MS). The procedures for instrumental analysis and quantification have previously been described in detail (1). Briefly, the analysis was performed on a Waters Acquity Ultra high pressure liquid chromatography (UHPLC) system, consisting of a binary LC-pump, an autosampler and a column oven, coupled to a Xevo TQ-S MS with an electrospray ionization unit. Electrospray ionization in the negative ion mode was applied for ionization of the analytes and multi-reaction monitoring mode for recording of the specific transitions.

For the quantification of the results, Masslynx with Targetlynx version 4.1 (Waters) was used.

The instrumental analysis and quantification of the results was done by senior scientist and special advisor Sandra Huber at the Environmental Pollutant Laboratory, University Hospital of Northern Norway.

4.2.14 Evaluation of the membrane integrity by mannitol

To investigate the integrity of the membrane after the exposure to PFOS, PFHxS and PFBS, a bidirectional transport study was conducted by the same principle as described in chapter 4.2.8, followed by a transport study with mannitol, carried out in the same manner. Caco-2 cell monolayers were incubated for 90 minutes with PFOS, PFHxS and PFBS of the desired concentrations (0.001-10 μM), dissolved in HBSS supplemented with 20 mM HEPES. The solutions were then discarded and replaced with 55 μM mannitol dissolved in HBSS supplemented by 20 mM HEPES in the donor chamber and fresh HBSS in the recipient chamber and incubated for 90 more minutes. Mannitol is a sugar molecule whose

permeability across the membrane is very low and is thus used as a membrane integrity marker. Aliquots were taken from the recipient chamber and diluted 1:10 with methanol. Mannitol internal standard of 5 µM was added. Standard solutions of following concentrations were prepared: 1024, 512, 256, 128, 64, 32, 16, and 8 nM and diluted similarly as the samples, with the addition of internal standard. The permeability was analyzed using LC-MS/MS.

4.2.15 Statistics

A Shapiro-Wilk test was used to evaluate normally distribution of the data set, and Brown-Forsythe test was used to test equal variance. Comparison of the different groups of the transport study were analyzed by One-Way Analysis of Variance (ANOVA) test followed by a post-hoc Dunnett's test for comparison against the control group. Rank-based ANOVA was used if the normality test failed. Dunn's test was used for comparison against the control group following rank-based ANOVA if the sizes of the treatment groups were unequal. Differences were considered significant at $p < 0.05$.

4.2.16 Data analysis

The transport rate of the test compound is usually expressed as apparent permeability coefficient. The apparent permeability of digoxin, as well as PFOS, PFHxS and PFBS was calculated using the following equation:

$$P_{app} = Vr \cdot \frac{dC}{dt} \cdot \frac{1}{A \cdot C_0}$$

where Vr is the volume in the recipient compartment, dC/dt is the slope of the cumulative concentration of the compound in the receiver compartment over time, A is the surface area of the membrane, and C0 is the initial concentration of the compound in the donor chamber.

The efflux ratio (ER) was calculated by the formula:

$$ER = P_{app\ (BA)} / P_{app\ (AB)}$$

where BA represents the apparent permeability of digoxin in the basolateral to apical direction, and AB represents the apparent permeability in the apical to basolateral direction. An efflux ratio above 2 is an indicator of active efflux.

5 Results

In this study, three perfluoroalkyl sulfonic acids of different carbon chain length, PFOS, PFHxS and PFBS, were investigated for their effect on the transport of digoxin, a P-gp substrate. Additionally, the transport of these perfluoroalkyl sulfonic acids themselves, was studied across the Caco-2 cell monolayer. Moreover, it was investigated whether PFOS, PFHxS and PFBS are substrates for P-gp, and whether P-gp is involved in the active efflux of these substances. The transport of PFOS, PFHxS and PFBS was thus studied with and without well-known P-gp inhibitors, quinidine and verapamil.

5.1 Quality control of cell growth

5.1.1 Proliferation assay

A proliferation assay was conducted using IncuCyte to ensure that the cell line had a healthy growth rate prior to conducting further experiments. The results of the proliferation assay are shown in the graphs below. The graphs are generated by the Incucyte software and show phase area confluence versus time in days, as seen in Figure 9 and 10.

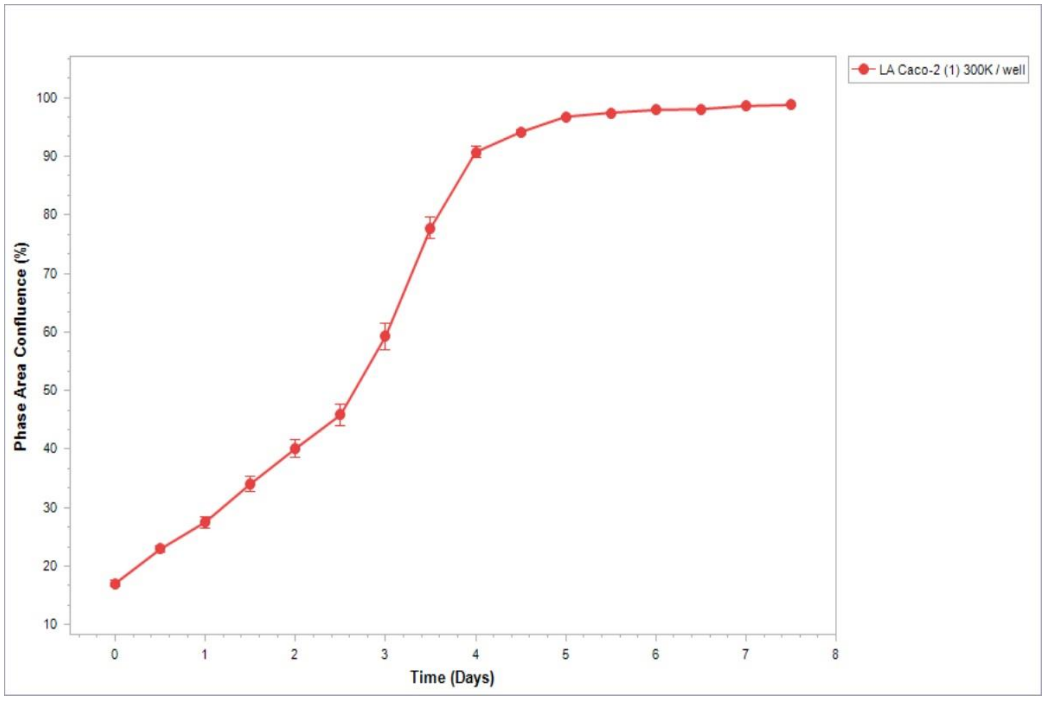

Figure 9: Growth curve of the Caco-2 cell line (batch 1) generated by IncuCyte. The proliferation of the cells is shown as phase area confluence versus time in days.

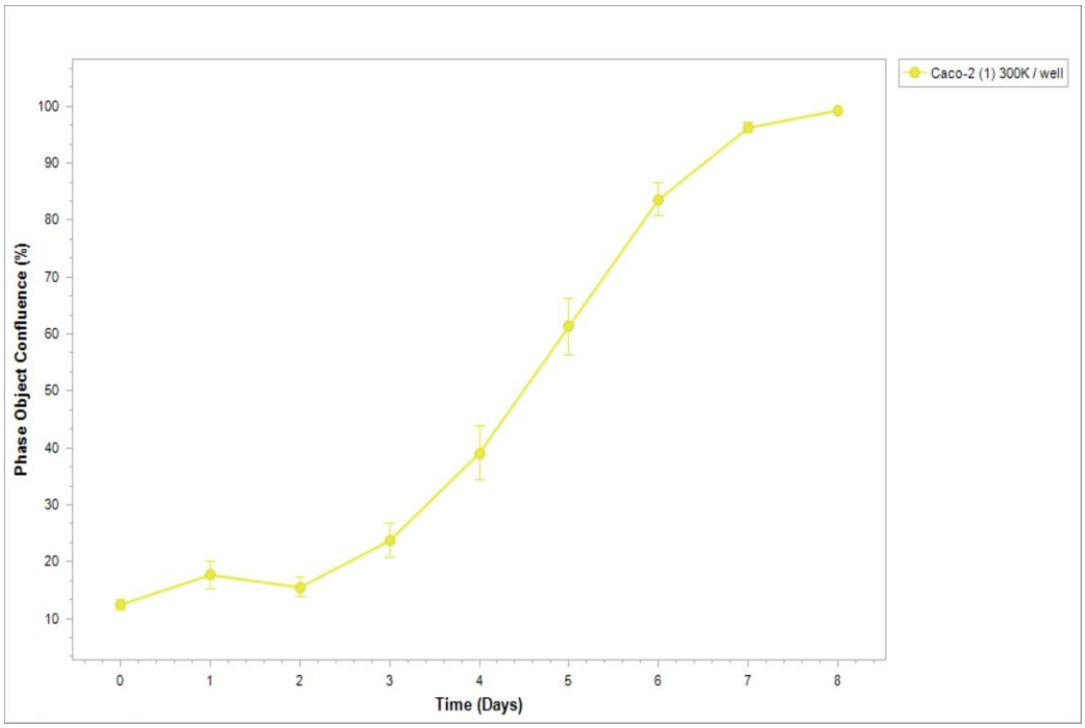

Figure 10: Growth curve of the Caco-2 cell line (batch 2) generated by IncuCyte. The proliferation of the cells is shown as phase area confluence versus time in days.

5.2 Electron microscopy

When grown in appropriate culture conditions, Caco-2 cells are known to differentiate and polarize to develop the morphology of enterocytes with tight junctions and microvilli. As a quality control, it was thus of interest to assess whether Caco-2 cells, cultured on permeable membrane inserts, are is fully differentiated with well-developed tight junctions and microvilli after 21 days in culture. For this purpose, SEM and TEM was applied.

5.2.1 Scanning electron microscopy

The images taken using SEM (Figure 11) show that the cells have differentiated and formed well-developed microvilli after 21 days in culture. The image shows the surface of the Caco-2 monolayer covered in microvilli.

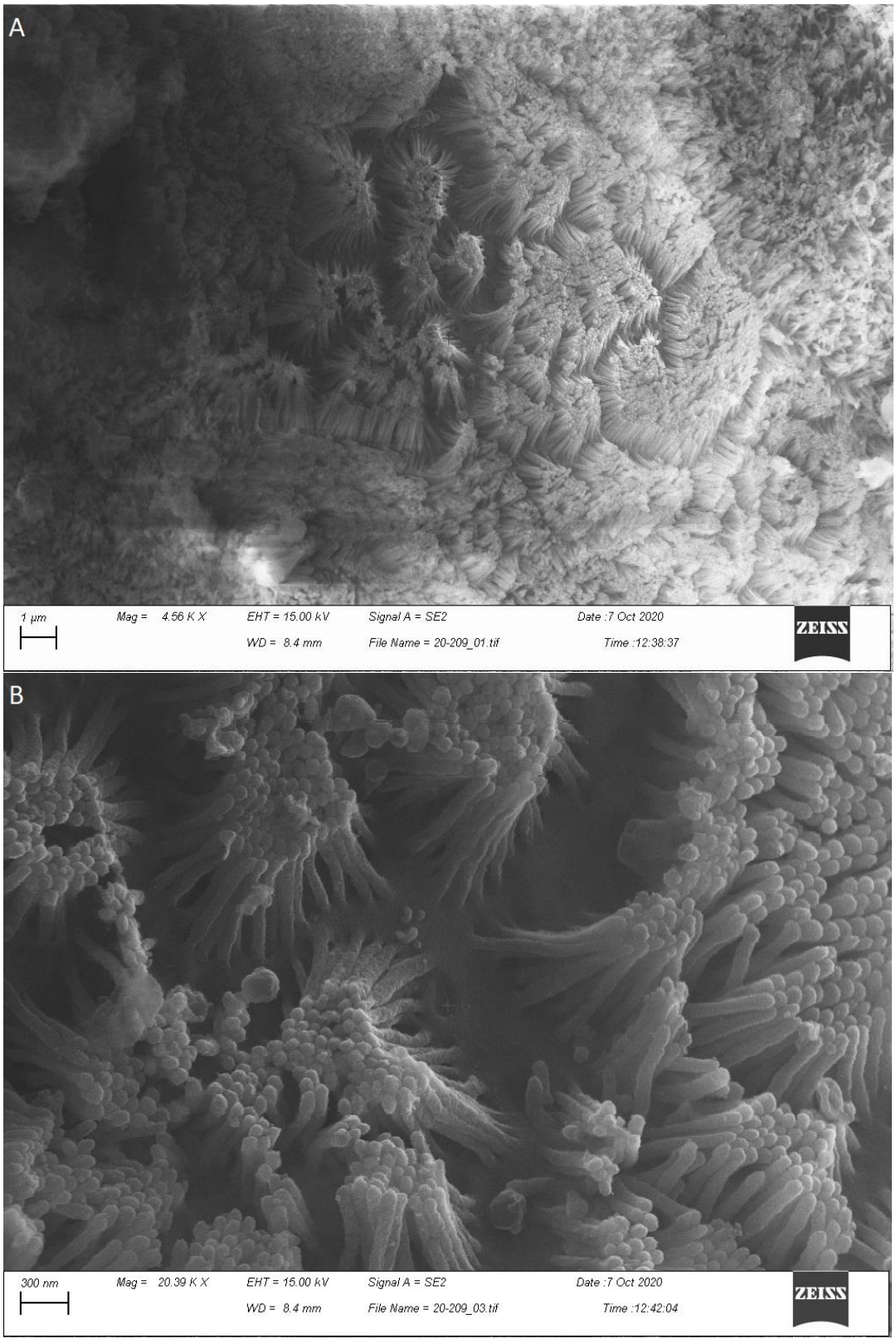

Figure 11: SEM (scanning electron microscopy) images of the Caco-2 cell monolayer after 21 days in culture, showing the surface of the cells covered microvilli. The cell density is $1 \cdot 10^5$ cells/mL. Image A covers a larger surface area, while image B is taken with increased magnification, giving a close-up image of the microvilli.

5.2.2 Transmission electron microscopy

The images below are cross-sections of Caco-2 cells taken by TEM (Figure 12 A, B, C) The images of the cross-sections show that after 21 days of culture, Caco-2 cells are well differentiated, and have formed tight junctions that are connecting the cells at the apical surface, in addition to a well-developed brush border of microvilli.

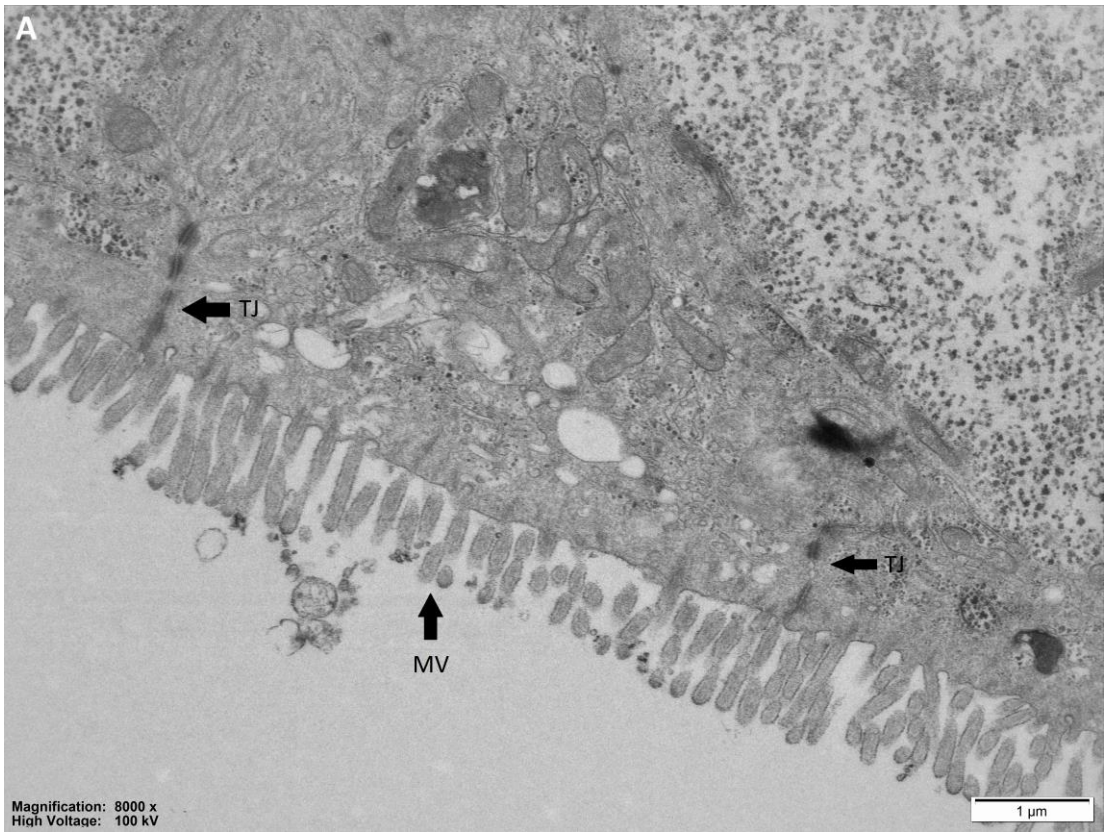

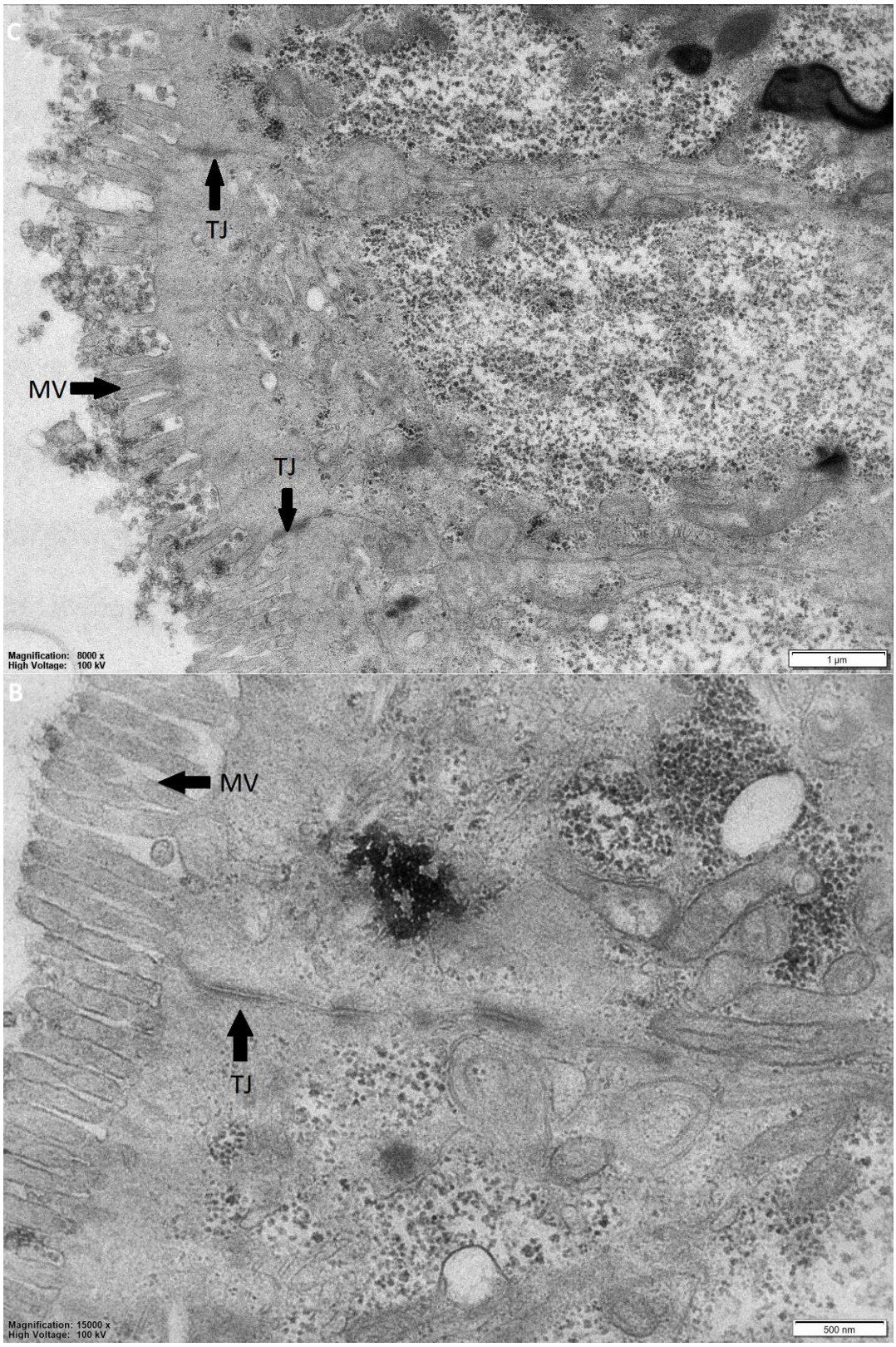

Figure 12: TEM (transmission electron microscopy) images showing a cross section of a Caco-2 cell after 21 days in culture, with well-developed tight junctions (TJ) and the presence of microvilli (MV.). The cell density in these images is $1 \cdot 10^5$ cells/mL.

5.2.3 Confocal microscopy

As a quality check of the Caco-2 monolayer, images were taken using the fluorescence microscope to ensure that the cells grow in a monolayer (Figure 13). The cell nucleus is dyed blue, and the cell membrane is dyed green. The red dots presumably represent the mitochondria. According to the images taken, the cells grow in a monolayer, because a single layer of cell nuclei is visible in the different planes of the cross-sections.

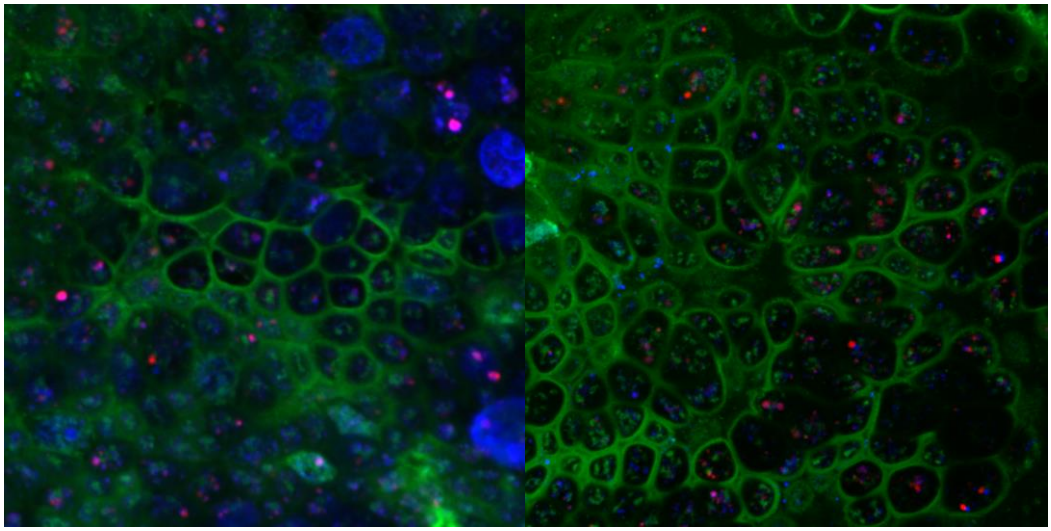

Figure 13: Live fluorescence microscope image of the Caco-2 cell monolayer after 21 days in culture, showing the cell nucleus (blue) the plasma membrane (green.) and mitochondria (red). The cell nucleuses were positioned in one plane, indicating that the cells grow in a monolayer.

5.3 PFAS background identification in equipment and solutions

PFAS of different carbon chain lengths were detected in some equipment and solutions used initially. This equipment and the background contaminated solutions were eliminated from the study and replaced with equipment and solutions that were PFAS-free. The results of the equipment and solutions tested is provided in Table 4 in the appendix.

5.4 The effect of PFAS on digoxin transport

Caco-2 cells were cultured on Transwell permeable supports, and the effect of increasing concentrations of PFOS, PFHxS and PFBS on the transport of digoxin by P-gp was

determined by conducting a bidirectional transport study. The apparent permeability (P_{app}) of digoxin across the monolayer was calculated, and the efflux ratio (ER) was determined.

The results are shown as a mean of five time-independent parallels, with standard deviations. One Way Analysis of Variance (ANOVA) on Ranks was performed due to failed normality test (Shapiro-Wilk). The transport of digoxin was compared in the apical to basolateral direction separately from the transport of digoxin in the basolateral to apical direction. There were no statistically significant differences between the groups exposed to PFOS, PFHxS and PFBS compared to the control group (n=5). The difference between the median values among the groups were not great enough to exclude the possibility that the difference is due to random sampling variability.

5.4.1 Digoxin and PFOS

As the results show (Figure 14), PFOS did not affect the transport of digoxin across the Caco-2 monolayer. Moreover, the apparent permeability of digoxin did not change with increased concentrations of PFOS.

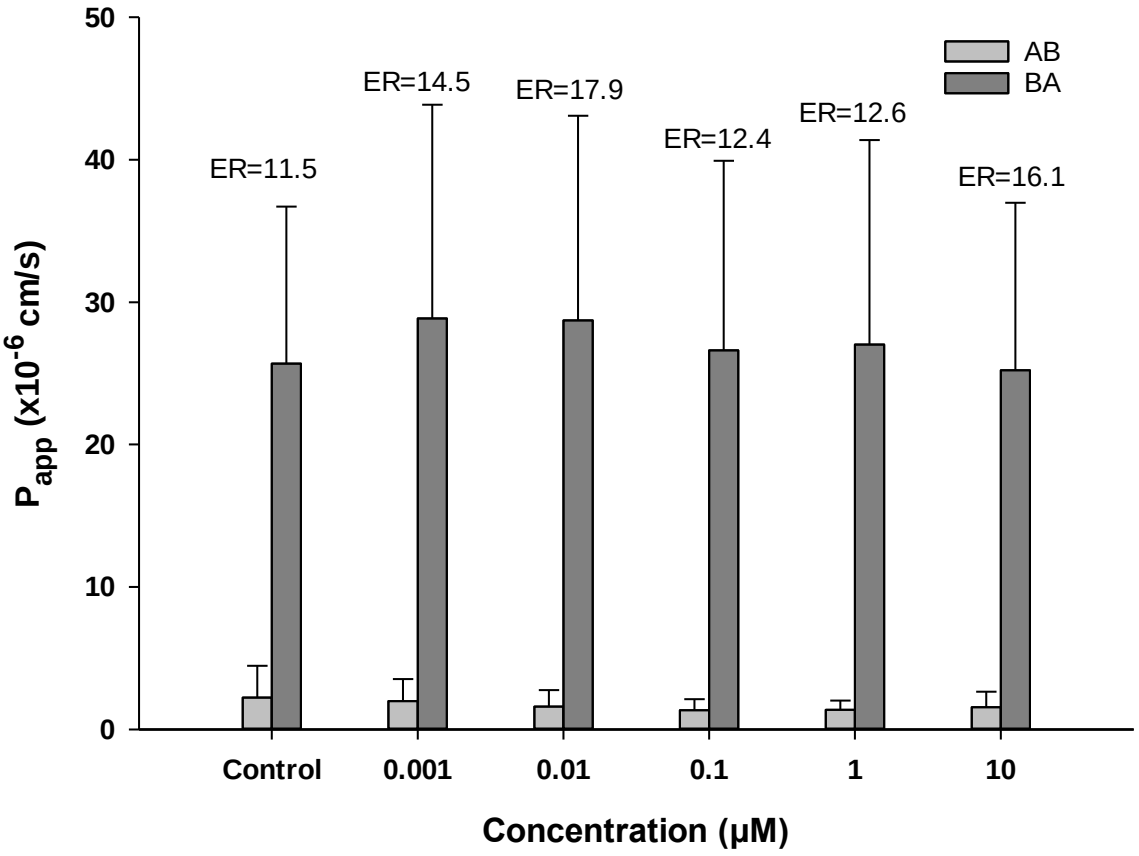

Figure 14: Determined bi-directional apparent permeability of D3-digoxin across the Caco-2 cell monolayer exposed to PFOS (0.001-10 µM), showing the transport rate of digoxin in the apical to basolateral direction (AB) and in the basolateral to apical direction (BA). Efflux ratio (ER) is shown. Data is expressed as the mean with standard deviation (n=5).

5.4.2 Digoxin and PFHxS

PFHxS did not affect the transport of digoxin across the monolayer (Figure 15), and there is no evidence that the apparent permeability of digoxin changed with increased concentrations of PFHxS.

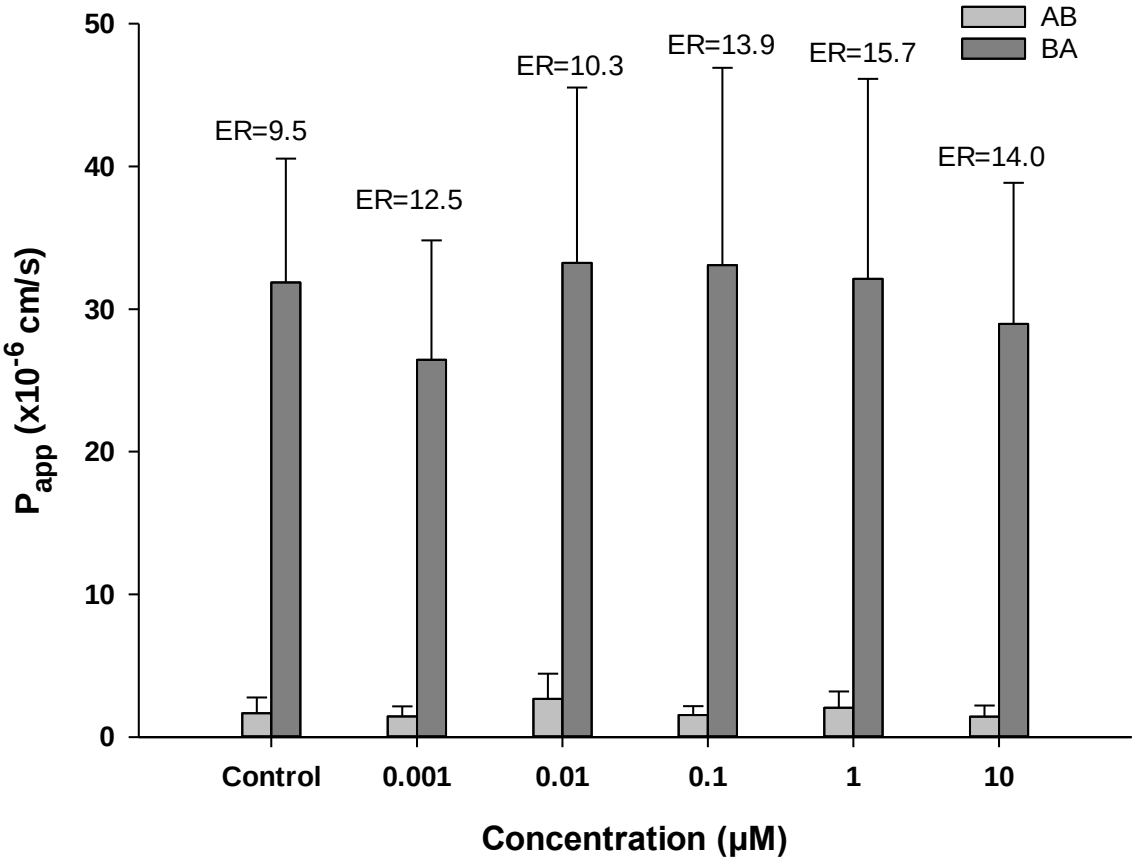

Figure 15: Determined bi-directional apparent permeability of D3-digoxin across the Caco-2 cell monolayer exposed to PFHxS (0.001-10 µM), showing the transport rate of digoxin in the apical to basolateral direction (AB) and in the basolateral to apical direction (BA). Efflux ratio (ER) is shown. Data is expressed as the mean with standard deviation (n=5).

5.4.3 Digoxin and PFBS

PFBS did not affect the transport of digoxin across the Caco-2 monolayer (Figure 16), and the increase in concentration of PFBS did not have any effect on the apparent permeability of digoxin.

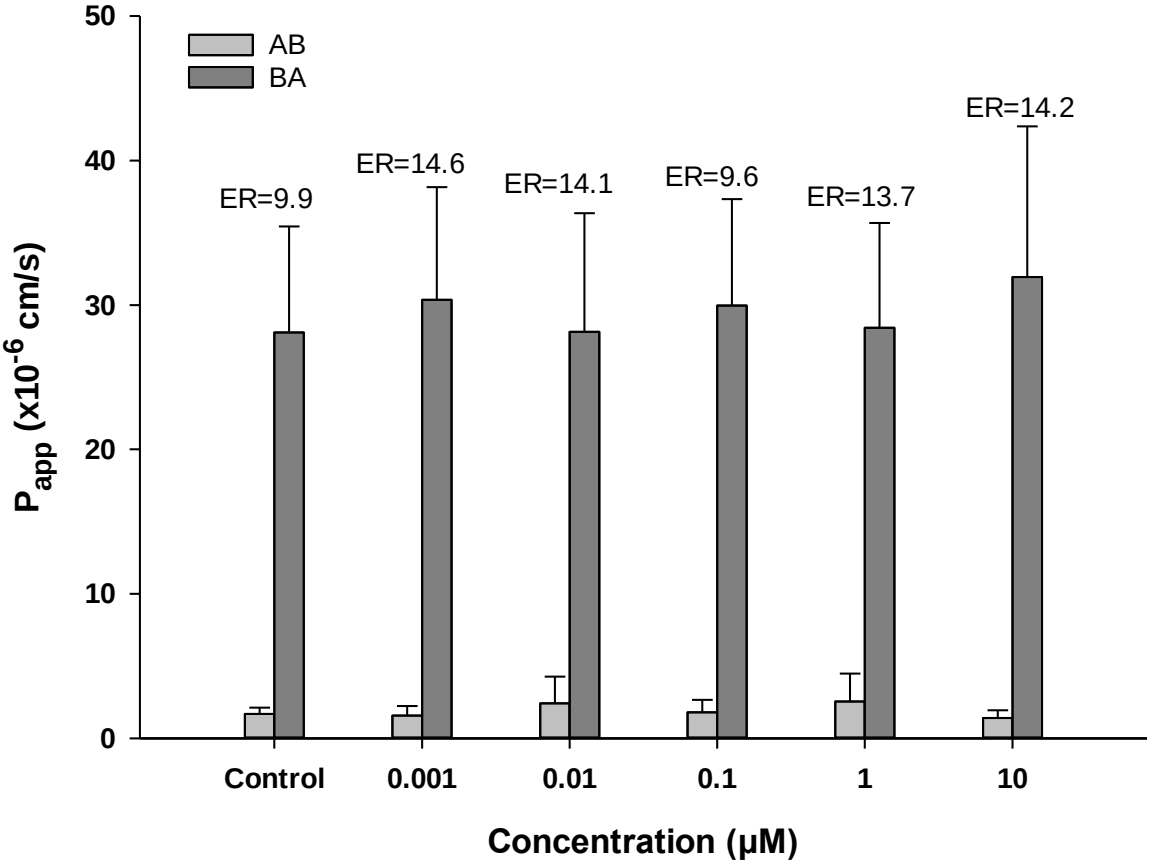

Figure 16: Determined bi-directional apparent permeability of D3-digoxin across the Caco-2 cell monolayer exposed to PFBS (0.001-10 µM), showing the transport rate of digoxin in the apical to basolateral direction (AB) and in the basolateral to apical direction (BA). Efflux ratio (ER) is shown. Data is expressed as the mean with standard deviation (n=5).

5.5 Transport of PFAS across the Caco-2 cell monolayer

While examining the effects of PFOS, PFHxS and PFBS on the transport of digoxin across the Caco-2 monolayer, it was observed that PFOS crossed the monolayer. This was investigated further, to assess whether PFOS, PFHxS and PFBS are transported across the Caco-2 monolayer, and if there are any differences in the transport of perfluoroalkyl sulfonic

acids of different carbon chain lengths. The results show that PFOS, PFHxS and PFBS crossed the Caco-2 monolayer. One-way ANOVA, or one-way ANOVA on ranks, was performed, and there were no statistically significant differences between the transport rates of the groups with different concentrations of PFOS, PFHxS and PFBS.

5.5.1 Transport of PFOS across the Caco-2 cell monolayer

The results (Figure 17) demonstrated that PFOS crossed the Caco-2 cell monolayer both in the apical to basolateral direction and in the basolateral to apical direction. However, 0.001 µM PFOS was not detected in the apical to basolateral direction by the LC-MS analysis. The results show no significant changes in transport with increased concentrations. The efflux ratio is below two for all the concentrations testes, which might suggest that there is no active efflux of PFOS by P-gp.

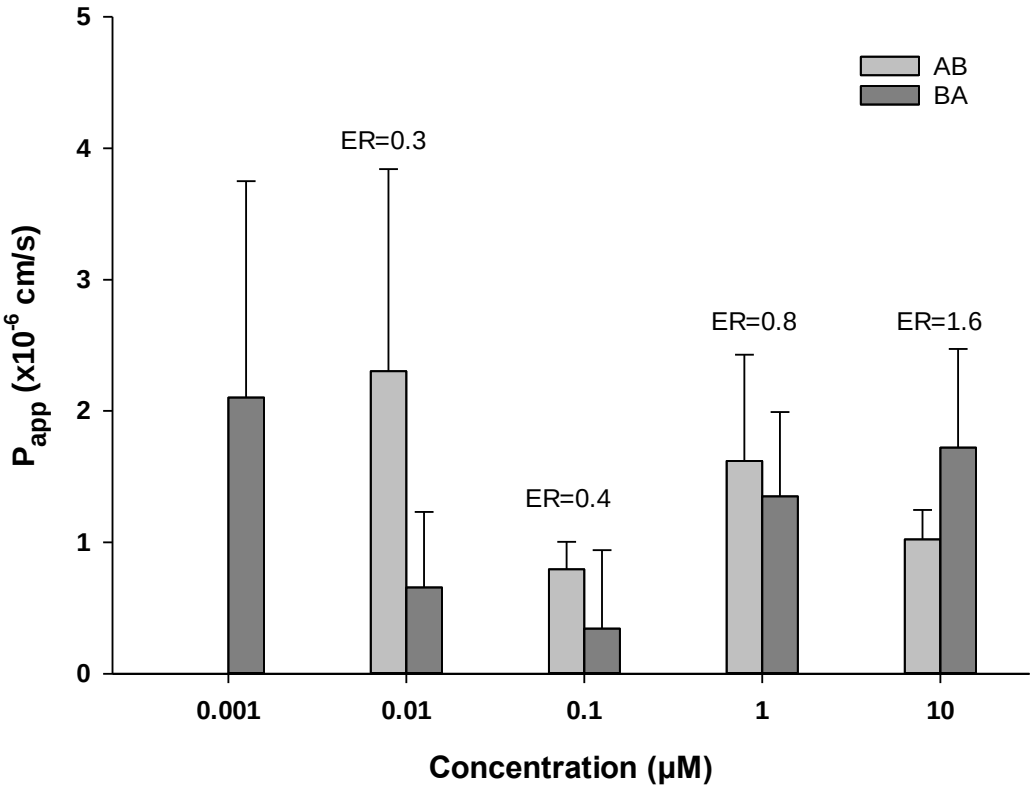

Figure 17: Determined bi-directional apparent permeability of PFOS 0.001-10 µM across the Caco-2 cell monolayer, showing the transport rate of PFOS in the apical to basolateral direction (AB) and in the basolateral to apical direction (BA). Efflux ratio (ER) is shown. Data is expressed as the mean with standard deviation (n=3).

5.5.2 Transport of PFHxS across the Caco-2 monolayer

PFHxS stands out compared to PFOS, as the transport rate of PFHxS, in both the apical to basolateral direction and in the basolateral to apical direction, appears considerably higher than the transport rate of PFOS (Figure 18). Although efflux ratios higher than two might indicate active efflux, the transport of PFHxS appears to be mostly equal in both directions.

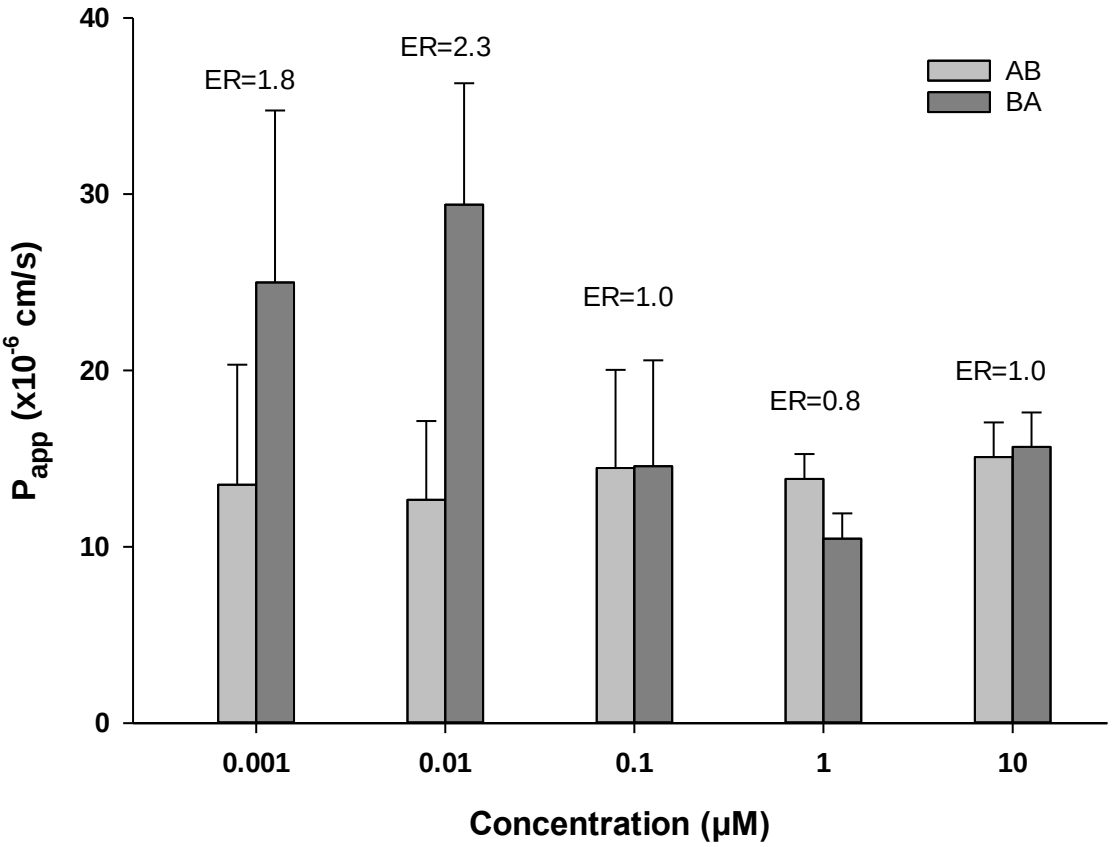

Figure 18: Determined bi-directional apparent permeability of PFOS 0.001-10 µM across the Caco-2 cell monolayer, showing the transport rate of PFOS in the apical to basolateral direction (AB) and in the basolateral to apical direction (BA). Efflux ratio (ER) is shown. Data is expressed as the mean with standard deviation (n=3).

5.5.3 Transport of PFBS across the Caco-2 monolayer

The transport rate of PFBS is lower compared to PFHxS, but higher compared to PFOS. As the results show, the PFBS crosses the cell monolayer both in the apical to basolateral direction, and in the basolateral to apical direction. As seen in Figure 19, the transport of PFBS seem to cease with increased in the apical to basolateral direction. For the higher concentrations (1 μM and 10 μM), the efflux ratio of higher than two, which could indicate active efflux in the basolateral to apical direction.

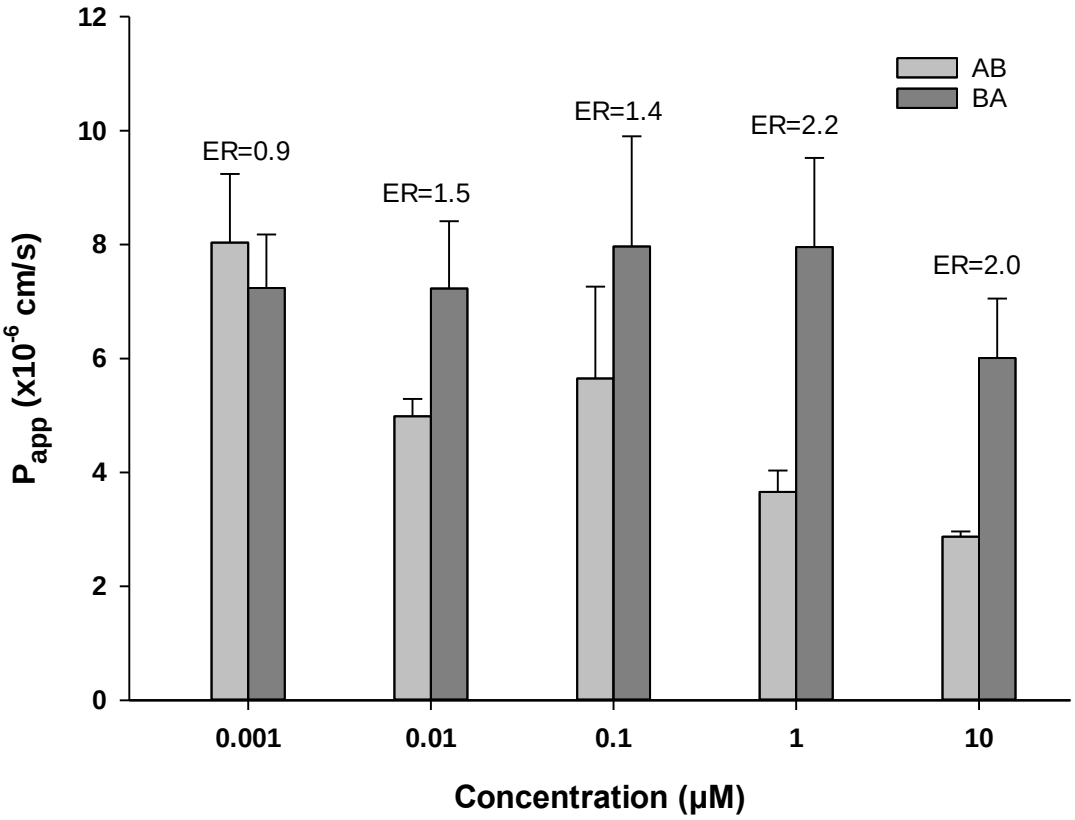

Figure 19: Determined bi-directional apparent permeability of PFOS 0.001-10 μM across the Caco-2 cell monolayer, showing the transport rate of PFOS in the apical to basolateral direction (AB) and in the basolateral to apical direction (BA). Efflux ratio (ER) is shown. Data is expressed as the mean with standard deviation (n=3).

5.6 Time trend for transport of PFAS across the Caco-2 monolayer

The linearity of the transport of PFOS, PFHxS and PFBS across the cell monolayer was proved by conducting a time trend on 1 µM PFOS, PFHxS and PFBS over a time period of 150 minutes. The results (Figure 20-22) show a rather linear transport of PFOS, PFHxS and PFBS across the Caco-2 monolayer, both for the apical to basolateral and basolateral to apical transport. Based on the results, 1 µM was chosen for further studies with P-gp inhibitors.

5.6.1 Time trend for transport of PFOS across the Caco-2 monolayer

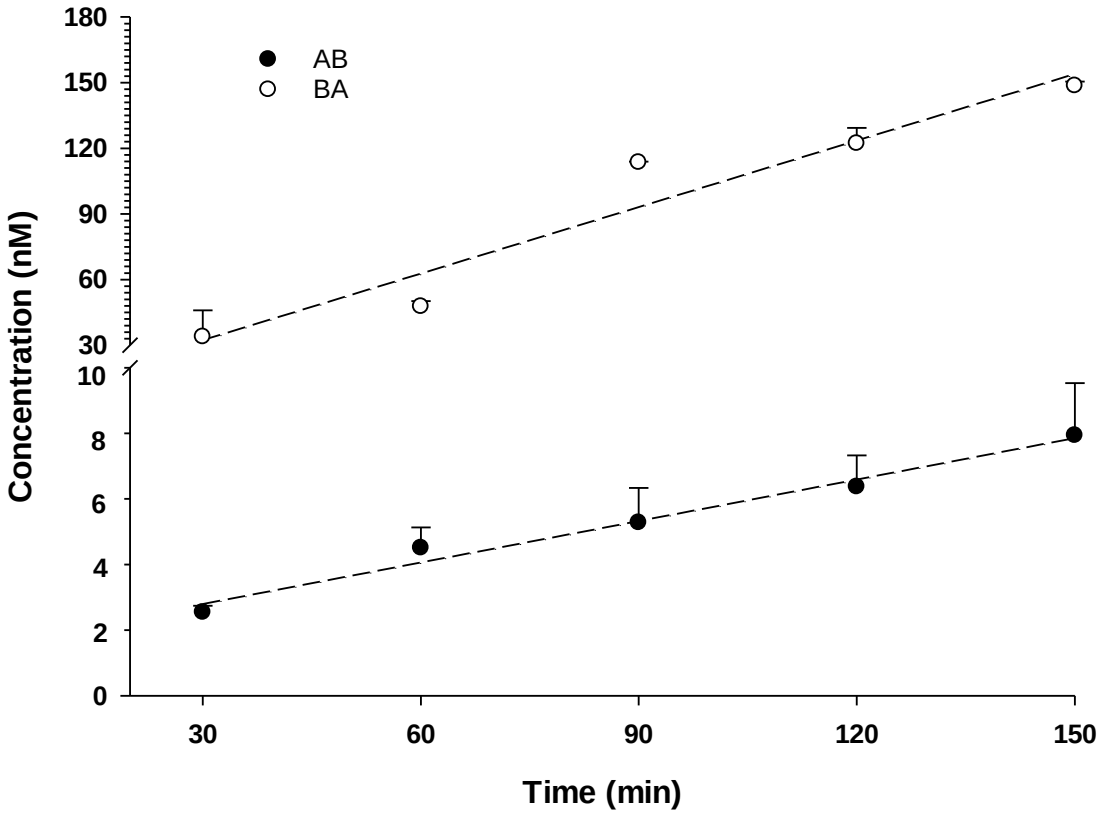

Figure 20: Time trend for transport of 1 µM PFOS across the Caco-2 monolayer, showing the transport in the apical to basolateral direction (AB) (R^2=0.964) and the basolateral to apical direction (BA) (R^2=0.88). The transport is expressed in concentration (nM) per time (min), and data is expressed as mean with standard deviation (n=2).

5.6.2 Time trend for transport of PFHxS across the Caco-2 monolayer

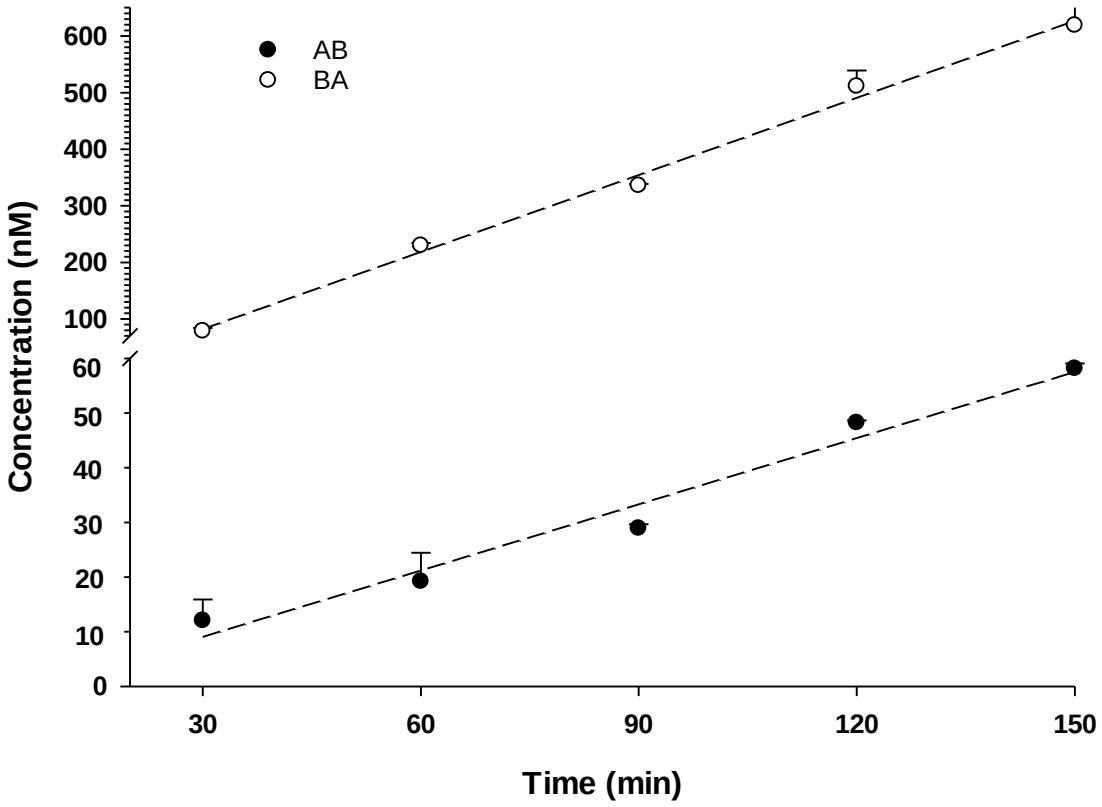

Figure 21: Time trend for transport of 1 µM PFHxS across the Caco-2 monolayer, showing the transport in the apical to basolateral direction (AB) (R^2=0.96) and the basolateral to apical direction (BA) (R^2=0.96). The transport is expressed in concentration (nM) per time (min), and data is expressed as mean with standard deviation (n=2).

5.6.3 Time trend for transport of PFBS across the Caco-2 monolayer

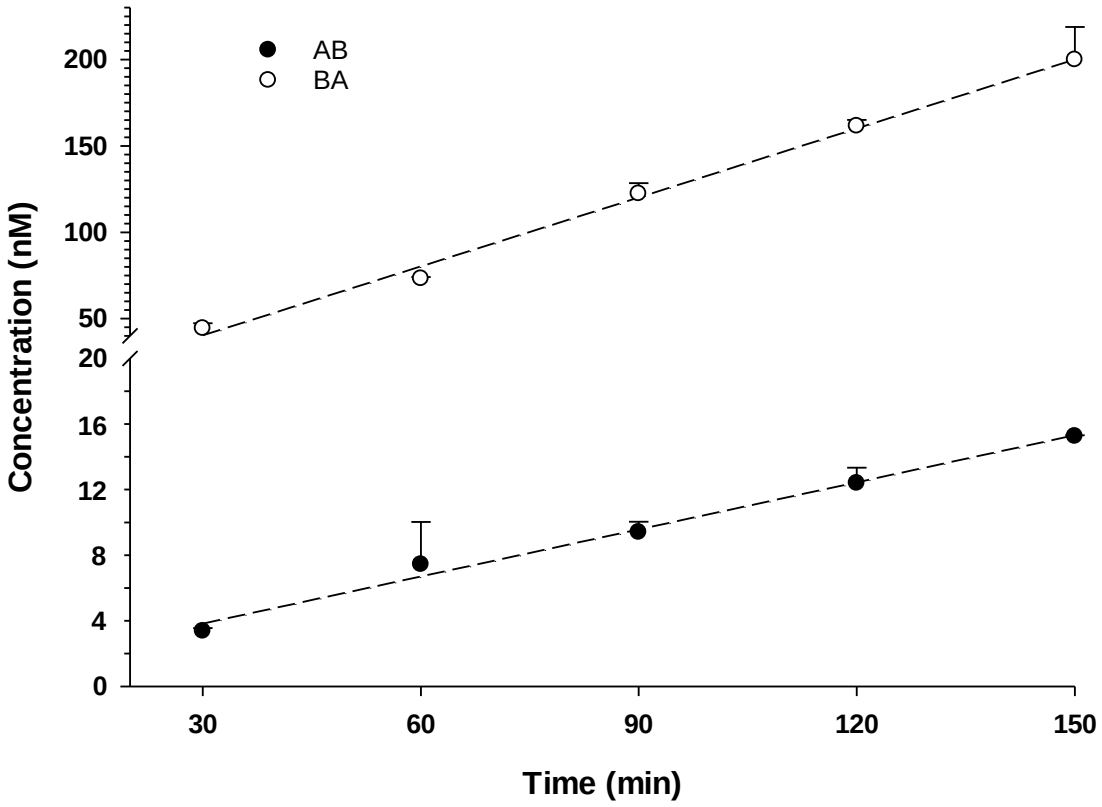

Figure 22: Time trend for transport of 1 µM PFBS across the Caco-2 monolayer, showing the transport in the apical to basolateral direction (AB) (R^2=0.98) and the basolateral to apical direction (BA) (R^2=0.97). The transport is expressed in concentration (nM) per time (min), and data is expressed as mean with standard deviation (n=2).

5.7 Transport of PFAS across the Caco-2 monolayer with P-glycoprotein inhibitors

The involvement of P-gp in the active efflux of PFOS, PFHxS and PFBS was studied. A bidirectional transport study was conducted on 1 µM PFOS, PFHxS and PFBS with known P-gp inhibitors – quinidine and verapamil of increasing concentrations (0.01, 0.1, 1, 10 and 100 µM). Each transport study was conducted in three time-independent parallels. Both verapamil and quinidine are known inhibitors of P-gp, but verapamil is less selective than quinidine.

5.7.1 PFOS and quinidine

Lower concentrations (0.01 and 0.1 μM) of quinidine seem to increase the transport rate of PFOS across Caco-2 monolayer in the basolateral to apical direction, as seen in Figure 23. However, higher concentrations (1 and 10 μM) appear to decrease the permeability both in the basolateral to apical direction and in the apical to basolateral direction. One-way Analysis of Variance (ANOVA) on Ranks was conducted due to fail test of equal variance. Dunn's post hoc test revealed that there was no statistical difference between the groups compared with the control group for the transport in apical to basolateral direction. For the transport of PFOS in the basolateral apical direction, there was no statistically significant difference between the groups.

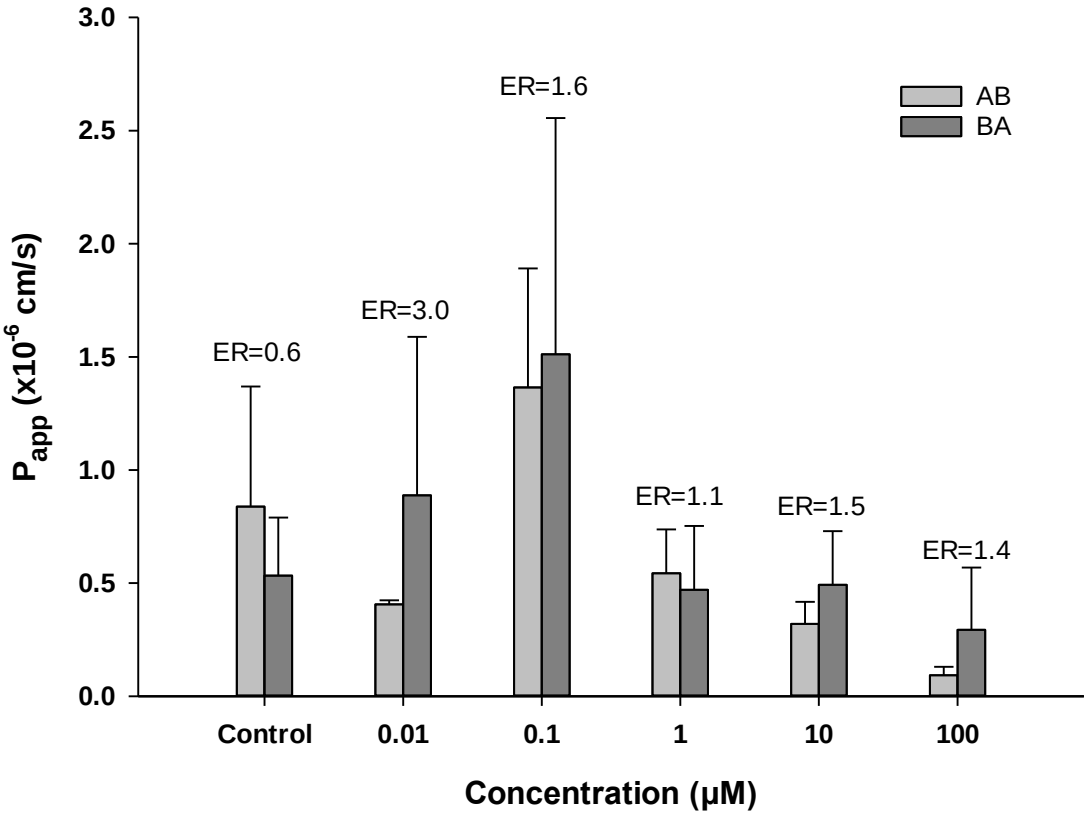

Figure 23: Determined bi-directional apparent permeability of 1 μM PFOS across the Caco-2 cell monolayer in the presence of 0.01-100 μM P-gp inhibitor quinidine. The transport rate of PFOS is shown in the apical to basolateral direction (AB) and in the basolateral to apical direction (BA). Efflux ratio (ER) is displayed. Data is expressed as the mean with standard deviation (n=3).

5.7.2 PFHxS and quinidine

The transport rate of PFHxS appears to be considerably higher than that of PFOS. The results (Figure 24) show a minor decrease in the transport rate of PFHxS in the basolateral to apical direction with increased concentrations of quinidine. In the apical to basolateral direction, the permeability of PFHxS show a minor decrease with the highest concentration of quinidine (100 µM). There was no statistically significant differences between the groups.

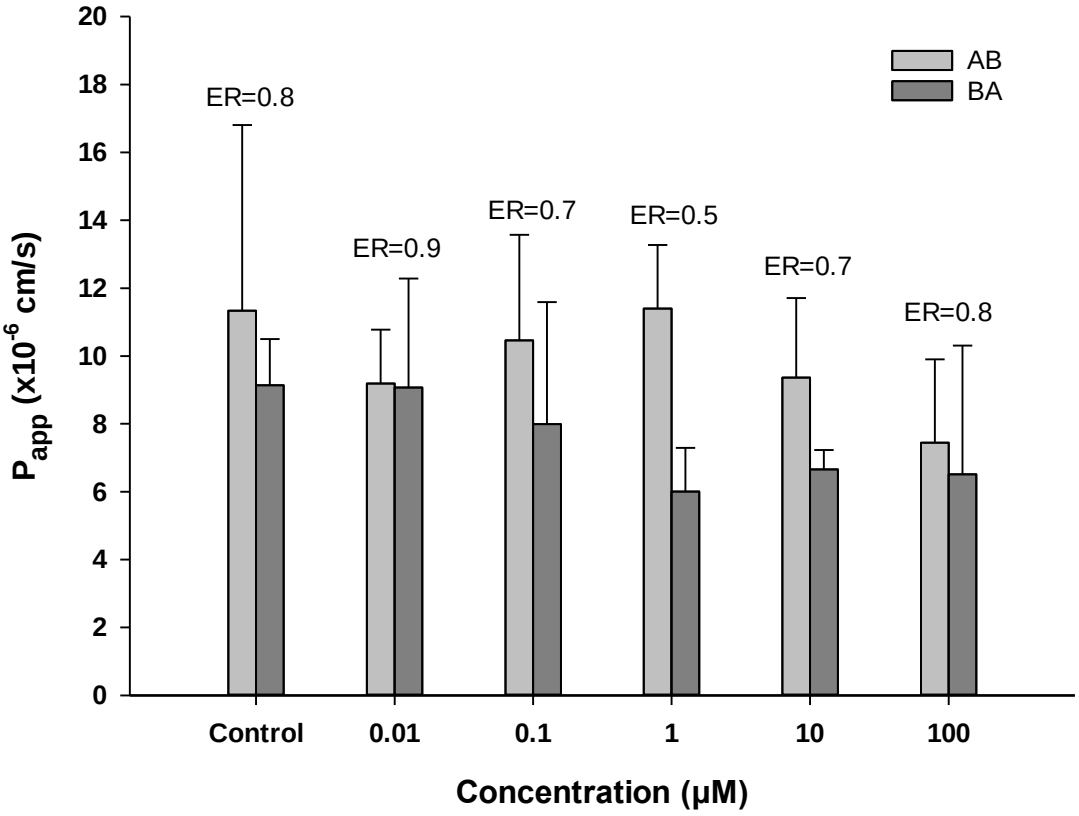

Figure 24: Determined bi-directional apparent permeability of 1 µM PFHxS across the Caco-2 cell monolayer in the presence of 0.01-100 µM P-gp inhibitor quinidine. The transport rate of PFHxS is shown in the apical to basolateral direction (AB) and in the basolateral to apical direction (BA). Efflux ratio (ER) is displayed. Data is expressed as the mean with standard deviation (n=3).

5.7.3 PFBS and quinidine

According to the results shown in Figure 25, there is no evidence that transport of PFBS is inhibited by quinidine, as there is no decrease in the apparent permeability with increasing

concentrations of quinidine. Moreover, the transport of PFBS in both directions is seemingly equal.

One-way ANOVA was performed on the apical to basolateral transport. Dunnett's post hoc test revealed a statistically significant difference between the control group and the group with 0.1 µM quinidine (P=0.02). For the basolateral to apical transport, there was no statistically significant difference.

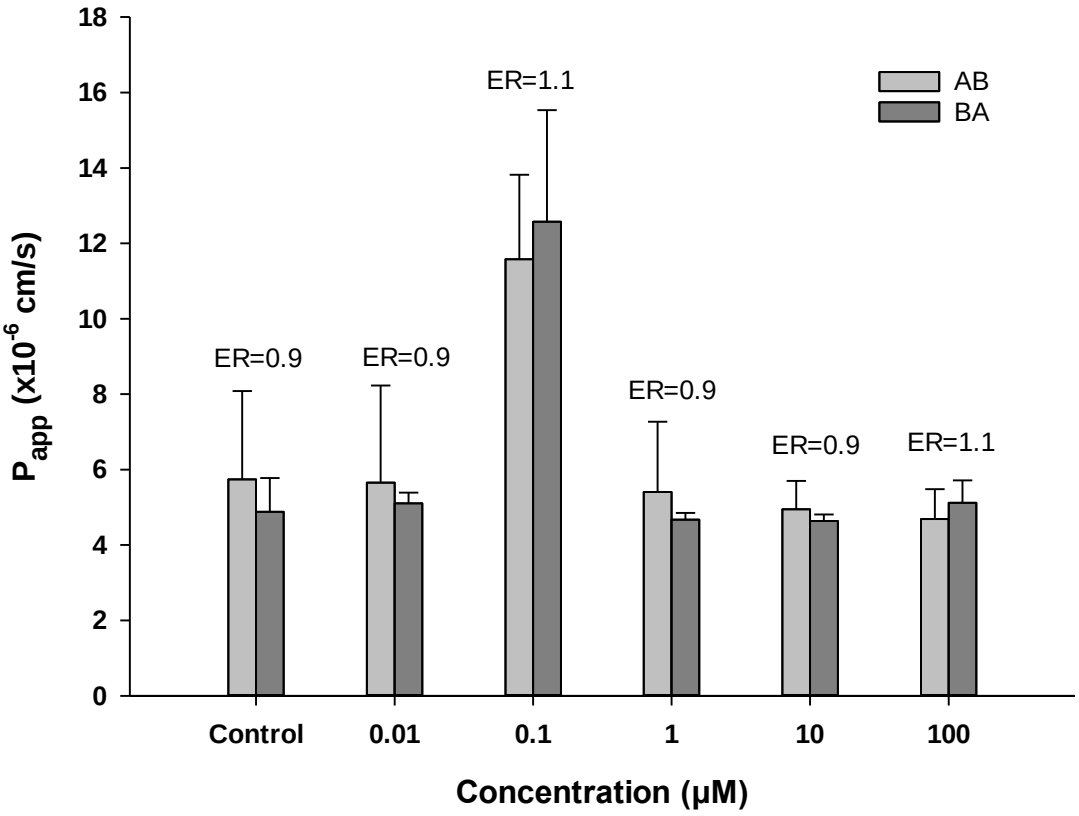

Figure 25: Determined bi-directional apparent permeability of 1 µM PFBS across the Caco-2 cell monolayer in the presence of 0.01-100 µM P-gp inhibitor quinidine. The transport rate of PFBS is shown in the apical to basolateral direction (AB) and in the basolateral to apical direction (BA). Efflux ratio (ER) is displayed. Data is expressed as the mean with standard deviation (n=3).

5.7.4 PFOS and verapamil

The results displayed in Figure 26 show a decrease in the permeability both in the basolateral to apical direction, and in the apical to basolateral direction, with increasing concentrations of verapamil. One-way ANOVA analysis was performed, followed by Dunnett's post hoc test,

which revealed a statistically significant difference in the mean values of the groups with 1 µM verapamil (p=<0.001), 10 µM verapamil (P=<0.001), and 100 µM verapamil (P=0.010) versus the control group, in the apical to basolateral direction. The mean values are greater than would be expected by chance, for the transport in the apical to basolateral direction.

In the basolateral to apical direction, the difference in the mean values among the groups was not great enough to exclude the possibility that the difference is due to random sampling variability, and there is no statistically significant difference among the groups.

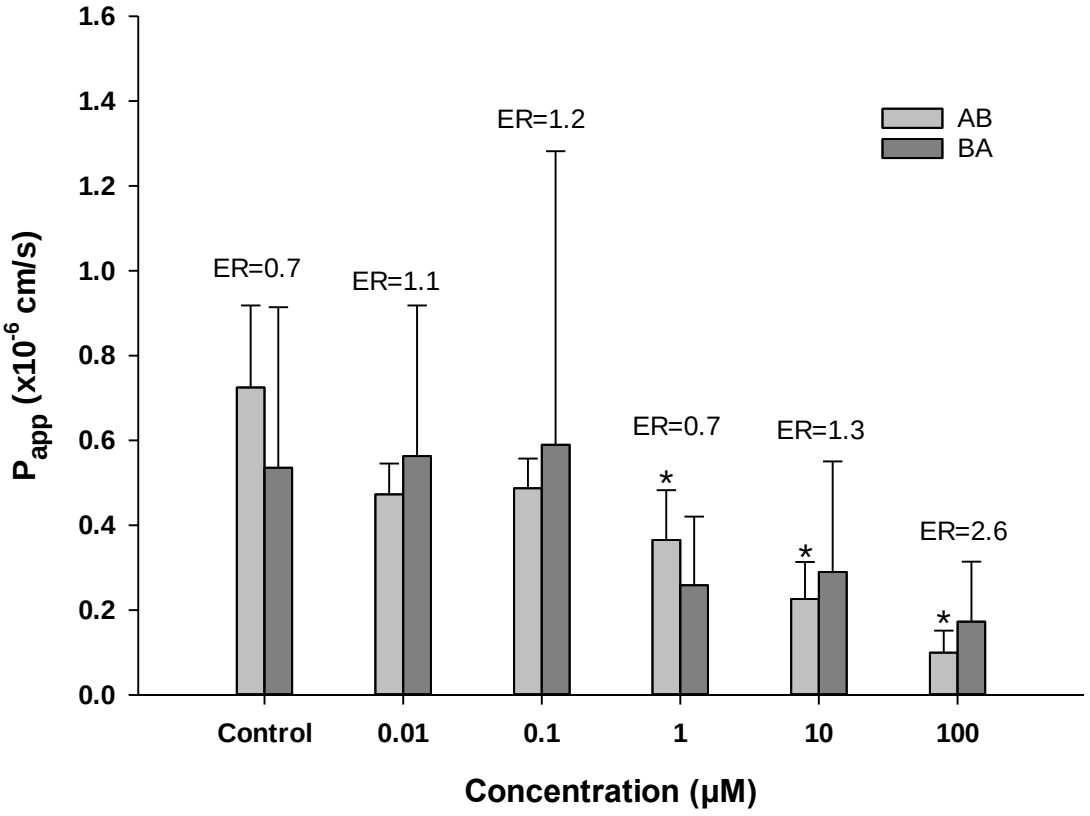

Figure 26: Determined bi-directional apparent permeability of 1 µM PFOS across the Caco-2 cell monolayer in the presence of 0.01-100 µM P-gp inhibitor verapamil. The transport rate of PFOS is shown in the apical to basolateral direction (AB) and in the basolateral to apical direction (BA). Efflux ratio (ER) is displayed. Data is expressed as the mean with standard deviation (n=3).

5.7.5 PFHxS and verapamil

It is evident that the transport rate of PFHxS is considerably higher than that of PFOS. The apparent transport rate in the basolateral to the apical direction seem to decrease with increased concentrations of verapamil, which is also true for the transport rate in the apical to basolateral direction (Figure 27).

One-way ANOVA was performed, however, there is no statistically significant difference in the transport of PFHxS neither in the apical to basolateral direction among, nor in the basolateral to apical direction between the different groups. The difference in means between the groups is not great enough to exclude the possibility that the difference is due to random sampling.

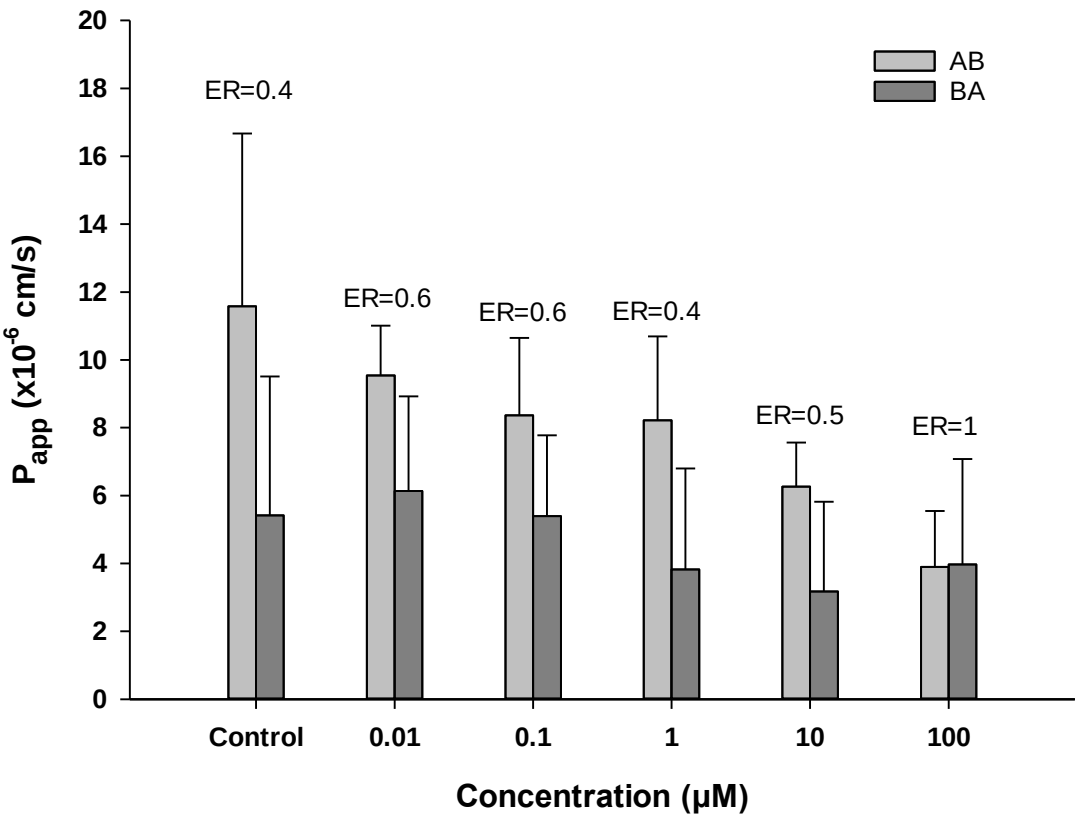

Figure 27: Determined bi-directional apparent permeability of 1 µM PFHxS across the Caco-2 cell monolayer in the presence of 0.01-100 µM P-gp inhibitor verapamil. The transport rate of PFHxS is shown in the apical to basolateral direction (AB) and in the basolateral to apical direction (BA). Efflux ratio (ER) is displayed. Data is expressed as the mean with standard deviation (n=3).

5.7.6 PFBS and verapamil

According to the results shown in Figure 28, verapamil has no effect on the permeability of PFBS across Caco-2 monolayer. The transport rate is nearly equal in both directions. There is no statistically significant difference between the groups.

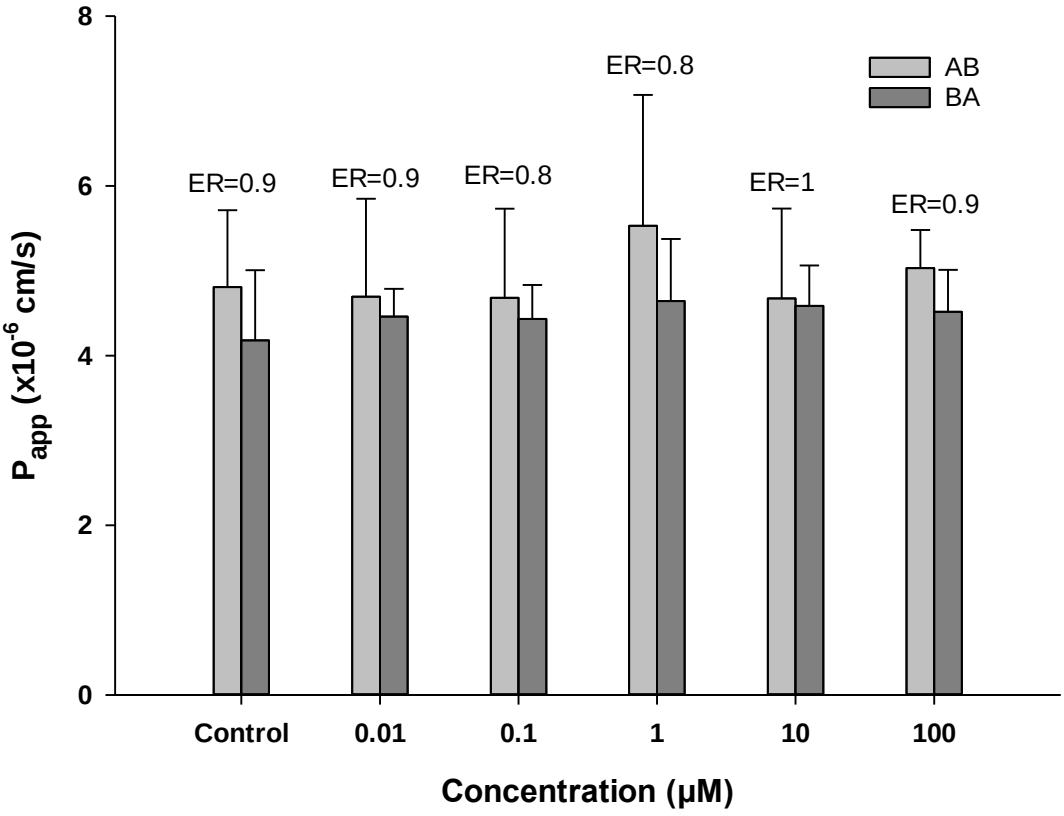

Figure 28: Determined bi-directional apparent permeability of 1 µM PFBS across the Caco-2 cell monolayer in the presence of 0.01-100 µM P-gp inhibitor quinidine. The transport rate of PFBS is shown in the apical to basolateral direction (AB) and in the basolateral to apical direction (BA). Efflux ratio (ER) is displayed. Data is expressed as the mean with standard deviation (n=3).

5.8 Evaluation of membrane integrity

Mannitol was used to evaluate the membrane integrity of Caco-2 cell monolayer after exposure to PFOS, PFHxS and PFBS, to ensure that the membrane complete. Apparent permeability was not calculated for mannitol, however, the results of the samples exposed to the individual PFSAs were compared to the control groups and showed that there was no difference between the groups.

6 Discussion

In recent years, PFAS, and especially compounds within the groups perfluoroalkyl carboxylic acids (PFCA) and perfluoroalkyl sulfonic acids (PFSA), have received great amount of attention due to the concerns regarding resistance to degradation in ecosystems, bioaccumulation in organisms and the potential toxic effects on humans. However, the research on potential toxic effects in humans is limited, and little knowledge is available about effects of PFAS on the activity of transporter proteins, P-gp in particular, with only few articles published in this topic (76, 89, 91, 108). In the small intestine, P-gp plays an important role in the detoxification of the organism and protects the human body from xenobiotics and toxins that enters the organism through ingestion, by active efflux into the lumen of the intestine. Clinically, P-gp thus has a great impact on the absorption and distribution of drugs, by limiting the absorption of many drugs (108). However, P-gp also has a detoxifying and protective role in other tissues, such as the blood-brain-barrier, retina, testes, placenta, developing fetus, kidney and liver, where it contributes to the active efflux of toxicants and removal of harmful agents from the body (108). Potential interaction of PFAS with P-gp, could alter the absorption and distribution of drugs and other toxicants entering the organism. It was hypothesized that P-gp could be involved in active efflux of particular PFSAs, thereby protecting the body from the potential toxic effects of these substances. The Caco-2 cell line model is widely used to study the intestinal absorption of various compounds because of the morphological and functional resemblance of human intestinal epithelial cells (109). The Caco-2 cell line model is in addition used to screen new chemicals for potential drug-drug interactions. Therefore, this model was used in the present study to investigate the effect of PFOS, PFHxS and PFBS on the transport of digoxin by P-gp. Digoxin is a specific substrate of P-gp. PFOS, PFHxS and PFBS consists of carbon chains of eight, six and four carbon atoms, respectively. It was of interest to investigate whether the carbon chain length affected the potential of these substances to inhibit P-gp activity. It was also of interest to investigate whether PFOS, PFHxS and PFBS crossed the Caco-2 monolayer, and whether the difference in carbon chain length affected the rate of transport across the membrane. Transport experiments were in addition conducted with verapamil and quinidine, which are known modulators of P-gp, in order to identify whether PFOS, PFHxS and PFBS might be P-

gp substrates and to evaluate if P-gp is involved in the possible detoxification mechanisms of PFSAs in the human body.

6.1 The effect of PFOS, PFHxS and PFBS on the transport of digoxin by P-gp

The results of the present study showed that neither PFOS, PFHxS nor PFBS affected the transport of digoxin by P-gp across the Caco-2 cell monolayer. There was no statistically significant difference in transport rate of digoxin among the groups exposed to increased concentrations of PFOS, PFHxS and PFBS and the control group. Moreover, it is evident that the difference in the carbon chain length between the individual compounds tested did not affect the flux of digoxin through P-gp in the Caco-2 cell line model. It can, thus, be argued that, in this *in vitro* model, PFOS, PFHxS and PFBS did not alter or modulate P-gp activity.

Several previously published studies have, however, demonstrated the potential of environmental toxicants causing synergistic toxic effects when combined with other compounds *in vivo* and *in vitro* (95, 110, 111). One of the mechanisms that might be involved is the inhibition of transporter proteins responsible for the efflux of toxic compounds, so-called chemosensitization. Chemosensitization might be a common effect of man-made environmental pollutants, including PFAS, and other compounds not considered harmful on their own (95). In zebrafish embryos, PFOS has been shown to enhance the accumulation and inhibited the clearance of rhodamine B, which is a chemical compound often used in biological research as a tracer dye. Moreover, the mortality by vinblastine, which is a substrate of multixenobiotic resistance transporters, increased when it was co-administrated with PFOS. This was seen upon as disrupted efflux activity of transporter proteins (95). These results might suggest that PFOS could interact with P-gp or other ABC-transporters responsible for the efflux of xenobiotics and modulate the transporter activity. However, the mechanisms of action are yet to be discovered. The same study conducted in addition an ATPase activity assay with recombinant zebrafish ABCB4, which confirmed the interference of ABCB4 function, as the transporter activity was reduced by PFOS (95).

Although the study described above suggested that PFOS interacts with ABC transporters and inhibits the efflux of vinblastine, the involvement of P-gp is not known. In the present study, the effect of PFOS, PFHxS and PFBS on the transport rate of digoxin across the Caco-2 cell

monolayer was studied directly and showed that the individual PFSAs did not affect the efflux of digoxin by P-gp. Digoxin is a specific P-gp substrate, and the results might imply that the individual PFSAs tested in the present study do not alter the activity P-gp in Caco-2 cells. Moreover, it could be suggested that they most likely are not competitive inhibitors of P-gp in the Caco-2 cell line model. Moreover, different model organisms were used in the present study and in the previously conducted study described above. In the present study, the Caco-2 cell line model was used, which is derived from human colorectal adenocarcinoma and is morphologically and functionally similar to human intestinal enterocytes. The model is widely used by pharmaceutical industries to predict drug-drug interactions, and intestinal absorption of different compounds, since the permeability coefficients obtained using the Caco-2 cell line model show a good correlation with *in vivo* permeability coefficients in human intestine (112). The U.S. Food and Drug Administration (FDA) therefore approves the Caco-2 model as one of the methods utilized to determine the permeability of a drug substance from the gastrointestinal tract (113). The Caco-2 cells are grown on a membrane insert, and as for intestinal enterocytes, the cells encompass several ways of transport across the membrane, such as passive paracellular and transcellular transport, facilitated transport and active transport. Thus, the model is a decent representation of the normal physiology of intestinal enterocytes. Although it has been shown that in zebrafish, PFOS interacts with ABC transporters and inhibits the efflux of a cytotoxic substrate, the results obtained in the present study might be more representative for the interactions of PFSAs with P-gp in humans (95).

There might be significant differences in the physiological and cellular processes between humans and model organisms of other species. Although ABC-genes are conserved between species, it can be argued that the expression, activity, and substrate specificity of P-gp can vary between humans and model organisms of different species (114-116). It has been demonstrated that there are several differences in the elimination kinetics of different PFAS, depending on species, sex, as well as the functional group and the length of the carbon chain of PFAS (44). The elimination half-live varies between species and individuals and is generally much longer in humans (45). Membrane transporters have received much attention in the attempt of explaining these kinetic differences. This might support the possibility that the different findings in the present study compared to the findings in other published studies might be caused by biological variability between model organisms and cell lines used, and that other model organisms might potentially have more efficient detoxification mechanisms

in other species due to possibly distinct or wider substrate specificities of the involved transporter.

Another previously conducted study showed that GenX (ammonium 2,3,3,3,3-tetrafluoro-2-(heptafluoropropoxy) propanoate) reduces the activity of P-gp, breast cancer resistance protein, and multidrug resistance-associated protein 2 at the blood-brain barrier (108). GenX is a chemical precursor used in the production of polytetrafluoroethylene (Teflon), and has been used as a substitute for both PFOS and PFOA, as it has been shown to be less bioaccumulative (117). However, the observations regarding lower bioaccumulation of GenX could be explained by a shorter emission period compared to the now regulated PFOS and PFOA, in addition to few published studies including GenX in their research investigation. In the study on GenX, the transporter activity was measured in isolated rat brain capillaries by a confocal microscopy based method, and the results showed that exposure of rat brain capillaries to low nanomolar concentrations (0.1-100 nM) of GenX, significantly reduced the transport activity of P-gp after 1-2 hours (108). In that study, fluorescent cyclosporine A was used as substrate for P-gp. Reversibility assays was performed, which showed that after GenX removal, the P-gp transport activity returned to control levels after 1 hour in males and after two hours in females (108). The same study showed that GenX did not reduce P-gp-associated ATPase activity in an *in vitro* transport assay system composed of vesical membranes and purified P-gp transporter proteins, thus, it was suggested that GenX did not inhibit P-gp transport by direct contact with the transporter (108). The study also suggested that GenX affected the transporter activity, but not its expression (108). The same study additionally performed growth inhibition assays on two human-derived P-gp overexpressing ovarian tumor and breast cancer cell lines (NCI/ADR-RES and MX-MCF-7), to determine if the effect of GenX observed in rats occurred in human cells (108). GenX as a single compound was not toxic to the cells, however, when co-administrated with Adriamycin, a cytotoxic P-gp substrate, the substrate toxicity increased, suggesting that GenX can inhibit the efflux of the cytotoxic agent in human cancer cell lines (108).

These are interesting findings. However, the different methods applied in the present study and the published study described above, together with differences in model organisms and cell lines used, in addition to structural differences between GenX and the individual PFSAs tested in the present study, might have led to different findings. GenX is a branched

perfluoroalkyl substance with six carbon atoms, an oxygen-bridge bond that makes the molecule polar to some degree, and a carboxylic acid as the functional group. Structurally, GenX differs from PFOS, PFHxS and PFBS used in the present study, which are a technical mixture of linear and branched species, and have a functional group consisting of sulfonic acid. The functional group of a compound determines the reactivity, solubility and other physical properties of the compound that can affect its biological role in living organisms. Compounds with different functional groups can thus interact differently with their surroundings. The structural differences between GenX and the investigated compounds in the present study could possibly explain the difference in the results when it comes to the inhibition of P-gp. In the present study, individual PFSAs were chosen to examine whether the potential to inhibit P-gp is affected by the carbon chain length of the substance. However, it would be interesting to examine the effects of perfluoroalkyl carboxylic acid on P-gp activity in the Caco-2 cell line model with digoxin as the P-gp substrate.

Moreover, in the study on the effects of GenX on P-gp, rat brain capillaries and P-gp overexpressing human ovarian tumor and breast cancer tumor cell lines were utilized, in comparison to Caco-2 cells used in the present study (108). In the present study, P-gp was not overexpressed, and it could be argued that the model is a more accurate representation of the normal physiology.

It is evident from the results obtained in the present study, that in the Caco-2 cell line model, PFOS, PFHxS and PFBS did not reduce the activity of P-gp. In contrast, other studies have conducted growth inhibition assays, utilizing cytotoxic P-gp substrates to measure the effects of different PFAS on the cell viability, and thus estimating possible interactions of PFAS with P-gp or other efflux transporters in the efflux of PFAS. It could be assumed that GenX and Adriamycin might have synergistic effects on the toxicity of the cancer cell lines utilized. Although P-gp is an important transporter that is involved in the efflux of many cytotoxic drugs and xenobiotics, it cannot be excluded that several transporters might be involved in the efflux of PFAS, as different transporters may have overlapping substrate specificity.

Another study showed that different environmental toxicants differentially target ABC-transporters in the blood-testis barrier and affect Leydig cell testosterone secretion *in vitro* (89). The same study performed an uptake assay using membrane vesicles overexpressing

several ABC transporters, including P-gp, and showed that PFOA and PFOS had the strongest observable effect on P-gp activity, where 100 μM led to 71 % and 84 % inhibition by PFOA and PFOS respectively (89). In the same study, the accumulation of PFOA was studied in transporter-overexpressing Madin-Darby canine kidney (MDCK) cells and normal MDCK cells, with and without the P-gp inhibitor elacridar, and showed that there was no difference in PFOA accumulation between P-gp overexpressing MDCK cells compared to normal control MDCK cells (89). This indicated that P-gp, most likely, was not responsible for the transport of neither PFOA nor the other environmental toxicants tested. This might suggest that PFOA modulate the activity of P-gp not necessarily directly, but through other possible mechanisms of action. These findings support the hypothesis that more complex mechanisms of action might be involved in the potential of PFAS to inhibit efflux transporters.

Although these interesting findings contradict with the findings in the present study, it can be argued that the differences in the results could be caused by the different methods applied to study the effects of PFAS on P-gp. In the published study described above, P-gp overexpressing membrane vesicles were used to study the interaction between PFOA, PFOS and P-gp (89). Moreover, the concentrations that caused the inhibitory effect were considerably higher (100 μM) than the highest concentrations used in the present study (10 μM). It could be argued that many compounds in such high concentrations, would interact with and possibly inhibit the transporter molecule, however, not necessarily by the same mechanisms of action as lower concentrations of the same compound. The range in concentrations in the present study was based on the concentrations of PFOS and PFHxS detected in human serum, thus, it can be argued that these are more representative when it comes to potential physiological effects in humans.

Although the findings in the present study showed that PFOS, PFHxS and PFBS did not affect the flux of digoxin by P-gp in the Caco-2 cell line model, it cannot be stated with certainty that the same will occur *in vivo*. It is uncertain whether these compounds will affect the absorption and distribution of drugs or toxicants entering the human body by ingestion. Moreover, PFOS, PFHxS and PFBS could possibly interact with P-gp or other ABC transporters involved in the absorption and distribution of drugs or toxicants *in vivo*, as they might be involved in more complex pathways that are difficult to study in the Caco-2 cell line

or other models. It is, nevertheless, an interesting and novel finding, that PFOS, PFHxS and PFBS did not interact with P-gp or modulate its activity in the Caco-2 cell line.

It is possible that individual PFAS interact with P-gp or other ABC transporters by mechanisms of action that have not been described in literature yet. It has been shown that GenX did not inhibit transporter activity by direct contact with the transporter protein (108). The same study showed that GenX might potentially disrupt the biological signaling pathways known to regulate ABC transporters (108). Previously published studies have suggested that PFAS might interact with peroxisome proliferator-activated receptor alpha (PPAR-α), the activity of which has been related to the activity and expression of P-gp. Signaling pathways dynamically regulate the activity and expression of P-gp, amongst other ABC transporter proteins (108). PPARs are nuclear receptors that are activated by endogenous fatty acids and some lipid-like xenobiotics (18). The effect of GenX and PPAR-γ on P-gp activity has been studied, and it was shown that the transport by P-gp transport that was reduced by GenX, was restored when co-treating with PPAR-γ inhibitor, in male rat brain capillaries (108). Although it has been shown that PPAR-α regulates the expression of the blood-brain barrier efflux transporter, it might not necessarily be involved in the regulation of expression of efflux transporters in the small intestine (118). However, PPAR-γ and PPAR-α are expressed in Caco-2 cells, and it has been shown that the expression increases with gradual differentiation of the cells (119). Thus, it could be suggested that PFOS, PFHxS and PFBS do not interact with PPAR-γ and PPAR-α in Caco-2 cells, to alter the expression of P-gp, or that expression of PPAR-γ and PPAR-α was not great enough to affect P-gp activity. Nevertheless, since the expression PPAR-γ and PPAR-α was not studied in in the Caco-2 cell line model in the present study, it is not certain whether an interaction between the individual PFSAs tested in the present study, and the PPAR receptors did occur.

6.2 PFOS, PFHxS and PFBS are transported across the Caco-2 cell monolayer

PFAS are bioaccumulating and biomagnifying in the food chain and are present in many consumer products that surrounds us in our daily lives, including in stain- and waterproof coatings for clothing and furniture, personal care products, and food packaging materials (120). PFAS are therefore known to be life-style related chemicals and are ubiquitously

distributed in the environment. It was thus of interest to determine whether PFOS, PFHxS and PFBS cross the Caco-2 cell monolayer and whether the individual PFSAs might be subjects for active efflux by P-gp as part of the detoxification process of toxicants entering the body by ingestion. The present study demonstrated that PFOS, PFHxS and PFBS crossed the Caco-2 cell monolayer in all the concentrations tested (0.001-10 μM) both in the apical to basolateral direction, and in the basolateral to apical direction. An exception was 0.001 μM PFOS in the apical to basolateral direction, that was not detected during the analysis. The results are inconsistent, and it is challenging to conclude whether active efflux or uptake of PFOS, PFHxS and PFBS does occur. Compared to the previously described findings of the present study, in which the flux of digoxin across the Caco-2 membrane was studied, it might seem that active efflux is not necessarily involved in the transport of PFOS, PFHxS and PFBS out of the cells. This could possibly imply that there are no effective mechanisms of detoxification of PFOS, PFHxS and PFBS in the Caco-2 cells, and potentially also not in intestinal enterocytes either.

Moreover, the transport rates of the compounds in both directions are mostly equal (Efflux ratio; ER=1), and the efflux ratio is below two for nearly all test compounds and concentrations tested. An efflux ratio greater than two might indicate that active efflux is involved. PFHxS 0.01 μM, as well as PFBS 1 and 10 μM, nevertheless, stand out with an efflux ratio higher than two. It was problematic to interpret the results and conclude whether active efflux might be involved for these specific concentrations, or whether reproducibility of the experiments due to challenges in handling cell experiments have had an impact on the results. Nevertheless, the results could indicate that the uptake in human intestinal enterocytes occurs at the same rate as the efflux of these individual PFSAs, suggesting that there are no protective mechanisms of action dealing with environmental toxicants like PFAS, when these enter the body by ingestion.

PFBS stands out compared to the other two compounds tested. It appears that the transport rate of PFBS in the apical to basolateral direction decreases with increased concentration of the compound. It could be assumed that there is some sort of inhibition involved, and that PFBS alters or inhibits its own uptake into the cell. A possible mechanism could be by saturation of a transporter involved in the uptake of PFBS. Digoxin was present in the incubation solutions, as some of the transport studies with PFOS, PFHxS and PFBS and

digoxin were carried out in the same assay as transport studies to investigate the permeability of PFOS, PFHxS and PFBS across the Caco-2 monolayer. It could be considered, that if active uptake through P-gp is involved, that digoxin could compete with PFBS for the uptake through possible uptake transporters.

Nevertheless, previously published studies have shown that long chain PFAS, like PFOS can be incorporated in biological membranes and thus affect the permeability of compounds (61, 121-123). One study showed that exposure of human placental choriocarcinoma cell line JEG-3 to a mixture eight perfluoroalkyl substances of 0.6 μM, including PFOS, PFHxS and PFBS, led to a 3.4-fold increase of several lipid classes, including phosphatidylcholines, plasmalogen and lyso plasmalogen, indicating that the PFAS interfered with the membrane lipids (61). What is interesting, the strongest alteration in cell lipids was observed at the lowest concentrations tested (0.6 μM) (61). Another study has previously shown that PFOS may cause adverse biological effect by alteration of the fluidity of the lipid assemblies of the plasma membrane (124). In the present study, it could be observed that highest transport rate across the membrane was for the lower concentrations of PFHxS (0.001, 0.01 μM) in the basolateral to apical direction. Although the incorporation of the individual PFSAs in the cell membrane was not tested in the present study, it could be hypothesized that the higher rate in the lower concentrations could be caused by the incorporation of the PFSAs in the cell membrane and its altered fluidity, making the membrane more permeable. A different study showed that PFOS increased membrane fluidity in fish leukocytes in a dose-dependent manner (5-15 mg/L) (125). Moreover, the same study showed that the mitochondrial membrane potential was affected by the same concentration range, which suggested that PFOS effects membrane properties at lower concentrations than those associated with other adverse effects (125). Another study studied the interactions of PFAS with a phospholipid bilayer by neutron reflectometry, and showed that all PFAS tested did interact with the phospholipid bilayer by incorporation (123). Longer chain PFAS showed higher tendency to penetrate into the bilayer compared to the short chain PFAS (123). This could possibly explain the inconsistency of the results regarding PFOS. Moreover, the disorder of the bilayer was in that study observed to increase with increased concentrations of PFAS, especially of short chain substances such as PFBS, and it was suggested that it could be an indication of aggregation of PFAS in the phospholipid bilayer (123). This is an interesting finding. In the present study it was observed that the rate of PFBS decreases with increased concentrations of

PFBS, and it could be suggested that the rate decreased due to incorporation and aggregation in the phospholipid bilayer. However, the measured concentrations in that study were much higher than in the present study, 0-0.07, 0-5.2 and 0-88 mmol/L for PFOS, PFHxS and PFBS respectively, thus, the results do not necessarily reflection the effects of PFAS within the physiological range that is detected in human serum (123). Nevertheless, these findings are very intriguing, and it would be an interesting follow-up to study PFAS incorporation and accumulation in the Caco-2 cell line in future studies.

In the present study, it was hypothesized that active transport was involved in the efflux of PFOS, PFHxS and PFBS. In the case of involvement of active transporters, the transport rate is dependent on the availability of the substrate to the transporter. In order to achieve a constant transport rate during incubation, the transporter needs to be saturated with its substrate, or the substrate need to be in excess. Only then, representative results of the transport rate can be obtained. A decrease in substrate concentration could significantly affect the transport activity. If the substrates, PFOS, PFHxS and PFBS were not in excess, the transporter activity could decrease with time due to decreased substrate availability in the donor chamber.

Time trends were conducted for 1 μM of PFOS, PFHxS and PFBS, which showed linear transport. It was concluded that at 1μM of PFOS, PFHxS and PFBS, the transporter activity is constant. However, only one time-independent study was conducted, but then in parallels. Conducting a single time-independent study excludes biological variations. The standard deviation was, on the other hand, very small, and the parallels within the study were almost identical. In an optimal way, several time-independent time trends should have been conducted for all concentrations used, however, this would have been beyond the scope of the present master's thesis.

The incubation lasted for 90 minutes straight. It cannot be excluded that the transport of PFOS, PFHxS and PFBS was reversed to the opposite direction, when the substrate concentration reached sufficient levels in the recipient chamber, back to the donor chamber. Then, an equilibrium would have been established. To avoid this in subsequent studies, samples should be taken in shorter intervals, as for example every 30 or even 15 minutes and

at the same time replacing the volume that was sampled, with fresh HBSS buffer added to the recipient chamber. In that way it would be easier to control the flux of substances.

Working with PFAS is challenging, as PFAS is known to adsorb to surfaces. The adsorption of PFOS, PFHxS and PFBS to the plate wells and inserts during the incubation cannot be excluded and could have led to the inconsistent results. PFAS with longer carbon chains tend to adsorb with a higher rate than PFAS with short carbon chains.

It has previously been shown that the toxicity of PFAS is dependent of the functional group attached, and increases with increased carbon chain length (61, 126). It was shown that the toxicity was greater for PFAS with a sulfonic acid functional group compared to carboxyl group. This could be connected to the rate of transport of PFAS into the cell. It was thus also of interest to study whether the transport rate across the Caco-2 cell monolayer differs between PFAS of different carbon chain lengths. PFOS, PFHxS and PFBS have chains of eight, six and four carbon atoms respectively. In the present study, it was observed that PFHxS crosses the monolayer at a seemingly higher rate compared to PFOS and PFBS. The rate was higher both in the apical to basolateral direction and in the basolateral to apical direction. Thus, it could be suggested that the cell membrane of Caco-2 cells is more permeable for PFHxS.

It is, however, rather difficult to conclude at this time how PFOS, PFHxS and PFBS cross the Caco-2 cell monolayer. A contribution of active transporters in addition to passive or facilitated diffusion could be involved.

6.3 Quinidine and verapamil influenced the transport of PFOS, PFHxS and PFBS across the Caco-2 monolayer

To study the involvement of P-gp in the active efflux and detoxification of PFOS, PFHxS and PFBS when entering body by ingestion, these substances were individually incubated with Caco-2 cell monolayers and known P-gp inhibitors. This was done in order to investigate whether PFOS, PFHxS and PFBS might be P-gp substrates. Verapamil and quinidine are known and widely used inhibitors of P-gp. Quinidine is more selective for P-gp than verapamil. It was hypothesized that if P-gp was involved in the active efflux of PFOS, PFHxS

and PFBS, efflux of these individual substances would decrease with increased concentrations of the inhibitors.

Although the results were not statistically significant, it can appear that the transport rate of PFOS and PFHxS decreases both in the apical to basolateral and in the basolateral to apical direction with increased concentrations of inhibitors. In contrast, the transport rate of PFBS is constant both in the apical to basolateral direction and in the basolateral to apical direction and the transport does not seem to be affected by the increased concentrations of neither quinidine nor verapamil.

The effect of quinidine on transport rate of PFOS is inconsistent, however, it shows a decrease in transport rate for the highest concentration of quinidine (100 μM) compared to the control group. The decrease is greater for the transport rate in the apical to basolateral direction than for the transport rate in the basolateral to apical direction. While it can appear that the control group has a higher flux of PFOS from the apical to basolateral chamber, than efflux from the basolateral to apical chamber (ER=0.6), the group exposed to 100 μM quinidine, shows a considerably lower rate of PFOS in the apical to basolateral direction than the efflux in the basolateral to apical direction (ER=1.4). It was hypothesized that quinidine would inhibit P-gp, and by these means decrease the transport rate of PFOS in the basolateral to apical direction, in case PFOS being a P-gp substrate. Although there is a small decrease in the transport rate in the basolateral to apical direction with increased concentrations of quinidine, it might appear that quinidine affected the influx of PFOS more than its efflux.

Similar effect on the transport rate of PFOS is seen with verapamil. For the control group, the efflux rate is 0.7, suggesting that the influx of PFOS into the cell is higher than the efflux. However, it appears that the transport rate of PFOS decreases with increased concentrations of verapamil (1, 10 and 100 μM), both in the apical to basolateral direction, and in the basolateral to apical direction. Similar as observed with quinidine, it might appear that verapamil inhibits the influx of PFOS.

Both inhibitors seem to decrease the transport rate of PFHxS to some degree, mostly in the basolateral to apical direction. However, the rate of PFHxS in the apical to basolateral direction decreased to some degree with increased concentrations of verapamil. This might imply that PFOS, PFHxS and PFBS cross the cell membrane in different ways with different

transport mechanisms involved. It could be hypothesized that PFBS, who's chemical structure consists of four carbons, diffuses more easily across the membrane, while PFHxS and PFOS requires facilitated active transport to cross the membrane.

A previously published study suggested that PFOA was not a substrate of P-gp, as the accumulation of PFOA in MDCK cells did not change when incubated with the P-gp inhibitor elacridar (89). In the present study, although the decrease of PFOS and PFHxS was not statistically significant, a trend could be observed, where flux of these substances decreased to some degree with increased concentrations of quinidine and verapamil. This might imply that active efflux might be involved, and that PFOS and PFHxS, but not PFBS could be substrates of P-gp. However, it is not excluded that PFOS, PFHxS and PFBS cross the Caco-2 monolayer by simple diffusion in addition to being actively transported. The Caco-2 model encompasses all these routes of transport across the membrane, including transcellular and paracellular diffusion, facilitated diffusion and active transport. It is possible that PFOS, PFHxS and PFBS cross the cell membrane by different mechanisms, thus, it is challenging to differentiate between these ways of transport when using the Caco-2 cell line model. It could be suggested that the Caco-2 cell line model was not the ideal model to study the transport of the individual PFSAs across the monolayer. The model might not be sensitive enough to differentiate between the different ways of transport across the membrane, especially considering that PFAS are compounds that are difficult to study.

However, in previously published studies it has been demonstrated that PFOS, PFHxS and PFBS are substrates of several human organic anion transporting polypeptides (OATP), including human OATP1B1, OATP1B3, OATP2B1, and rat OATP1A1, OATP1B2, OATP2B1, OATP1A5 (44). These transporters are involved in the uptake of different PFAS and are expressed in hepatocytes and enterocytes in humans and rats. OATPs are sodium-independent transporters that mediate the uptake of different endogenous and exogenous compounds like taurocholate, estrone-3-sulfate, bilirubin and several drugs including statins (109). These experiments were conducted using Chinese hamster ovary cells and HEK-cells (44). Further it has been demonstrated that OATP1B2, as well as OATP1A2 are present in the human intestinal enterocytes and are known to be expressed in the Caco-2 cell line model (109). However, the expression levels of OATP1B2 are higher than for the other OATP isoforms in intestinal enterocytes and also in Caco-2 cells. It has been suggested that

OATP1A2 is not involved in the uptake of PFOA, thus, it was suggested that OATP2B1 mediates the uptake of PFOA into Caco-2 cells (109). OATPs could therefore have contributed to the uptake of PFOS, PFHxS and PFBS into Caco-2 cells in the present study. It has also been shown that PFBS was transported with the lowest efficiency by all three human OATPs (44). However, the results of the present study showed that the transport rate of PFBS, in both directions, was higher than of PFOS.

OATP1A2, which has been shown to be involved in transport of PFAS, is inhibited by verapamil (127). However, this transporter is not expressed in the Caco-2 cell line model. Nevertheless, it seems that verapamil and quinidine inhibit the transport rate in the apical to basolateral direction of both PFOS and PFHxS. This suggests that there might be other transporters, that are expressed in the Caco-2 cell line model, and which are involved in the uptake of these substances. Inhibition of these unknown/other transporters could be useful in order to limit the absorption of PFOS and PFHxS entering the body through ingestion.

6.4 Limitations of the study and future aspects

There are several limitations to the present study that could have affected the results. These should be improved and accounted for in follow-up and future studies.

First, in the present study, the flux of substances across the membrane and back to the initial chamber was not controlled. Although the concentration gradient is presumably the driving force of the flux of substances, there is no guarantee that the concentrations measured are the actual concentrations transported of the substance in one direction. If the transport rate of a substance was fast, this could have led to an equilibrium being established after some time during the incubation. However, this was not investigated, and it cannot be stated with certainty that an equilibrium was established within the 90 minutes of incubation. However, to improve this, it could be suggested to take samples from the recipient chamber in shorter intervals, as for example every 15 or 30 minutes in comparison to incubating for 90 minutes straight. Moreover, samples could be taken in a way to reduce the volume of the recipient chamber in half, and after, replacing this volume with fresh HBSS. This way, the concentration of the substances in the recipient chamber would be reduced and thus

minimized the diffusion from the recipient to donor chamber across the monolayer. The flux of the substance would be limited to the transport from the donor chamber to the recipient chamber.

It might be that calculation of apparent permeability for PFAS in Caco-2 cell line model was not the perfect way to measure the transport across the biological membranes. It was hypothesized that PFOS, PFHxS and PFBS are substrates for P-gp, however, it might be a better way of presenting the permeability of a compound, when other ways of transport are involved.

Second, this study did not account for biological variation and the data was not normalized. Due to limitations in the number of inserts per plate, it was prioritized to test more concentrations, instead of including membrane integrity markers, such as mannitol and propranolol, with every transport study. The cell membranes could have been incubated with the integrity markers subsequent the incubation with the individual PFSAs, however, in this case, time was the limiting factor. The extraction of digoxin was supposed to occur as fast as possible to limit its degradation. However, it would be preferred to include inserts with integrity markers with every transport study, which could then be used for the normalization of data and correct for biological variations. The expression of P-gp might differ between cells of different passage number, and the number of transporters might differ between 21 and 28 days of culture. Culture conditions also affect the differentiation and polarization of the cells, and thus, also the expression of P-gp. The expression of P-gp is closely related to the measured transport activity, as a greater number of transporters would result in a greater transport rate. With increased passage number of the cells, morphological and genetic changes might occur in the cells. These changes might affect the characteristics of the cells, including expression of transporter proteins, and it is thus recommended that the passage number of cells does not exceed 10. In this study, this was taken into account, thus, several batches of cells were used throughout the study. This could imply that there were biological differences among the different batches of cells used in the study, that could have affected and caused variations in the results. Thus, it is important to account for biological variation.

The selection of the concentrations was based on the levels of PFOS and PFHxS detected in human serum. Higher concentrations could be applied to observe an effect, however, in that

case, it would be much more challenging to conduct the experiments because PFAS contamination issues caused for example by carry over, and the results would not necessarily reflect the real-life scenario.

There are some limitations when it comes to the experimental setup of the transport studies, that could have affected the results. The size of the incubator used during the transport studies was too big to install it on a shaker, and too small to place the shaker inside. It is possible that the compounds were not evenly and properly mixed in the wells and inserts before taking an aliquot, although the plates were shaken by hand after ended incubation. PFAS readily adsorb to surfaces over time and are challenging substances to work with. Using a shaker during the incubation could have minimized the probability of an adsorption of PFAS to the plastic.

Further, the aliquots of 50 μL were stored at -20 degrees for later LC-MS analysis. Although the vials were mixed using a vortex prior to sample dilution and preparation for analysis, there exists a possibility that the samples were not mixed thoroughly well enough, and what could have introduced random errors. More time-independent parallels should have been conducted, but due to time limitations and limitations in the capacity of the instrument, it was not possible to conduct more experiments.

Some parallels had to be excluded as the amount of test substance detected was identical in both chambers, suggesting that the filter could have been punctured during washing or pipetting. To avoid using punctured filters, TEER could have been measured just beforehand the addition of incubation solutions. However, since TEER measurements were conducted every week during cell culture, to observe the growth and health of the cells, the Millipore was calibrated to be used in culture medium. Transport experiments were conducted in HBSS transport buffer, and in order to measure electrical resistance across the monolayer, the instrument had to be calibrated to this specific buffer. This was time consuming and inconvenient, however, for future studies, it could be suggested to obtain several electrodes that could be used to different purposes and buffers.

In the present study, the effect of three PFSAs of different carbon chain lengths on the transport of digoxin, was investigated. Additionally, it would be interesting studying other PFAS with different chain length and functional groups, to investigate and compare the effects of carbon chain length and effects of different functional groups on the transport of

digoxin across the Caco-2 cell monolayer. Although the Caco-2 model is a widely used model to study drug-drug interactions, it would be interesting to utilize different human cell lines expressing ABC transporter proteins and possibly also tissues containing efflux transporters to investigate whether this would affect the results. It could additionally be considered using knockout models to study specific transporters of interest, instead of inhibitors. Moreover, it would be interesting to investigate the synergistic effects of PFAS and cytotoxic substrates in the Caco-2 cell line, in order to examine whether the results from other published studies could be reproduced in Caco-2 cell line and potentially other human cell lines. Moreover, it would be interesting to examine the potential mechanisms of action of the synergy between PFAS and other toxic agents.

Aditionally, it would be of great interest to examine not only the transport of PFAS across the membrane, but also the accumulation of PFAS within the cells, as well as the incorporation of PFAS in the cell membrane in future studies.

7 Conclusion

To conclude, the findings in the present study showed that PFOS, PFHxS and PFBS did not affect the flux of digoxin by P-gp in the Caco-2 cell line model. It is still uncertain whether PFOS, PFHxS and PFBS could possibly interact with P-gp or other ABC transporters involved in the absorption and distribution of drugs or toxicants *in vivo*, as they might be involved in more complex pathways that are difficult to study in the Caco-2 cell line or other models. It is, nevertheless, an interesting and novel finding, that PFOS, PFHxS and PFBS did not interact with P-gp or modulate its activity in the Caco-2 cell line. Further, it was shown that PFOS, PFHxS and PFBS were transported across the Caco-2 cell monolayer with approximately the same rate in both the apical to basolateral direction and in the basolateral to apical direction. When the transport rate was measured using known P-gp inhibitors, it was observed that the transport rate decreased to some degree for PFOS and PFHxS in both the apical to basolateral direction and in the basolateral to apical direction, but not for PFBS, suggesting that active uptake and efflux might be involved in the transport of these substances across the Caco-2 cell monolayer. However, it is possible that other ways of transport are involved. Further research in the fields of permeability of PFAS across biological barriers as well as mechanisms of action involved in inhibition of efflux transporters is needed to assess the potential toxicity of these environmental toxicants.

Works cited

1. Huber S, Brox J. An automated high-throughput SPE micro-elution method for perfluoroalkyl substances in human serum. Analytical and Bioanalytical Chemistry. 2015;407(13):3751-61.
2. Pelch KE, Reade A, Wolffe TAM, Kwiatkowski CF. PFAS health effects database: Protocol for a systematic evidence map. Environ Int. 2019;130:104851.
3. Buck RC, Franklin J, Berger U, Conder JM, Cousins IT, de Voogt P, et al. Perfluoroalkyl and polyfluoroalkyl substances in the environment: terminology, classification, and origins. Integr Environ Assess Manag. 2011;7(4):513-41.
4. Schulz K, Silva MR, Klaper R. Distribution and effects of branched versus linear isomers of PFOA, PFOS, and PFHxS: A review of recent literature. Science of The Total Environment. 2020;733:139186.
5. Blake BE, Fenton SE. Early life exposure to per- and polyfluoroalkyl substances (PFAS) and latent health outcomes: A review including the placenta as a target tissue and possible driver of peri- and postnatal effects. Toxicology. 2020;443:152565-.
6. Liu Y, Cao Z, Zong W, Liu R. Interaction rule and mechanism of perfluoroalkyl sulfonates containing diferent carbon chains with human serum albumin. RSC Advances. 2017.
7. Ding N, Harlow SD, Randolph JF, Jr., Loch-Caruso R, Park SK. Perfluoroalkyl and polyfluoroalkyl substances (PFAS) and their effects on the ovary. Hum Reprod Update. 2020;26(5):724-52.
8. Foguth R, Sepúlveda MS, Cannon J. Per- and Polyfluoroalkyl Substances (PFAS) Neurotoxicity in Sentinel and Non-Traditional Laboratory Model Systems: Potential Utility in Predicting Adverse Outcomes in Human Health. Toxics. 2020;8(2):42.
9. Sinclair E, Kim SK, Akinleye HB, Kannan K. Quantitation of Gas-Phase Perfluoroalkyl Surfactants and Fluorotelomer Alcohols Released from Nonstick Cookware and Microwave Popcorn Bags. Environmental Science & Technology. 2007;41(4):1180-5.
10. Bradley EL, Read WA, Castle L. Investigation into the migration potential of coating materials from cookware products. Food additives and contaminants. 2007;24(3):326-35.
11. Trier X, Granby K, Christensen JH. Polyfluorinated surfactants (PFS) in paper and board coatings for food packaging. Environmental Science and Pollution Research. 2011;18(7):1108-20.
12. Schaider LA, Balan SA, Blum A, Andrews DQ, Strynar MJ, Dickinson ME, et al. Fluorinated Compounds in U.S. Fast Food Packaging. Environ Sci Technol Lett. 2017;4(3):105-11.
13. Hill PJ, Taylor M, Goswami P, Blackburn RS. Substitution of PFAS chemistry in outdoor apparel and the impact on repellency performance. Chemosphere. 2017;181:500-7.
14. Lee JH, Lee CK, Suh C-H, Kang H-S, Hong C-P, Choi S-N. Serum concentrations of per- and poly-fluoroalkyl substances and factors associated with exposure in the general adult population in South Korea. International Journal of Hygiene and Environmental Health. 2017;220(6):1046-54.
15. Kang H, Choi K, Lee H-S, Kim D-H, Park N-Y, Kim S, et al. Elevated levels of short carbon-chain PFCAs in breast milk among Korean women: Current status and potential challenges. Environmental research. 2016;148:351-9.

16. Harada K, Inoue K, Morikawa A, Yoshinaga T, Saito N, Koizumi A. Renal clearance of perfluorooctane sulfonate and perfluorooctanoate in humans and their species-specific excretion. Environmental research. 2005;99(2):253-61.
17. Kannan K, Koistinen J, Beckmen K, Evans T, Gorzelany JF, Hansen KJ, et al. Accumulation of perfluorooctane sulfonate in marine mammals. Environ Sci Technol. 2001;35(8):1593-8.
18. Szilagyi JT, Avula V, Fry RC. Perfluoroalkyl Substances (PFAS) and Their Effects on the Placenta, Pregnancy, and Child Development: a Potential Mechanistic Role for Placental Peroxisome Proliferator–Activated Receptors (PPARs). Current Environmental Health Reports. 2020;7(3):222-30.
19. Caron-Beaudoin É, Ayotte P, Laouan Sidi EA, Gros-Louis McHugh N, Lemire M. Exposure to perfluoroalkyl substances (PFAS) and associations with thyroid parameters in First Nation children and youth from Quebec. Environ Int. 2019;128:13-23.
20. Bao J, Li C-L, Liu Y, Wang X, Yu W-J, Liu Z-Q, et al. Bioaccumulation of perfluoroalkyl substances in greenhouse vegetables with long-term groundwater irrigation near fluorochemical plants in Fuxin, China. Environmental research. 2020;188:109751.
21. Hanssen L, Röllin H, Odland JØ, Moe MK, Sandanger TM. Perfluorinated compounds in maternal serum and cord blood from selected areas of South Africa: results of a pilot study. Journal of Environmental Monitoring. 2010;12(6):1355-61.
22. Langberg HA, Arp HPH, Breedveld GD, Slinde GA, Høiseter Å, Grønning HM, et al. Paper product production identified as the main source of per- and polyfluoroalkyl substances (PFAS) in a Norwegian lake: Source and historic emission tracking. Environ Pollut. 2021;273:116259.
23. Butenhoff JL, Olsen GW, Pfahles-Hutchens A. The applicability of biomonitoring data for perfluorooctanesulfonate to the environmental public health continuum. Environ Health Perspect. 2006;114(11):1776-82.
24. Cousins IT, Goldenman G, Herzke D, Lohmann R, Miller M, Ng CA, et al. The concept of essential use for determining when uses of PFASs can be phased out. Environ Sci Process Impacts. 2019;21(11):1803-15.
25. Sunderland EM, Hu XC, Dassuncao C, Tokranov AK, Wagner CC, Allen JG. A review of the pathways of human exposure to poly- and perfluoroalkyl substances (PFASs) and present understanding of health effects. J Expo Sci Environ Epidemiol. 2019;29(2):131-47.
26. Grandjean P, Clapp R. Perfluorinated Alkyl Substances: Emerging Insights Into Health Risks. New Solut. 2015;25(2):147-63.
27. Ateia M, Maroli A, Tharayil N, Karanfil T. The overlooked short- and ultrashort-chain poly- and perfluorinated substances: A review. Chemosphere. 2019;220:866-82.
28. Joerss H, Xie Z, Wagner CC, von Appen W-J, Sunderland EM, Ebinghaus R. Transport of Legacy Perfluoroalkyl Substances and the Replacement Compound HFPO-DA through the Atlantic Gateway to the Arctic Ocean-Is the Arctic a Sink or a Source? Environmental science & technology. 2020;54(16):9958-67.
29. Averina M, Hervig T, Huber S, Kjær M, Kristoffersen EK, Bolann B. Environmental pollutants in blood donors: The multicentre Norwegian donor study. Transfusion Medicine. 2020;30(3):201-9.
30. Göckener B, Weber T, Rüdel H, Bücking M, Kolossa-Gehring M. Human biomonitoring of per- and polyfluoroalkyl substances in German blood plasma samples from 1982 to 2019. Environ Int. 2020;145:106123.

31. Duffek A, Conrad A, Kolossa-Gehring M, Lange R, Rucic E, Schulte C, et al. Per- and polyfluoroalkyl substances in blood plasma – Results of the German Environmental Survey for children and adolescents 2014–2017 (GerES V). International Journal of Hygiene and Environmental Health. 2020;228:113549.
32. Arbuckle TE, MacPherson S, Foster WG, Sathyanarayana S, Fisher M, Monnier P, et al. Prenatal perfluoroalkyl substances and newborn anogenital distance in a Canadian cohort. Reproductive Toxicology. 2020;94:31-9.
33. Colles A, Bruckers L, Den Hond E, Govarts E, Morrens B, Schettgen T, et al. Perfluorinated substances in the Flemish population (Belgium): Levels and determinants of variability in exposure. Chemosphere. 2020;242:125250.
34. Forsthuber M, Kaiser AM, Granitzer S, Hassl I, Hengstschläger M, Stangl H, et al. Albumin is the major carrier protein for PFOS, PFOA, PFHxS, PFNA and PFDA in human plasma. Environ Int. 2020;137:105324.
35. Caron-Beaudoin É, Ayotte P, Blanchette C, Muckle G, Avard E, Ricard S, et al. Perfluoroalkyl acids in pregnant women from Nunavik (Quebec, Canada): Trends in exposure and associations with country foods consumption. Environ Int. 2020;145:106169.
36. Eriksson U, Mueller JF, Toms LL, Hobson P, Kärrman A. Temporal trends of PFSAs, PFCAs and selected precursors in Australian serum from 2002 to 2013 : Supplementary materials. Environ Pollut. 2017;220(Pt A).
37. Andersen ME, Clewell HJ, Tan Y-M, Butenhoff JL, Olsen GW. Pharmacokinetic modeling of saturable, renal resorption of perfluoroalkylacids in monkeys—Probing the determinants of long plasma half-lives. Toxicology. 2006;227(1):156-64.
38. Sinclair GM, Long SM, Jones OAH. What are the effects of PFAS exposure at environmentally relevant concentrations? Chemosphere. 2020;258:127340.
39. Rotander A, Toms L-ML, Aylward L, Kay M, Mueller JF. Elevated levels of PFOS and PFHxS in firefighters exposed to aqueous film forming foam (AFFF). Environ Int. 2015;82:28-34.
40. OECD. Summary Report on updating the OECD 2007 List of Per- and Polyfluoroalkyl Substances. 2018. Report No.: ENV/JM/MONO(2018)7.
41. Yue Y, Li S, Qian Z, Pereira RF, Lee J, Doherty JJ, et al. Perfluorooctanesulfonic acid (PFOS) and perfluorobutanesulfonic acid (PFBS) impaired reproduction and altered offspring physiological functions in Caenorhabditis elegans. Food and Chemical Toxicology. 2020;145:111695.
42. Calafat AM, Kato K, Hubbard K, Jia T, Botelho JC, Wong L-Y. Legacy and alternative per- and polyfluoroalkyl substances in the U.S. general population: Paired serum-urine data from the 2013-2014 National Health and Nutrition Examination Survey. Environ Int. 2019;131:105048-.
43. Agency SC. Annex XV report: Proposal for identification of a substance of very high concern on the basis of the criteria set out in REACH Article 57. Substance name(s): Perfluorohexane-1-sulphonic acid and its salts. 2017.
44. Zhao W, Zitzow JD, Weaver Y, Ehresman DJ, Chang S-C, Butenhoff JL, et al. Organic Anion Transporting Polypeptides Contribute to the Disposition of Perfluoroalkyl Acids in Humans and Rats. Toxicol Sci. 2017;156(1):84-95.
45. Pizzurro DM, Seeley M, Kerper LE, Beck BD. Interspecies differences in perfluoroalkyl substances (PFAS) toxicokinetics and application to health-based criteria. Regulatory Toxicology and Pharmacology. 2019;106:239-50.

46. Li Y, Fletcher T, Mucs D, Scott K, Lindh CH, Tallving P, et al. Half-lives of PFOS, PFHxS and PFOA after end of exposure to contaminated drinking water. Occupational and environmental medicine. 2018;75(1):46.
47. Olsen GW, Chang S-C, Noker PE, Gorman GS, Ehresman DJ, Lieder PH, et al. A comparison of the pharmacokinetics of perfluorobutanesulfonate (PFBS) in rats, monkeys, and humans. Toxicology. 2009;256(1):65-74.
48. Zeng Z, Song B, Xiao R, Zeng G, Gong J, Chen M, et al. Assessing the human health risks of perfluorooctane sulfonate by in vivo and in vitro studies. Environ Int. 2019;126:598-610.
49. Pérez F, Nadal M, Navarro-Ortega A, Fàbrega F, Domingo JL, Barceló D, et al. Accumulation of perfluoroalkyl substances in human tissues. Environ Int. 2013;59:354-62.
50. Han R, Zhang F, Wan C, Liu L, Zhong Q, Ding W. Effect of perfluorooctane sulphonate-induced Kupffer cell activation on hepatocyte proliferation through the NF-κB/TNF-α/IL-6-dependent pathway. Chemosphere. 2018;200:283-94.
51. Wan C, Han R, Liu L, Zhang F, Li F, Xiang M, et al. Role of miR-155 in fluorooctane sulfonate-induced oxidative hepatic damage via the Nrf2-dependent pathway. Toxicology and Applied Pharmacology. 2016;295:85-93.
52. Fai Tse WK, Li JW, Kwan Tse AC, Chan TF, Hin Ho JC, Sun Wu RS, et al. Fatty liver disease induced by perfluorooctane sulfonate: Novel insight from transcriptome analysis. Chemosphere. 2016;159:166-77.
53. Chang ET, Adami H-O, Boffetta P, Wedner HJ, Mandel JS. A critical review of perfluorooctanoate and perfluorooctanesulfonate exposure and immunological health conditions in humans. Crit Rev Toxicol. 2016;46(4):279-331.
54. Govarts E, Iszatt N, Trnovec T, de Cock M, Eggesbø M, Palkovicova Murinova L, et al. Prenatal exposure to endocrine disrupting chemicals and risk of being born small for gestational age: Pooled analysis of seven European birth cohorts. Environ Int. 2018;115:267-78.
55. Grandjean P, Heilmann C, Weihe P, Nielsen F, Mogensen UB, Timmermann A, et al. Estimated exposures to perfluorinated compounds in infancy predict attenuated vaccine antibody concentrations at age 5-years. J Immunotoxicol. 2017;14(1):188-95.
56. Steenland K, Tinker S, Frisbee S, Ducatman A, Vaccarino V. Association of perfluorooctanoic acid and perfluorooctane sulfonate with serum lipids among adults living near a chemical plant. American journal of epidemiology. 2009;170(10):1268-78.
57. Fei C, McLaughlin Joseph K, Tarone Robert E, Olsen J. Perfluorinated Chemicals and Fetal Growth: A Study within the Danish National Birth Cohort. Environ Health Perspect. 2007;115(11):1677-82.
58. Kristensen SL, Ramlau-Hansen CH, Ernst E, Olsen SF, Bonde JP, Vested A, et al. Long-term effects of prenatal exposure to perfluoroalkyl substances on female reproduction. Human Reproduction. 2013;28(12):3337-48.
59. Joensen UN, Veyrand B, Antignac J-P, Blomberg Jensen M, Petersen JH, Marchand P, et al. PFOS (perfluorooctanesulfonate) in serum is negatively associated with testosterone levels, but not with semen quality, in healthy men. Human Reproduction. 2013;28(3):599-608.
60. Lin C-Y, Wen L-L, Lin L-Y, Wen T-W, Lien G-W, Hsu SHJ, et al. The associations between serum perfluorinated chemicals and thyroid function in adolescents and young adults. Journal of Hazardous Materials. 2013;244-245:637-44.

61. Gorrochategui E, Pérez-Albaladejo E, Casas J, Lacorte S, Porte C. Perfluorinated chemicals: Differential toxicity, inhibition of aromatase activity and alteration of cellular lipids in human placental cells. Toxicology and Applied Pharmacology. 2014;277(2):124-30.
62. Mao Z, Xia W, Wang J, Chen T, Zeng Q, Xu B, et al. Perfluorooctane sulfonate induces apoptosis in lung cancer A549 cells through reactive oxygen species-mediated mitochondrion-dependent pathway. Journal of applied toxicology : JAT. 2013;33(11):1268-76.
63. Chou HC, Wen LL, Chang CC, Lin CY, Jin L, Juan SH. From the Cover: l-Carnitine via PPARγ- and Sirt1-Dependent Mechanisms Attenuates Epithelial-Mesenchymal Transition and Renal Fibrosis Caused by Perfluorooctanesulfonate. Toxicol Sci. 2017;160(2):217-29.
64. Soloff AC, Wolf BJ, White ND, Muir D, Courtney S, Hardiman G, et al. Environmental perfluorooctane sulfonate exposure drives T cell activation in bottlenose dolphins. Journal of applied toxicology : JAT. 2017;37(9):1108-16.
65. Tang LL, Wang JD, Xu TT, Zhao Z, Zheng JJ, Ge RS, et al. Mitochondrial toxicity of perfluorooctane sulfonate in mouse embryonic stem cell-derived cardiomyocytes. Toxicology. 2017;382:108-16.
66. Chen J, Zheng L, Tian L, Wang N, Lei L, Wang Y, et al. Chronic PFOS Exposure Disrupts Thyroid Structure and Function in Zebrafish. Bulletin of Environmental Contamination and Toxicology. 2018;101(1):75-9.
67. Chen X, Nie X, Mao J, Zhang Y, Yin K, Jiang S. Perfluorooctanesulfonate induces neuroinflammation through the secretion of TNF-α mediated by the JAK2/STAT3 pathway. NeuroToxicology. 2018;66:32-42.
68. Chan LMS, Lowes S, Hirst BH. The ABCs of drug transport in intestine and liver: efflux proteins limiting drug absorption and bioavailability. European Journal of Pharmaceutical Sciences. 2004;21(1):25-51.
69. Widmaier E, Raff, H, Strang, KT. Vander's Human Physiology: The Mechanisms of Body Function. New York: McGraw-Hill Education; 2016.
70. Kong S, Zhang YH, Zhang W. Regulation of Intestinal Epithelial Cells Properties and Functions by Amino Acids. Biomed Res Int. 2018;2018:2819154-.
71. van Breemen RB, Li Y. Caco-2 cell permeability assays to measure drug absorption. Expert Opinion on Drug Metabolism & Toxicology. 2005;1(2):175-85.
72. Walsh C, Schwartz-Bloom, RD. Levine's Pharmacology Drug Actions and Reactions. UK: Taylor & Francis; 2005.
73. Hardin J, Bertoni, G, Kleinsmith, LJ. Becker's World of the Cell San Fransisco: Pearson Benjamin Cummings; 2012.
74. Boudker O, Verdon G. Structural perspectives on secondary active transporters. Trends Pharmacol Sci. 2010;31(9):418-26.
75. Elsby R, Surry DD, Smith VN, Gray AJ. Validation and application of Caco-2 assays for the in vitro evaluation of development candidate drugs as substrates or inhibitors of P-glycoprotein to support regulatory submissions. Xenobiotica; the fate of foreign compounds in biological systems. 2008;38(7-8):1140-64.
76. Rusiecka I, Skladanowski AC. Induction of the multixenobiotic/multidrug resistance system in various cell lines in response to perfluorinated carboxylic acids. Acta biochimica Polonica. 2008;55(2):329-37.
77. Ravna AW, Sylte I, Sager G. Molecular model of the outward facing state of the human P-glycoprotein (ABCB1), and comparison to a model of the human MRP5 (ABCC5). Theor Biol Med Model. 2007;4:33-.

78. Ye Z, Lu Y, Wu T. The impact of ATP-binding cassette transporters on metabolic diseases. Nutr Metab (Lond). 2020;17:61-.
79. Ravna AW, Sylte I, Sager G. Binding site of ABC transporter homology models confirmed by ABCB1 crystal structure. Theor Biol Med Model. 2009;6:20-.
80. Ravna AW, Sager G. Molecular modeling studies of ABC transporters involved in multidrug resistance. Mini reviews in medicinal chemistry. 2009;9(2):186-93.
81. Silva R, Vilas-Boas V, Carmo H, Dinis-Oliveira RJ, Carvalho F, de Lourdes Bastos M, et al. Modulation of P-glycoprotein efflux pump: induction and activation as a therapeutic strategy. Pharmacology & therapeutics. 2015;149:1-123.
82. Shi Z, Tiwari AK, Patel AS, Fu L-W, Chen Z-S. Roles of Sildenafil in Enhancing Drug Sensitivity in Cancer. 2011;71(11):3735-8.
83. Juliano RL, Ling V. A surface glycoprotein modulating drug permeability in Chinese hamster ovary cell mutants. Biochimica et Biophysica Acta (BBA) - Biomembranes. 1976;455(1):152-62.
84. Saaby L, Brodin B. A Critical View on *In Vitro* Analysis of P-glycoprotein (P-gp) Transport Kinetics. Journal of Pharmaceutical Sciences. 2017;106(9):2257-64.
85. Zhang H, Xu H, Ashby Jr CR, Assaraf YG, Chen Z-S, Liu H-M. Chemical molecular-based approach to overcome multidrug resistance in cancer by targeting P-glycoprotein (P-gp). Medicinal Research Reviews. 2020;n/a(n/a).
86. Hunter J, Jepson MA, Tsuruo T, Simmons NL, Hirst BH. Functional expression of P-glycoprotein in apical membranes of human intestinal Caco-2 cells. Kinetics of vinblastine secretion and interaction with modulators. The Journal of biological chemistry. 1993;268(20):14991-7.
87. Kigen G, Edwards G. Drug-transporter mediated interactions between anthelminthic and antiretroviral drugs across the Caco-2 cell monolayers. BMC Pharmacol Toxicol. 2017;18(1):20-.
88. Awortwe C, Fasinu PS, Rosenkranz B. Application of Caco-2 cell line in herb-drug interaction studies: current approaches and challenges. J Pharm Pharm Sci. 2014;17(1):1-19.
89. Dankers ACA, Roelofs MJE, Piersma AH, Sweep FCGJ, Russel FGM, van den Berg M, et al. Endocrine Disruptors Differentially Target ATP-Binding Cassette Transporters in the Blood-Testis Barrier and Affect Leydig Cell Testosterone Secretion In Vitro. Toxicological Sciences. 2013;136(2):382-91.
90. Angelini A, Centurione L, Sancilio S, Castellani ML, Conti P, Di Ilio C, et al. The effect of the plasticizer diethylhexyl phthalate on transport activity and expression of P-glycoprotein in parental and doxo-resistant human sarcoma cell lines. Journal of biological regulators and homeostatic agents. 2011;25(2):203-11.
91. Nicklisch SCT, Rees SD, McGrath AP, Gökirmak T, Bonito LT, Vermeer LM, et al. Global marine pollutants inhibit P-glycoprotein: Environmental levels, inhibitory effects, and cocrystal structure. Sci Adv. 2016;2(4):e1600001-e.
92. Sreeramulu K, Liu R, Sharom FJ. Interaction of insecticides with mammalian P-glycoprotein and their effect on its transport function. Biochimica et Biophysica Acta (BBA) - Biomembranes. 2007;1768(7):1750-7.
93. Anselmo HMR, van den Berg JHJ, Rietjens IMCM, Murk AJ. Inhibition of cellular efflux pumps involved in multi xenobiotic resistance (MXR) in echinoid larvae as a possible mode of action for increased ecotoxicological risk of mixtures. Ecotoxicology. 2012;21(8):2276-87.

94. Moscovitz JE, Nahar MS, Shalat SL, Slitt AL, Dolinoy DC, Aleksunes LM. Correlation between Conjugated Bisphenol A Concentrations and Efflux Transporter Expression in Human Fetal Livers. Drug Metab Dispos. 2016;44(7):1061-5.
95. Keiter S, Burkhardt-Medicke K, Wellner P, Kais B, Färber H, Skutlarek D, et al. Does perfluorooctane sulfonate (PFOS) act as chemosensitizer in zebrafish embryos? Science of The Total Environment. 2016;548-549:317-24.
96. Kielberg V, Brünner, N., Briand, P. Celledyrkning: En praktisk håndbog i dyrkning af mammale celler: Foreningen af Danske Lægestuderendes Forlag 1993.
97. Langdon S. Cell Culture Contamination. In: Langdon SP, editor. Cancer Cell Culture: Methods and Protocols. Totowa, NJ: Humana Press; 2004. p. 309-17.
98. Zhao Yy, Fan Y, Wang M, Wang J, Cheng Jx, Zou Jb, et al. Studies on pharmacokinetic properties and absorption mechanism of phloretin: In vivo and in vitro. Biomedicine & Pharmacotherapy. 2020;132:110809.
99. Hidalgo IJ, Raub TJ, Borchardt RT. Characterization of the human colon carcinoma cell line (Caco-2) as a model system for intestinal epithelial permeability. Gastroenterology. 1989;96(3):736-49.
100. Gaillard JL, Finlay BB. Effect of cell polarization and differentiation on entry of Listeria monocytogenes into the enterocyte-like Caco-2 cell line. Infection and immunity. 1996;64(4):1299-308.
101. Vachon PH, Beaulieu JF. Transient mosaic patterns of morphological and functional differentiation in the Caco-2 cell line. Gastroenterology. 1992;103(2):414-23.
102. van Breemen RB, Li Y. Caco-2 cell permeability assays to measure drug absorption. Expert Opin Drug Metab Toxicol. 2005;1(2):175-85.
103. Grès MC, Julian B, Bourrié M, Meunier V, Roques C, Berger M, et al. Correlation between oral drug absorption in humans, and apparent drug permeability in TC-7 cells, a human epithelial intestinal cell line: comparison with the parental Caco-2 cell line. Pharmaceutical research. 1998;15(5):726-33.
104. Matsumoto T, Kaifuchi N, Mizuhara Y, Warabi E, Watanabe J. Use of a Caco-2 permeability assay to evaluate the effects of several Kampo medicines on the drug transporter P-glycoprotein. J Nat Med. 2018;72(4):897-904.
105. Fromm MF, Kim RB, Stein CM, Wilkinson GR, Roden DM. Inhibition of P-glycoprotein-mediated drug transport: A unifying mechanism to explain the interaction between digoxin and quinidine [seecomments]. Circulation. 1999;99(4):552-7.
106. Savaryn JP, Toby TK, Kelleher NL. A researcher's guide to mass spectrometry-based proteomics. Proteomics. 2016;16(18):2435-43.
107. Øiestad EL, Johansen U, Opdal MS, Bergan S, Christophersen AS. Determination of Digoxin and Digitoxin in Whole Blood. Journal of Analytical Toxicology. 2009;33(7):372-8.
108. Cannon RE, Richards AC, Trexler AW, Juberg CT, Sinha B, Knudsen GA, et al. Effect of GenX on P-Glycoprotein, Breast Cancer Resistance Protein, and Multidrug Resistance-Associated Protein 2 at the Blood-Brain Barrier. Environ Health Perspect. 2020;128(3):37002-.
109. Kimura O, Fujii Y, Haraguchi K, Kato Y, Ohta C, Koga N, et al. Uptake of perfluorooctanoic acid by Caco-2 cells: Involvement of organic anion transporting polypeptides. Toxicology Letters. 2017;277:18-23.
110. Nørgaard KB, Cedergreen N. Pesticide cocktails can interact synergistically on aquatic crustaceans. Environmental Science and Pollution Research. 2010;17(4):957-67.
111. Färber H, Jones P, Giesy J, Engwall M. Perfluorooctane Sulfonate Increases the Genotoxicity of Cyclophosphamide in the Micronucleus Assay with V79 Cells: Further Proof

of Alterations in Cell Membrane Properties Caused by PFOS (3 pp). Environmental Science and Pollution Research - International. 2007;14(2):85-7.
112. Hou TJ, Zhang W, Xia K, Qiao XB, Xu XJ. ADME Evaluation in Drug Discovery. 5. Correlation of Caco-2 Permeation with Simple Molecular Properties. Journal of Chemical Information and Computer Sciences. 2004;44(5):1585-600.
113. Larregieu CA, Benet LZ. Drug discovery and regulatory considerations for improving in silico and in vitro predictions that use Caco-2 as a surrogate for human intestinal permeability measurements. AAPS J. 2013;15(2):483-97.
114. Isenbarger TA, Carr CE, Johnson SS, Finney M, Church GM, Gilbert W, et al. The Most Conserved Genome Segments for Life Detection on Earth and Other Planets. Origins of Life and Evolution of Biospheres. 2008;38(6):517-33.
115. Annilo T, Chen Z-Q, Shulenin S, Costantino J, Thomas L, Lou H, et al. Evolution of the vertebrate ABC gene family: Analysis of gene birth and death. Genomics. 2006;88(1):1-11.
116. Anjard C, Loomis WF, Dictyostelium Sequencing C. Evolutionary analyses of ABC transporters of Dictyostelium discoideum. Eukaryot Cell. 2002;1(4):643-52.
117. Brandsma SH, Koekkoek JC, van Velzen MJM, de Boer J. The PFOA substitute GenX detected in the environment near a fluoropolymer manufacturing plant in the Netherlands. Chemosphere. 2019;220:493-500.
118. More VR, Campos CR, Evans RA, Oliver KD, Chan GN, Miller DS, et al. PPAR-α, a lipid-sensing transcription factor, regulates blood-brain barrier efflux transporter expression. Journal of cerebral blood flow and metabolism : official journal of the International Society of Cerebral Blood Flow and Metabolism. 2017;37(4):1199-212.
119. Huin C, Schohn H, Hatier R, Bentejac M, Antunes L, Plénat F, et al. Expression of peroxisome proliferator-activated receptors alpha and gamma in differentiating human colon carcinoma Caco-2 cells. Biology of the Cell. 2002;94(1):15-27.
120. Kotthoff M, Müller J, Jürling H, Schlummer M, Fiedler D. Perfluoroalkyl and polyfluoroalkyl substances in consumer products. Environ Sci Pollut Res Int. 2015;22(19):14546-59.
121. Fitzgerald NJM, Wargenau A, Sorenson C, Pedersen J, Tufenkji N, Novak PJ, et al. Partitioning and Accumulation of Perfluoroalkyl Substances in Model Lipid Bilayers and Bacteria. Environ Sci Technol. 2018;52(18):10433-40.
122. Hu Wy, Jones PD, DeCoen W, King L, Fraker P, Newsted J, et al. Alterations in cell membrane properties caused by perfluorinated compounds. Comparative Biochemistry and Physiology Part C: Toxicology & Pharmacology. 2003;135(1):77-88.
123. Nouhi S, Ahrens L, Campos Pereira H, Hughes AV, Campana M, Gutfreund P, et al. Interactions of perfluoroalkyl substances with a phospholipid bilayer studied by neutron reflectometry. Journal of colloid and interface science. 2018;511:474-81.
124. Xie W, Ludewig G, Wang K, Lehmler H-J. Model and cell membrane partitioning of perfluorooctanesulfonate is independent of the lipid chain length. Colloids and Surfaces B: Biointerfaces. 2010;76(1):128-36.
125. Hu W, Jones PD, DeCoen W, King L, Fraker P, Newsted J, et al. Alterations in cell membrane properties caused by perfluorinated compounds. Comp Biochem Physiol C Toxicol Pharmacol. 2003;135(1):77-88.
126. Berntsen HF, Bjørklund CG, Audinot J-N, Hofer T, Verhaegen S, Lentzen E, et al. Time-dependent effects of perfluorinated compounds on viability in cerebellar granule neurons: Dependence on carbon chain length and functional group attached. NeuroToxicology. 2017;63:70-83.

127. Kalliokoski A, Niemi M. Impact of OATP transporters on pharmacokinetics. Br J Pharmacol. 2009;158(3):693-705.

Appendix

Table 1. Fixation procedure for SEM and TEM

Step#	Description	User Prompt (on/off)	Time (Hr:min:sec)	Power (Watts)	Temp (ºC)	Load Cooler (off/auto/on)	Vacuum/ Bubbler Pump (off/ bub/ vac cycle/ vac on/ vap)	SteadyTemp pump (on/off)	SteadyTemp temp (ºC)
Protocol #9 Mal Green Fixation									
1	MalGreen GA fix	Off	0: 2: 0	100	50	Off	vacuum on	On	23
2	MalGreen GA fix	Off	0: 2: 0	0	50	Off	vacuum on	On	23
3	MalGreen GA fix	Off	0: 2: 0	100	50	Off	vacuum on	On	23
4	MalGreen GA fix	Off	0: 2: 0	0	50	Off	vacuum on	On	23
5	MalGreen GA fix	Off	0: 2: 0	100	50	Off	vacuum on	On	23
6	MalGreen GA fix	Off	0: 2: 0	0	50	Off	vacuum on	On	23
7	MalGreen GA fix	Off	0: 2: 0	100	50	Off	vacuum cycle	On	23
	2 bench washes								
8	PHEM Buffer	On	0: 0: 40	250	50	Off	Off	On	23
9	PHEM Buffer	On	0: 0: 40	250	50	Off	Off	On	23
10	Osmium	On	0: 2: 0	100	50	Off	vacuum cycle	On	23
11	Osmium	Off	0: 2: 0	0	50	Off	vacuum on	On	23
12	Osmium	Off	0: 2: 0	100	50	Off	vacuum on	On	23
13	Osmium	Off	0: 2: 0	0	50	Off	vacuum on	On	23
14	Osmium	Off	0: 2: 0	100	50	Off	vacuum on	On	23
15	Osmium	Off	0: 2: 0	0	50	Off	vacuum on	On	23
16	Osmium	Off	0: 2: 0	100	50	Off	vacuum cycle	On	23
	2 bench washes								
17	PHEM Buffer	On	0: 0: 40	250	50	Off	Off	On	23
18	PHEM Buffer	On	0: 0: 40	250	50	Off	Off	On	23
19	Tannic Acid	On	0: 1: 0	150	50	Off	vacuum cycle	On	23
20	Tannic Acid	Off	0: 1: 0	0	50	Off	vacuum on	On	23
21	Tannic Acid	Off	0: 1: 0	150	50	Off	vacuum on	On	23
22	Tannic Acid	Off	0: 1: 0	0	50	Off	vacuum on	On	23
23	Tannic Acid	Off	0: 1: 0	150	50	Off	vacuum on	On	23
24	Tannic Acid	Off	0: 1: 0	0	50	Off	vacuum on	On	23
25	Tannic Acid	Off	0: 1: 0	150	50	Off	vacuum cycle	On	23
	2 bench washes								
26	PHEM Buffer	On	0: 0: 40	250	50	Off	Off	On	23
27	Water	On	0: 0: 40	250	50	Off	Off	On	23
28	Water	On	0: 0: 40	250	50	Off	Off	On	23

	2 bench washes								
29	UA	On	0: 1: 0	150	50	Off	vacuum cycle	On	23
30	UA	Off	0: 1: 0	0	50	Off	vacuum on	On	23
31	UA	On	0: 1: 0	150	50	Off	vacuum on	On	23
32	UA	Off	0: 1: 0	0	50	Off	vacuum on	On	23
33	UA	Off	0: 1: 0	150	50	Off	vacuum on	On	23
34	UA	Off	0: 1: 0	0	50	Off	vacuum on	On	23
35	UA	Off	0: 1: 0	150	50	Off	vacuum cycle	On	23
36	Water	On	0: 0: 40	250	50	Off	Off	On	23
37	Water	On	0: 0: 40	250	50	Off	Off	On	23
38	25% ETOH	On	0: 0: 40	250	50	Off	Off	On	23
39	50% ETOH	On	0: 0: 40	250	50	Off	Off	On	23
40	70% ETOH	On	0: 0: 40	250	50	Off	Off	On	23
41	90% ETOH	On	0: 0: 40	250	50	Off	Off	On	23
42	100% ETOH	On	0: 0: 40	250	50	Off	Off	On	23
43	100% ETOH	On	0: 0: 40	250	50	Off	Off	On	23
44	100% ETOH	On	0: 0: 40	250	50	Off	Off	On	23
Protocol #11 - Resin infiltration									
1	Resin 1:2	On	0: 3: 0	250	50	Off	vacuum cycle	On	23
2	Resin 100	On	0: 3: 0	250	50	Off	vacuum cycle	On	23
3	Resin 100	On	0: 3: 0	250	50	Off	vacuum cycle	On	23

Table 2. PFAS dilutions – transport studies with and without inhibitors

Sample concentration (μM)	Volume of sample (μL)	ISTD (μL)	RSTD (μL)	MeOH (μL)	Milli-Q water (μL)	Total volume (μL)
Control	50	10	5	35	0	100
0.001	50	10	5	35	0	100
0.01	50	25	10	115	100	300
0.1	10	25	10	115	140	300
1	10	25	10	115	140	300
10	10	25	10	115	145	300

Table 3. PFAS dilutions – time trend

Sample concentration (μM)	Volume of sample (μL)	ISTD (μL)	RSTD (μL)	MeOH (μL)	Milli-Q water (μL)	Total volume (μL)
1	50	25	10	115	100	300

Table 4. Test of PFAS presence in equipment and solutions used in the study. The tests were performed in parallels.

Equipment/solution	Comment
Pipette tips 1-10 μL	Not detected
Pipette tips 1-100 μL	Not detected
Pipette tips 1-1000 μL	PFBS detected
Culture medium DMEM	Trace amount s of PFHpS. PFOS, PFNS detected, and maybe PFDS and 6:2 FTS
PBS	Not detected
HBSS	Not detected
Trypsin	6:2 FTS, but another test is required to conclude with certainty
Cell culture flask 25 cm^3	Trace amounts of PFNA. PFDA, PFUnDA, PFDoDA, PFTrDA, PFTeDA detected
Cell culture flask 75 cm^3	PFBA, PFPeA, PFHxA, PFHpA detected. Trace amounts of PFHxS
Transwell permeable membrane inserts and plate wells	PFNA, PFDA, PFUnDA, PFDoA, PFTrDA, PFTeDA detected
Serological pipettes 5 and 10 mL	Not detected
Water PCR-clean	Not detected
Milli-Q water	Not detected
Ethanol, MS grade	Not detected
Glass pipette	Not detected
Centrifuge tube 15, 50 mL	Not detected
Eppendorf tube	Not detected
MS grade methanol	Not detected